University of Stavanger

Faculty of Science and Technology

MASTER'S THESIS

Study program/ Specialization: Master in Petroleum Geoscience	Spring semester, 2012 Restricted access
Writer: Maren K. Bjørheim	*Maren Bjørheim* .... (Writer's signature)
Faculty supervisor: Alejandro Escalona External supervisor(s):	
Title of thesis: Reservoir potential in the Klappmyss Formation, Barents Sea.	
Credits (ECTS):30	
Key words: Early Triassic, Klappmyss Formation, Clinoform angles, Clinoform trajectories, reservoir prediction.	Pages: …76………………. + enclosure: ………… Stavanger, ………15.06.2012……….. Date/year

Acknowledgements

This master thesis has been carried out (spring 2012) at the Department of the Petroleum Engineering, University of Stavanger, Norway, under the supervision of Associate Professor in Petroleum Geoscience Alejandro Escalona and Andrew Rutherford and Lucy Ramsey, both in the exploration team in BG Norway.

I would like to thank Alejandro Escalona for supervising me during this work by supporting me with relevant literature, discussing my observations and giving me valuable feedback both regarding the thesis subject and thesis writing in general.

I also wish to express my gratitude to my supervisors in BG, Andrew and Lucy. Without you this thesis would not have been written. I am grateful for all guiding through the software, constructive comments along the way and the positive attitude in general. You are both inspiring in terms of knowledge and working spirit.

Also thanks to "colleagues" in BG. Thank for helping me with computer issues and showing me how much there is to learn about the petroleum industry.

Contents

Introduction

By May 2012 there are a total of 91 exploration and appraisal wells in the Norwegian sector of the Barents Sea, and more than 300 000 km of seismic reflection data. Moreover, estimation from Norwegian Petroleum Directorate (NPD) favours Barents Sea as the area with the highest potential for finding hydrocarbons (in Norway) in their resource calculation from 2011. Both oil and gas have been discovered in the South Barents basin and findings in well 7220/8-1 (Skrugard), and 7225/3-1 (Norvarg) have contributed to new optimism in the Barents Sea (www.npd.no), resulting in increased interest from numerous companies.

Most reserves are contained in Jurassic clastic reservoirs (eg. Shtokman), but recent drilling has verified effective reservoirs in the Triassic succession. The discovery of Triassic source and reservoir potentials have created increased interest for this interval. Goliat oil field (figure 1) will for instance start producing from Triassic reservoirs in 2013. However, the Triassic remains a secondary target and the number of wells drilled through Triassic is still limited.

Recent work in the western Barents Sea focussed on regional 2D lines where Triassic seismic sequence stratigraphy and paleogeography were interpreted (Glørstad-Clark et al., 2010). Further platform-margin deltas were interpreted based on mapping of clinoform geometries, clinoform angles and trajectories (Glørstad- Clark et al., 2011). This study has a similar approach; however, the main attention is on a smaller 3D area (figure 1) covering one of these platform margin deltas, and only Early Triassic Klappmyss Formation is considered. The main purpose is the petroleum significance in this area and to understand reservoir potential in the Klappmyss Formation in the Samson Dome area (figure 1), Barents Sea. This formation has had less focus regarding exploration potential and has been the primary objective in only one well (7228/9-1S).

By performing seismic stratigraphy and analyzing the clinoform configuration, facies distribution can be predicted, and thus reservoir properties in the Klappmyss Fm. These results might serve as a base for further exploration in Early Triassic.

In order to achieve this, a 3D seismic dataset tied to regional data and wells will be interpreted. Moreover, isopach and attribute maps will be generated to better predict the likelihood of deltas in reaching the shelf margin, and forming sand-rich deposits. Furthermore, seismic facies will be mapped and shelf edge trajectories analysed in order to make palaeographic reconstructions. Clinoform angles will be calculated and depth conversion will be performed to be able to consider different grain size possibilities and estimate reservoir volumes.
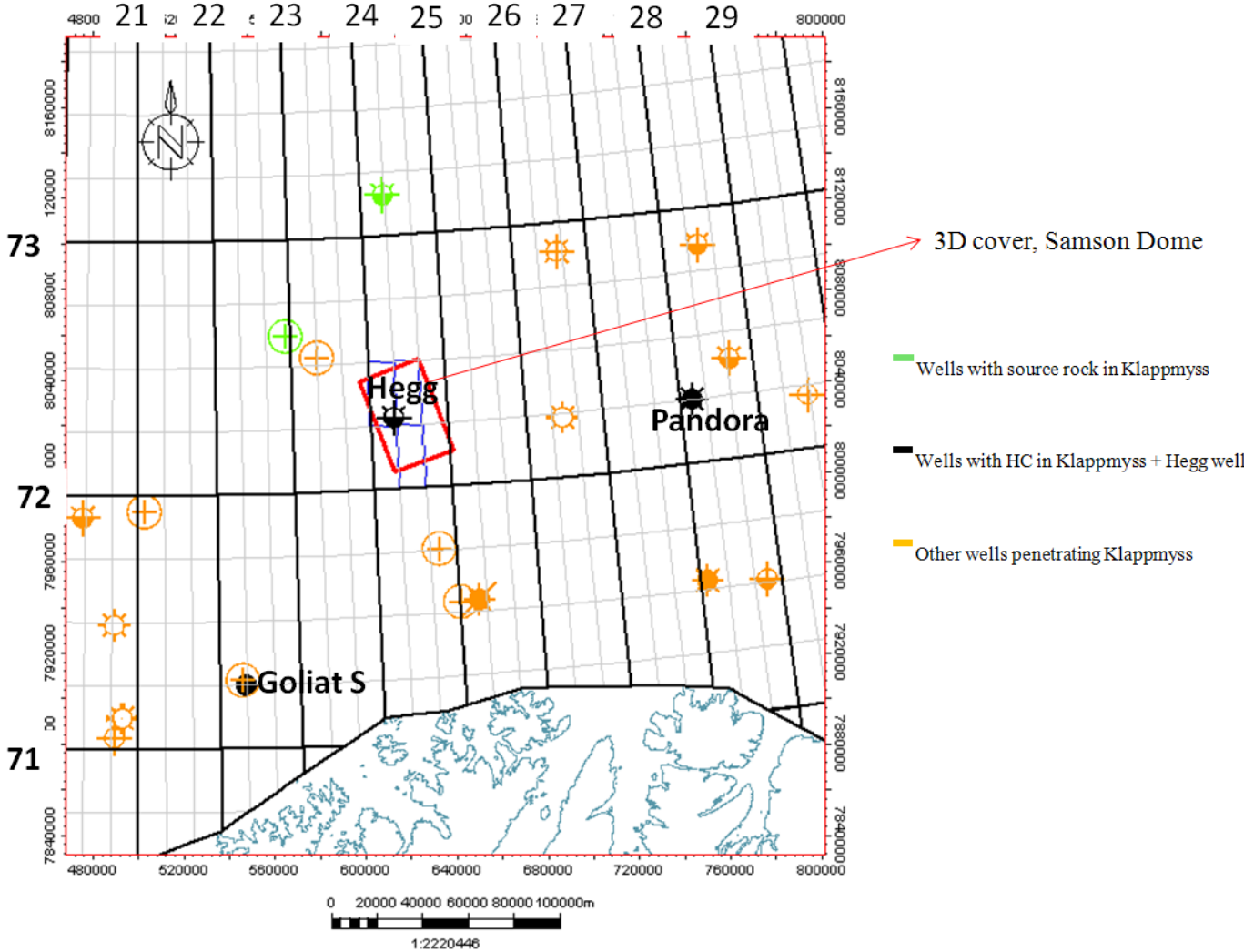

Figure 1 Map showing wells that penetrated the Klappmyss Fm. Area of project focus highlighted (3D seismic).Wells shown in green represent wells with source rock in the Klappmyss Fm., wells shown in black contained hydrocarbon or shows and will be further discussed in this paper. Wells displayed in orange are all other wells that penetrated the Klappmyss Fm. More information about these wells can be found in Appendix B.

Geological setting

The Barents Sea is situated on the northern margin of Eurasia. This large basin (figure 2) is located north of Norway and Russia on a passive continental margin (Dengo and Røssland, 1992). It is bounded to the west by the northeast Atlantic Ocean, east by the island Novaya Zemlya and northwest by the archipelago of Svalbard (figure 2). Its southern margin is defined by the Norwegian and Russian coastline following the Finnmark platform, the Timan Ridge and to the southeast by the Timan Pechora Platform (figure 2). The Barents Sea shelf comprises a history of rifting, thermal subsidence, inversion, uplift and erosion that have controlled the deposition of sediments since Early Palaeozoic (Faleide et. al., 1993). The major structural elements of the Barents were established already during Carboniferous or earlier but have been reactivated through time. This study has primary objective on the Klappmyss Formation (Early Triassic), therefore, the geological evolution up until the Triassic, will be described in detail. However, the Cenozoic geological history will be shortly described as well as this period may have affected the petroleum system, because of uplift and erosion.

Figure 2 showing the location of the Barents Sea, and the study area, after (www.worldatlas.com/aatlas/infopage/barents.gif).

Precambrian to Devonian

There is widespread agreement between several tectonic reconstructions that the Barents Sea shelf formed part of a passive margin extending from Baltica since Early Palaeozoic times (Ziegler, 1999, Worsley, 2006). The Caledonian Orogeny (400- 500 Ma) formed most of the regional basement during the collision between Laurentia and Baltica. This led to widespread deposition of thick continental clastic sediments (figure 3) between Late Silurian and Devonian times (Faleide et al., 1984; Glørstad- Clark et al., 2011).
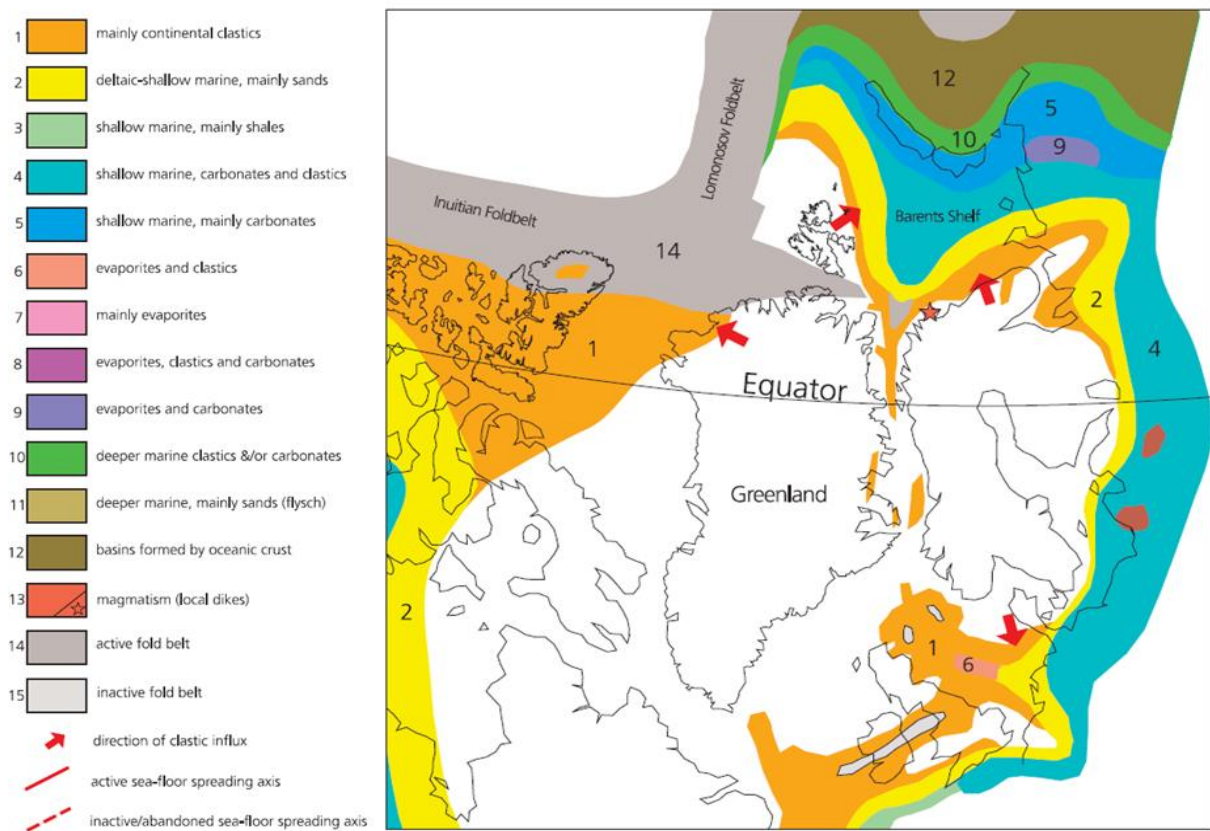
Figure 3 Devonian regional palaeogeography, modified after Torsvik et al., 2002

Carboniferous to Permian

Erosion of the Caledonian Orogeny led to the deposition of clastic sediments of alluvial fans and river plains into halfgrabens, formed during the initial phase of crustal extension (figure 4) between Greenland and Norway (Rønnevik, 1981, Worsley, 2006). This extension began in Early Carboniferous separating North Greenland, the Barents Sea shelf and Svalbard, and developed two linked rift systems. The Atlantic rift arm formed between Greenland and Norway (figure 4) and a continuous seaway opened between the Artic in north and the northwest European basins in the south (this seaway was closed during Triassic) (Stemmerik & Worsley, 2005).

Between the Carboniferous and the Permian the Barents Sea shelf was located around the equator and as the continent drifted northwards, the clastic deposition was followed by extensive post-rift carbonate platform deposition from late Carboniferous through Permian, as the Laurassia supercontinent drifted into subtropical latitudes (0°-30° N) (figure 4). Moreover, evaporate deposition occurred in local basins during lowstand (Worsley, 2006), that later formed diapirs (Stoupakova et al., 2011).
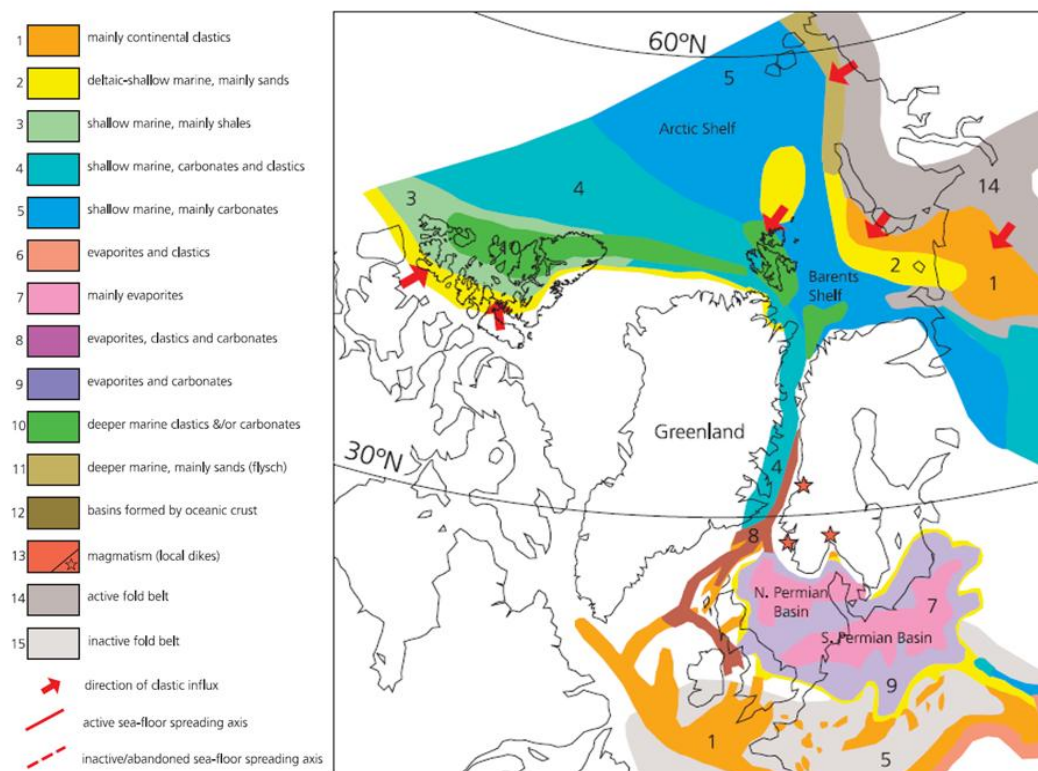

Figure 4 Permian regional palaeogeography, modified after Torsvik et al., 2002

Triassic

A significant extensional event marks the Late Permian –Early Triassic (Gudlaugsson et al., 1998, Johansen et al., 1994, Ziegler, 1988) contributing to Triassic subsidence as well as large amount of sediment influx. At this time the Barents was bordered by the Baltic continent to the south, the North American continent to the west, an open seaway to the northwest, and the developing Ural mountain (figure 5) to the east (Novaya Zemlya) (Glørstad- Clark et al ; 2011).

During the Triassic the Barents Sea was a wide, shallow, epicontinental seaway covering the continental shelf of north-western Eurasia, and the Triassic succession in the Barents shows a gradual infill of the basin prograding further west and northwest with time. Triassic deposits were mainly erosional products from Fennoscandia to the south and the Urals to the southeast, resulting in thick siliciclastic deposits both in the Norwegian and the Russian shelf. Sediment input from the Urals area is suggested by the plagioclase feldspar rich nature of the sands, this being linked with basaltic volcanism during the Lower and Middle Triassic (Bergan & Knarud, 1992). A provenance study by Mørk (1999) suggests three different source areas for the Triassic deposit (figure5), the Hammerfest Basin being sourced from the Caledonian orogeny, Svalbard from Greenland and the east Barents and Pechora from the Uralian mountains (figure 5). This conclusion is based on geochemical analyses and Sm-Nd ages, where Triassic samples from the Bjarmeland Platform and Nordkapp Basin show similar trends on Quartz-feldspar-lithics plots compared to Novaya Zemlya and Pechora Sea. Also the heavy mineral distribution show similarities, especially between the Bjarmeland Platform and Nordkapp Basin (Mørk, 1999).
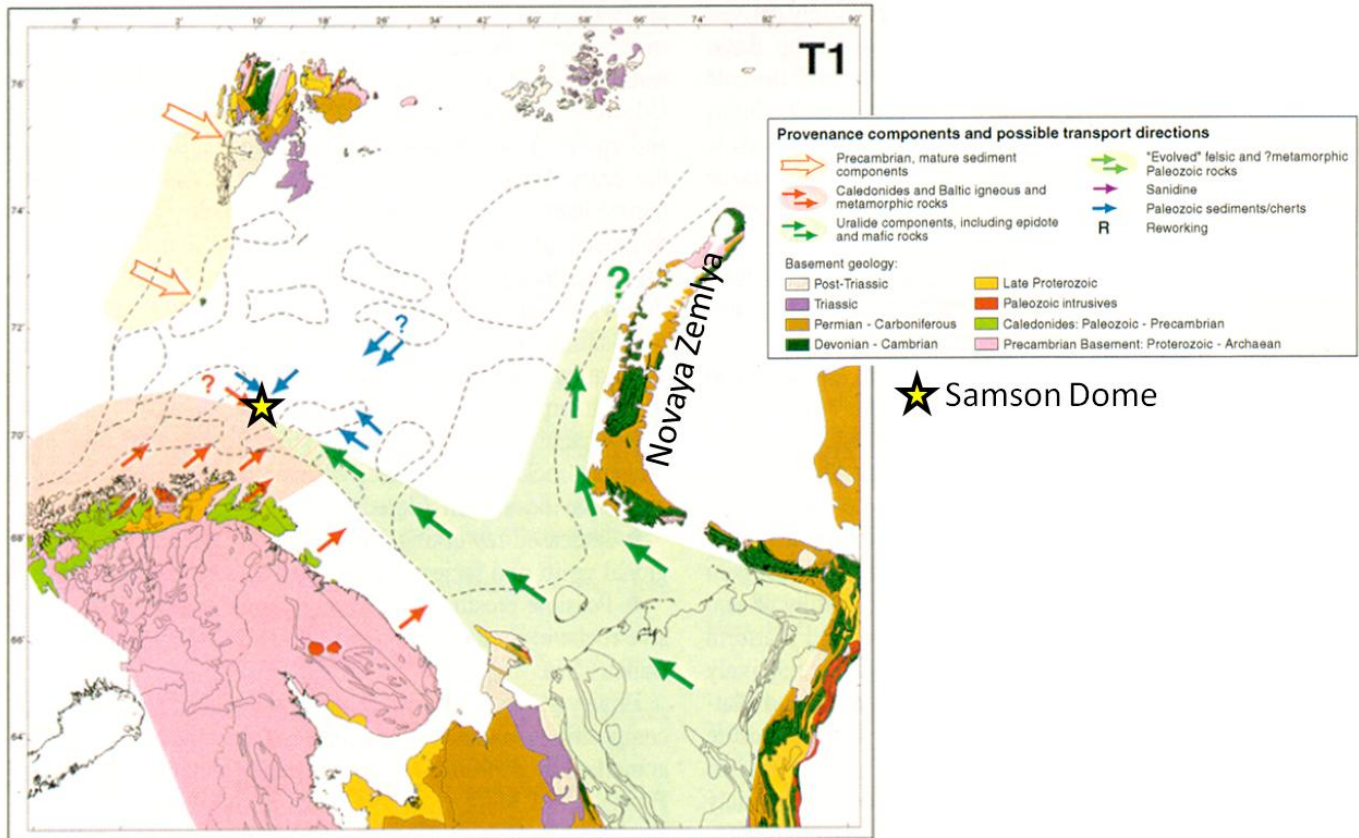
Figure 5 illustrating possible sediment transports during Early Triassic, after Mørk 1999.

Triassic was a relatively tectonic quiet period. However, the sedimentary succession was influenced by northwards drift and climate variation controlling the types of sediments (Glørstad-Clark et al., 2010).

The Early Triassic in the Barents Sea was dominated by prograding transgressive-regressive sequences. Glørstad-Clark`s study from 2011, illustrate the development of platform-margin deltas in Early Triassic in the Barents Sea. These were identified by mapping of clinoform geometries, clinoform angles and trajectories. Shelf/platform-margin deltas have got much attention from the oil industry related to the potential hydrocarbon reservoirs.

These reservoirs could be related to supply of sand to the deep sea, or storage of sand on the shelf edge itself (Porebski & Steel, 2002).These broad low-relief basins are strongly sensitive to changes in relative sea-level due to rapid emergence and submergence of wide areas, and to changes in position of major rivers supplying sand to the delta system (Glørstad- Clark et al., 2011).

The 3rd order sequence (Klappmyss Fm.) is dominated by a clinoform system prograding mainly from the Baltic Shield in the south toward an SSE-NNW direction (figure 6) (Glørstad- Clark et al ; 2011, Steel et al ; 2002).
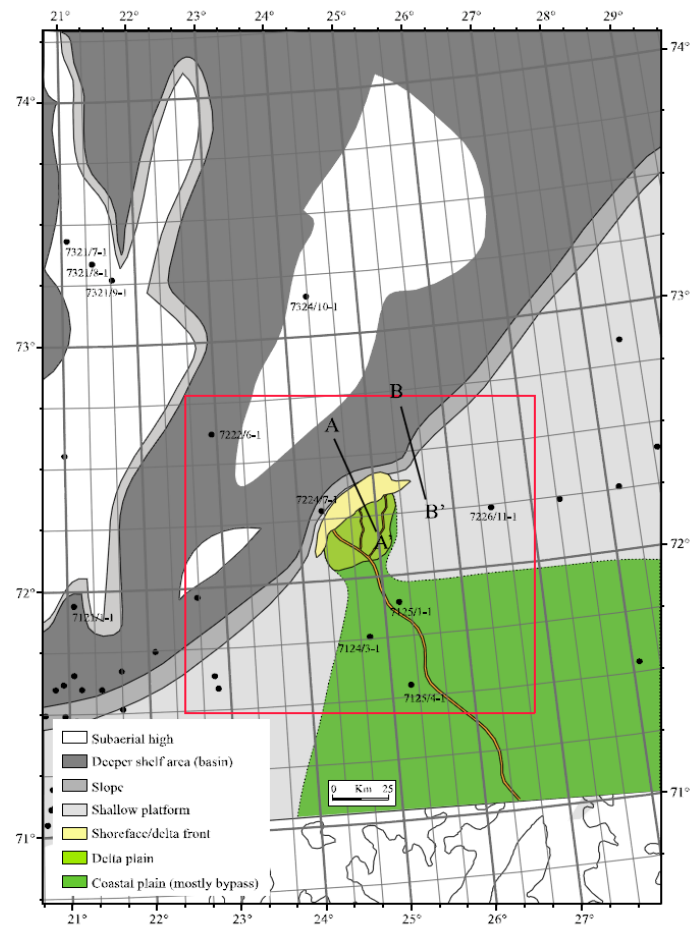

Figure 6 illustrating the prograding platform margin delta located close to the Hegg well, Samson Dome, after Glørstad-Clark et al., 2011.

The Triassic lithostratigraphy comprise the Fruholmen, Snadd, Kobbe, Klappmyss and Havert formations as seen in figure 7. The Klappmyss Fm. (Early Triassic), which is the formation of interest, consists mainly of medium to dark grey shale interbedded with silt and sandstone (where drilled) (www.npd.no).
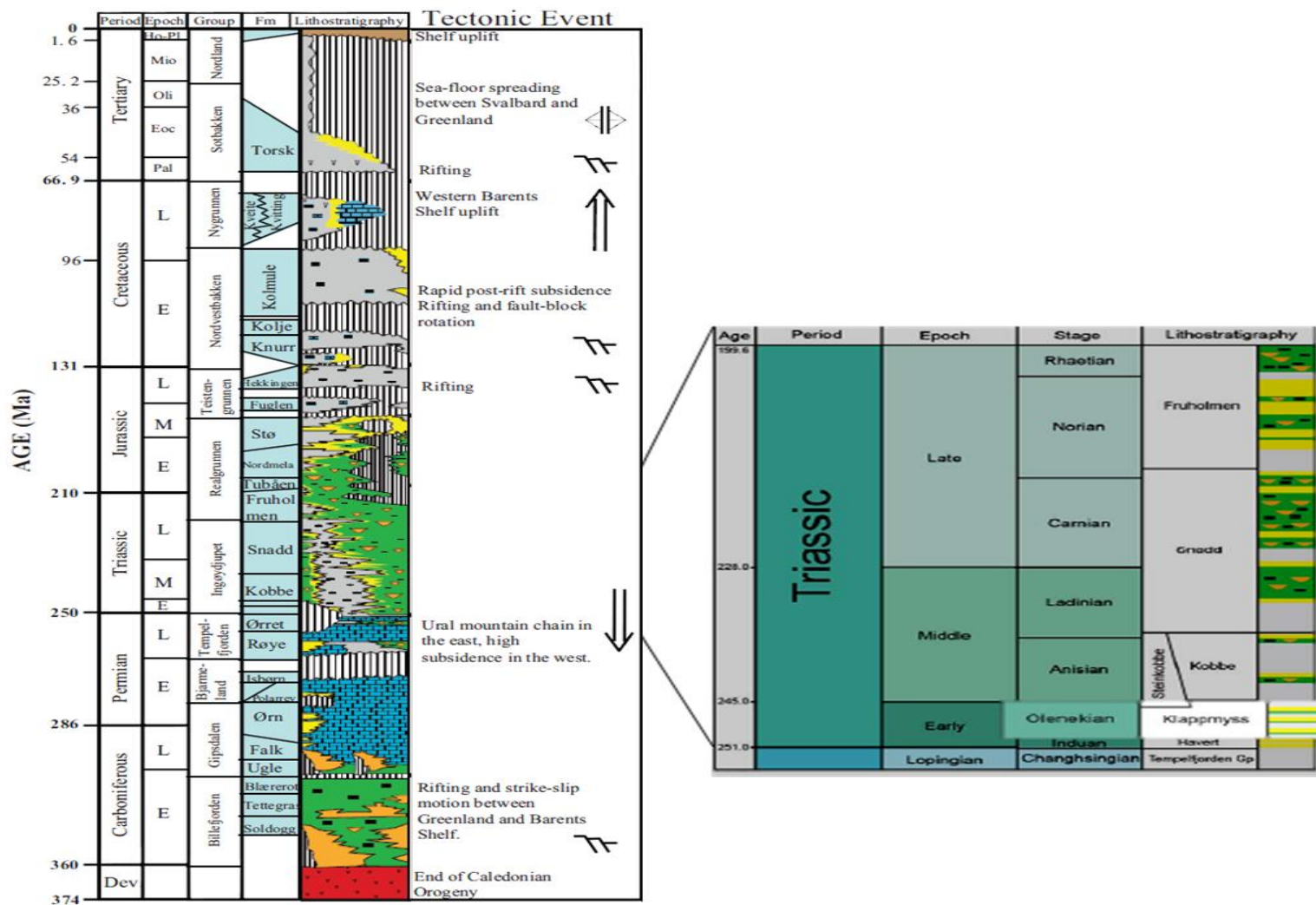
Figure 7: Lithostratigraphy in the Norwegian Barents Sea Triassic, lithostratigraphy is modified from Nøttvedt et al. (1993) while formation names are from Mørk et al. (1999).

Cenozoic

Tectonic activity during the Cenozoic was mainly related to progressive northward opening of the North Atlantic Oceeans (figure 8). This period also comprised deformation related to salt movement. Moreover, in the Neogene, most of the Barents Sea was uplifted and eroded, resulting in that most of Neogene is absent in the Barents Sea (Nøttvedt and Johannesen, 2008, Henriksen et al., 2011). Total erosion around the Bjarmelamd Platform area was about 1.5-2 km (Henriksen et al., 2011)..For some structures the removal of overburden has led to the leakage of hydrocarbon, causing the emptying of reservoirs or structures not being filled to spill point. Therefore, in most of the Barents Sea the reservoir quality at a particulary depth is generally lower than expected.
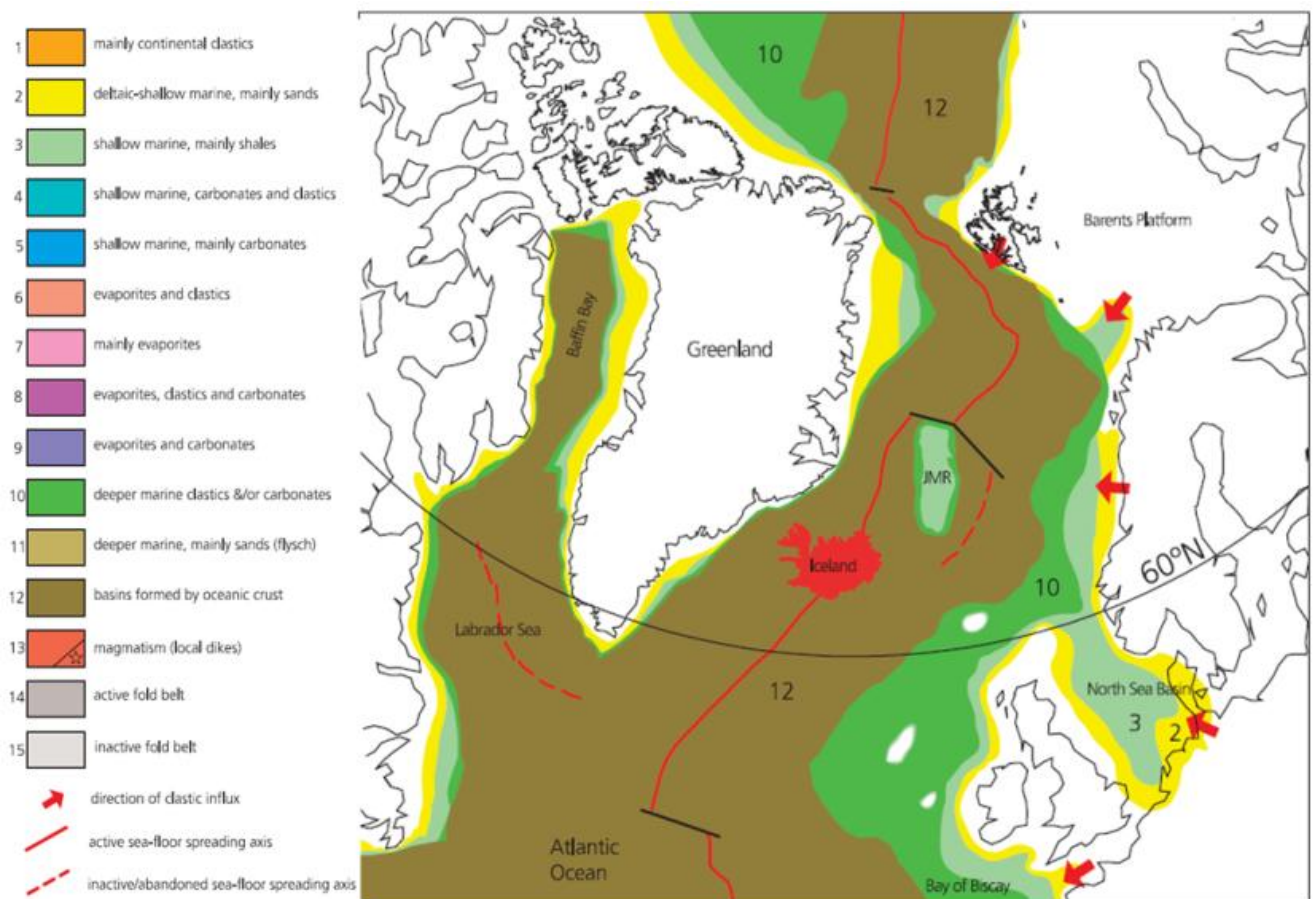

Figure 8 Cenozoic regional palaeogeography, modified after Torsvik et al., 2002.

13

Study area

The Samson Dome is a salt dome located within the Bjarmeland Platform (figure 9), bordered by the Loppa High to the west, Nordkapp Basin to south and Sørkapp and Bjørnøya Basins to the northwest (figure 9).
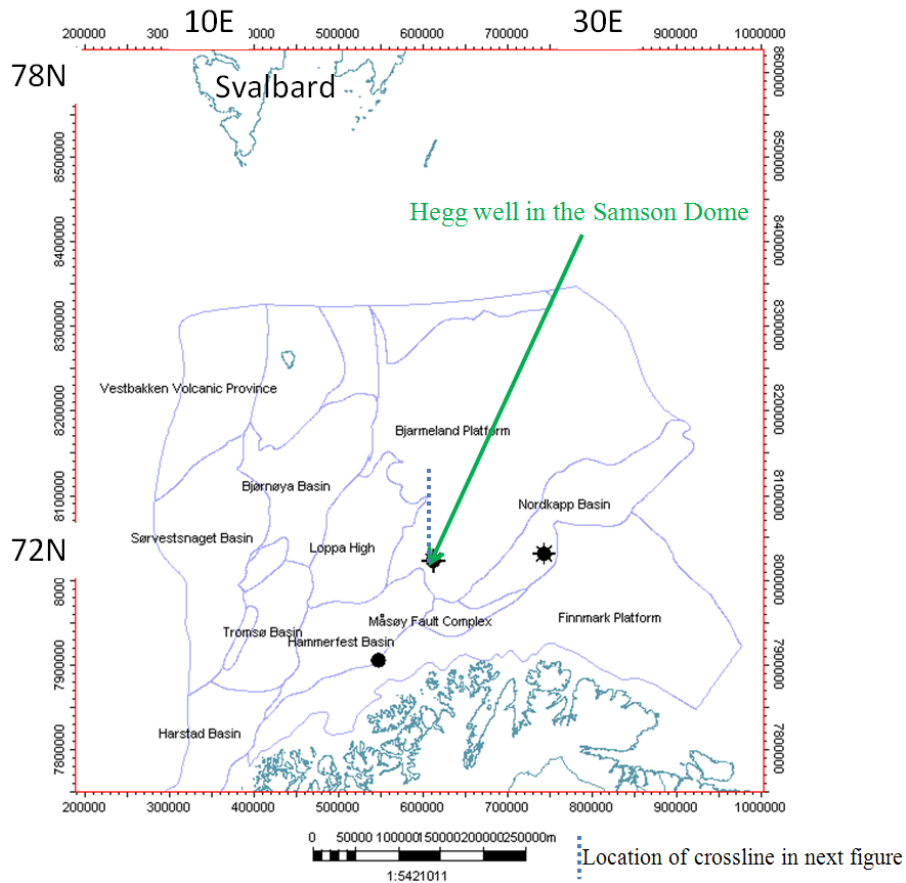
Figure 9 Regional structural elements of the Norwegian Barents Sea. Stippled line B (blue) shows the location of the seismic line in crossection below (figure 10).

Crossection of the dome can be seen in figure 10. Here the relatively thick Triassic deposit is underlain by Cretaceous rocks which thin out northwards. Note also the missing sections in Cenozoic times (figure 10) and the position of the salt.
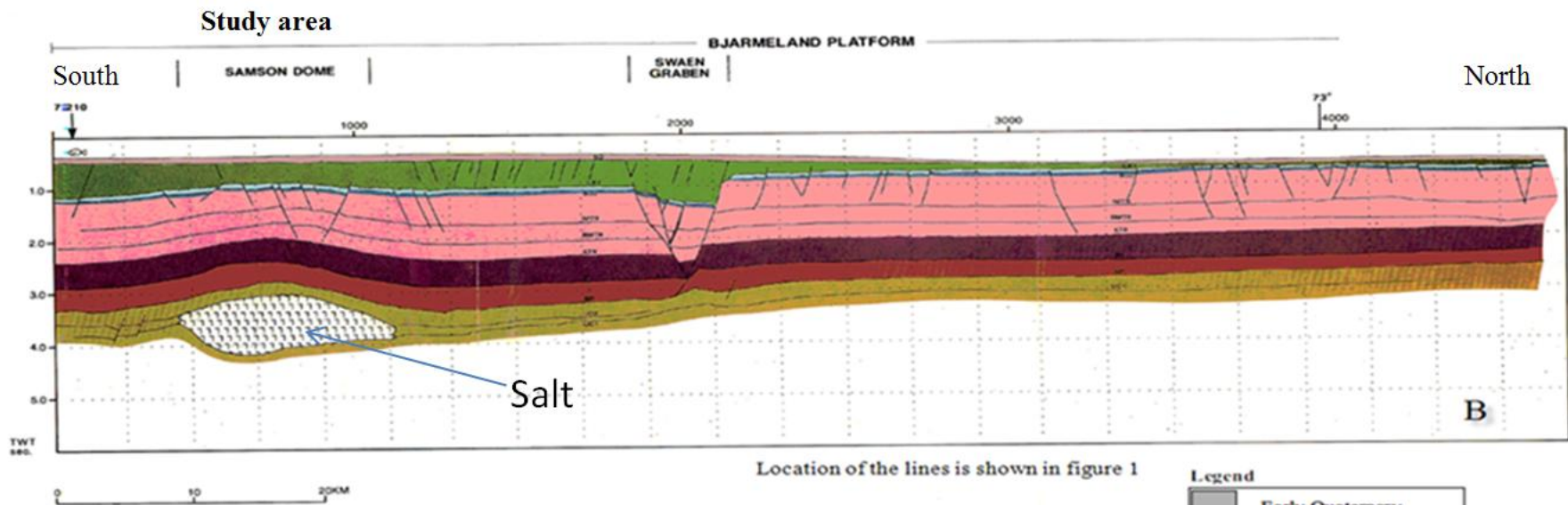
Cross section showing the Samson Dome and the Bjarmeland Platform, modified after Gabrielsen et al., 1990.

Figure 10 showing a crossection located north-south over the Samson Dome.

Database and methods

Three-Dimentional Seismic Data

A 3D seismic survey, bg1002, was used as the basis for the seismic interpretation (red square in figure 11). The data were acquired from CGGVeritas in October 2011. Moreover, the survey consists of about 1100 km^2, two-way traveltime data recorded to 5s and sampled at 4 ms. The data for this study were made available in a 16-bit display format which enables a detailed clinoform and amplitude analysis. For the lower Triassic interval, the dominant frequency is between 26 and 30 Hz, giving a minimum vertical resolution of 20 meters (see appendix A).

Conventional 3-D seismic data interpretation included the generation of synthetic seismograms using well logs to give correlations between seismic reflectors and well data. This synthetic was correlated with a wiggle representation of the seismic next to the well (Inline 1760) from the 3D survey (Appendix A). Also the caliper log was used to quality check the synthetic seismogram together with acoustic impedance to check consistency between AI versus the hard/ soft events seen on the real seismic lines. Seismic flattening on Top Havert was used to improve the seismic interpretation, as well as FS representing a flooding surface (timeline).

The quality of the data is mainly good, but due to salt and shallow gas, some areas are chaotic/masked and difficult to interpret. In Appendix A, table 1 list the name, year of acquisition and extent of survey.

Two-Dimentional Seismic Data

In addition, 2D seismic surveys covering approximately 24300 km^2 were interpreted to understand the regional geology on a much broader scale. Seismic quality was varying, where some lines had low frequency. As in the 3D data, salt affect the quality and also multiples are recognised in the seismic data. Appendix C, table 1 display the different surveys, year of acquisition and extent of survey. In addition, some comments on quality are included.

Seismic 2D/3D interpretation and map generation was carried out using the Petrel 2010 Interpretation software package.
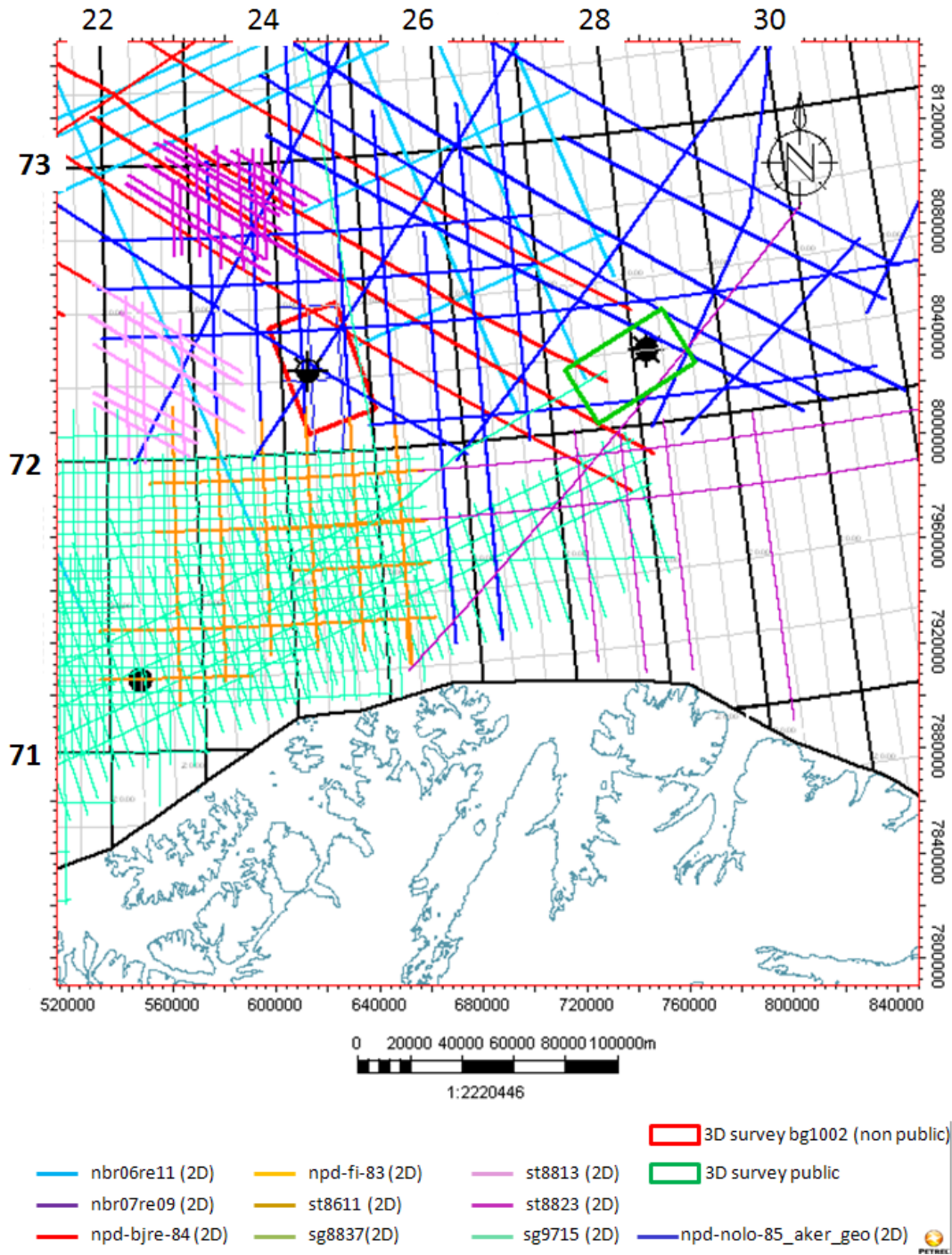

Figure 11: Basemap showing data coverage. Red square represents 3D non-public seismic over the Samson dome, while the green square represent public 3D seismic over the Pandora well. Other lines represent 2D seismic lines.

Well Data

Well data from 25 wells were considered (Appendix B) using the Norwegian Petroleum Directorate fact pages (www.npd.no). These wells penetrate the Klappmyss formation in the Barents Sea. As seen on figure 16, the wells are widely spaced and only well 7122/7-4S and 7228/7-1A have core information. However, even if the cores are more than 100km from the study area, they were incorporated in the study. Core descriptions for well 7122/7-4S were provided by Eni Norge and for well 7228/7-1A by Baker Huges Inteq. These descriptions were used to enhance age control and better define Triassic paleoenvironment.

The well tops from NPD were used as a basis for well log correlation.
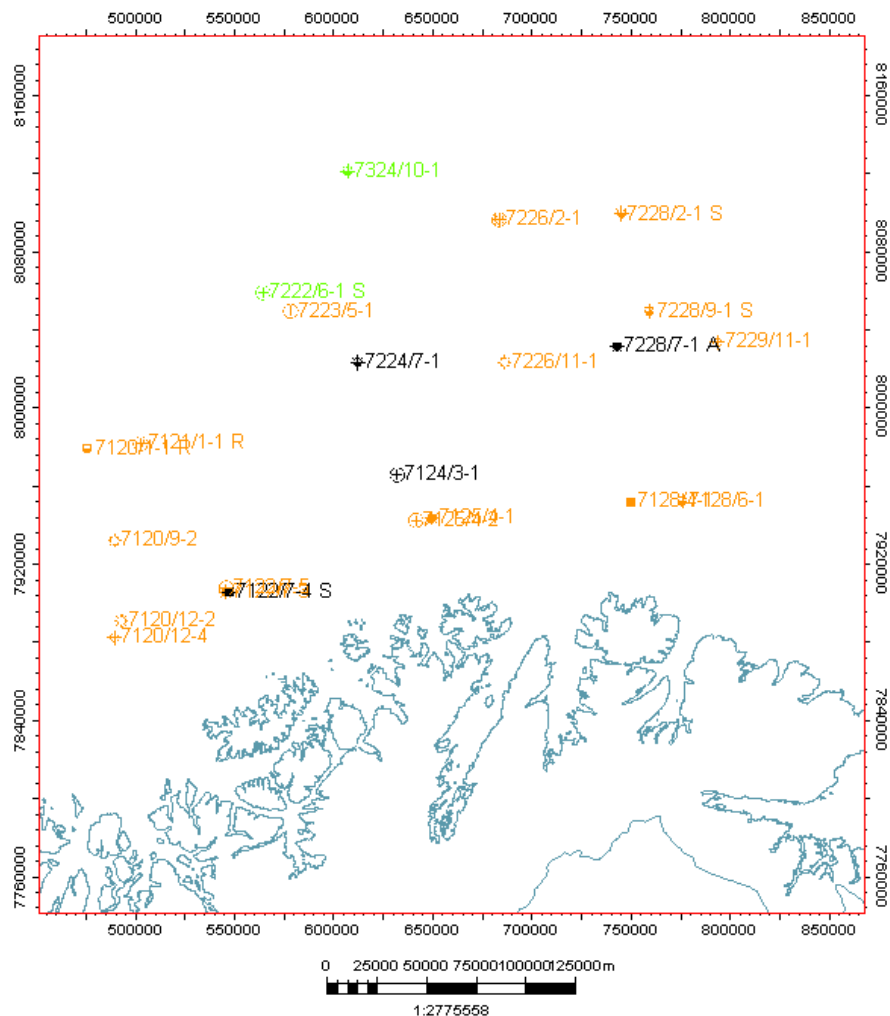

Figure 12, map showing wells penetrating Klappmyss Fm. Wells shown in green had source rock potentials while wells displayed in black had shows or discovery in Klappmyss Formation.

Study method

The overall goal in this study is to integrate seismic stratigraphy and studies in delta configuration to help predict facies distribution, grain size and thereby reservoir properties in the Klappmyss Fm.. Several steps will be followed in this study as seen in figure 13.
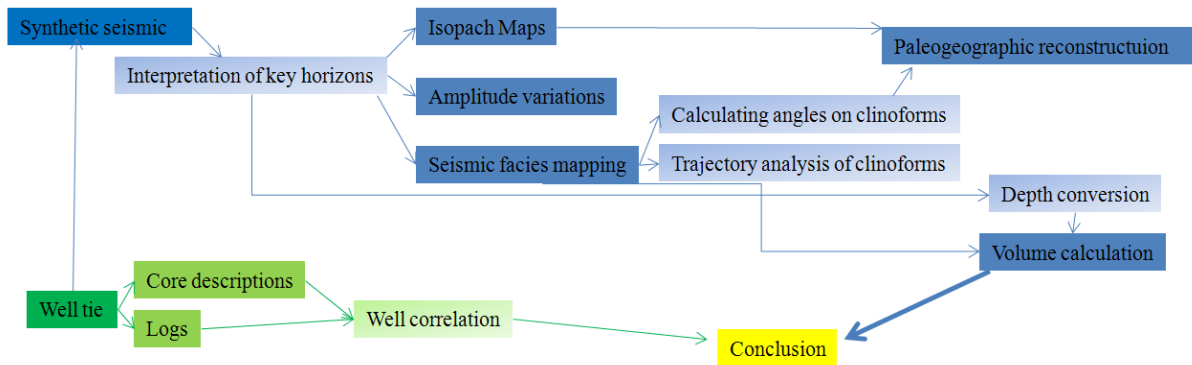

Figure 13 illustrating the different steps followed in this study

Synthetic seismogram were first generated by convolving the reflectivity derived from digitized acoustic and density logs with the wavelet derived from seismic data. Frequency was 28Hz (Appendix A).By comparing marker beds (lithogroups from www.npd.no) picked on well logs with major reflections on the seismic section. This tie helped improve the data interpretation. The acoustic log was calibrated with check-shots.

The marker Fuglen Fm. (late Jurassic age) was chosen because the reflector is very bright on the seismic and is easily traceable. By looking at the difference in depth between the seismic reflector and the well marker, the synthetic seismic was bulk-shifted 20ms. Photos from pre and post 20ms bulk-shifting (at Fuglen Fm. marker level) can be seen in Appendix. In addition, figure 14 and 15 shows the 20ms bulkshift on Klappmyss Fm. level. These figures illustrate the tie.
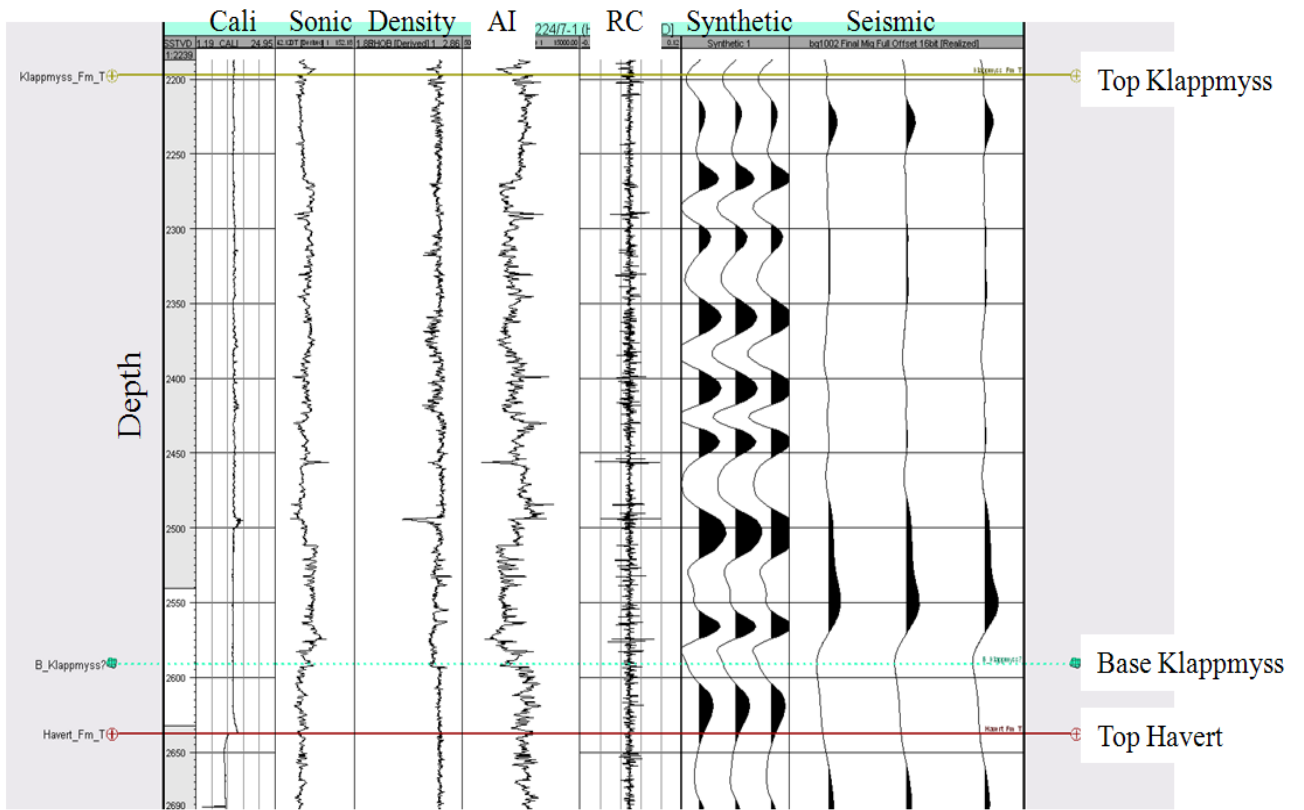
Figure 14 Snapshot of the created synthetic at Klappmyss level before bulkshift.
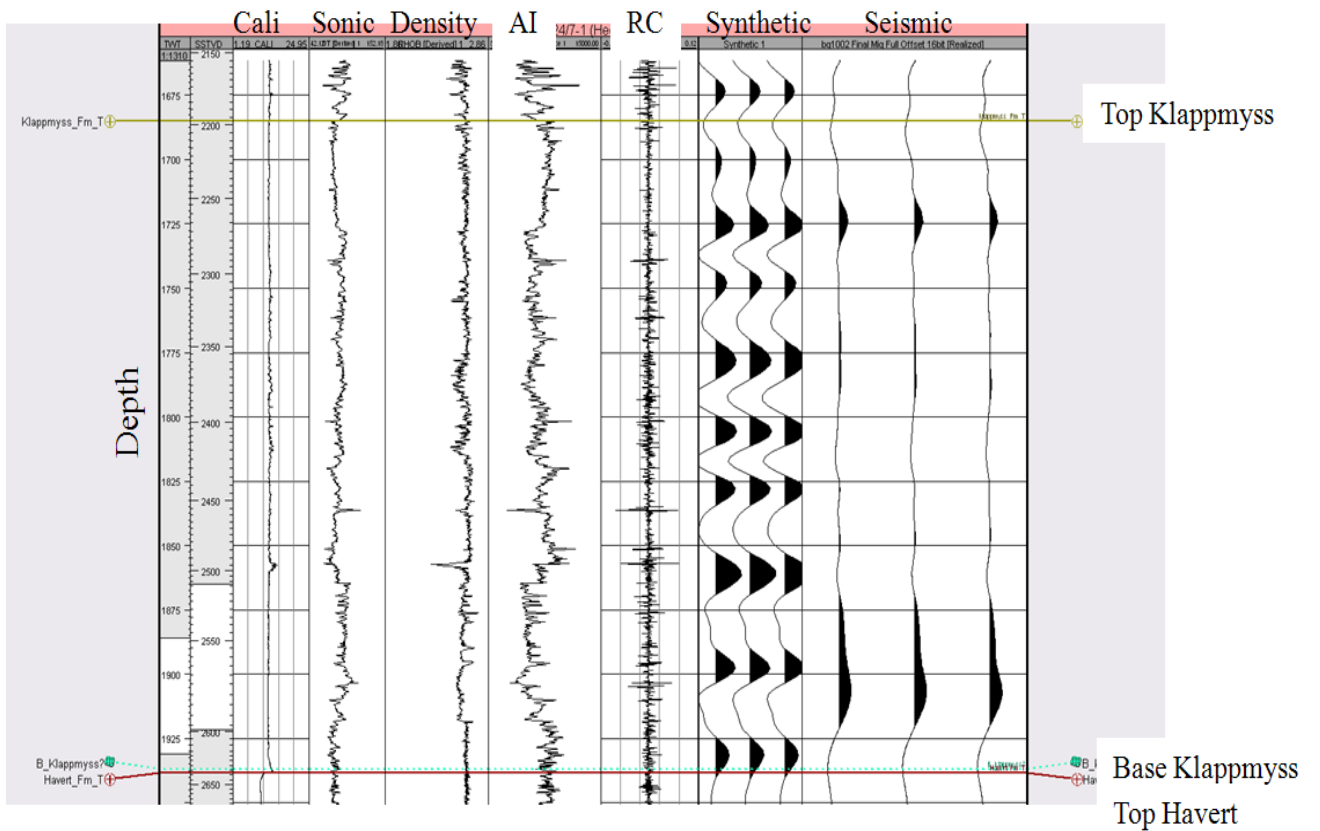

Figure 15 After bulkshift 20ms

Conventional seismic interpretation was preformed by picking and tracking laterally consistent seismic reflectors for the purpose of mapping geological structures, stratigraphy and reservoir architecture. Isopach maps were generatred and seismic facies was mapped in order to see changes in thickness and contribute in interpreting energy environment (oblique/ sigmoidal). In addition, the shape of the prograding clinoforms was analysed based on angles (in order to predict sediment grain size), and clinoform trajectories (to better predict lithology and storage of sediments). To improve the recognition of shelf edge trajectory trends and improve interpretation, seismic cross sections were flattened on maximum flooding surfaces which represent time lines.

Decompaction of clinoforms was preformed to get real geometries at the time the progradation and development of the platform edge delta took place. In order to achieve this also depth conversion was needed. Depth conversion was also later used when calculating reservoir volumes.

A preliminary volume calculation were performed to enable an insight into the economic aspect of the study which could contribute to a higher probability for making a good decision on the commercial value on this potential prospect.

Logs (GR, Caliper , Resistivity, Sonic and Density-Neutron) contributed to better prediction/interpretation of sediment lithology, and understanding of the hydrocarbon distribution. In addition, correlation between relevant wells was preformed using flooding surfaces and stacking pattern.

Stratigraphic considerations

Seismic stratigraphy is a technique for interpreting strata information from seismic data and reconstructing the paleogeography (Vail et al., 1977). This technique fills the gap between sedimentology, basin analysis, and the various types of conventional stratigraphy which can be used in the exploration of oil and gas (Catuneanu et al., 2002). The term "Clinoform" was originally introduced to describe the shape of a depositional surface at the scale of the entire continental margin.

In current literature, this term denotes strata packages with oblique internal layering, best imaged on seismic reflection profiles where three geometric elements are recognised: "topset" (figure 17), the most shallow and low angle area, "foreset" (figure 17) the central and steepest area and "bottomset", the flat area farther basinward (figure 17) (Catuneanu et al., 2002). Further, Sangree and Windmier (1977) defined the shape of the clinoforms either sigmoid or oblique (figure 12). Sigmoid (figure 16) is characterized by aggradational topsets and gradual increase in slope from the topset to the foreset, and is often interpreted to represent low energy environment. In contrast, oblique clinoforms (figure 16) has abrupt change in slope from topset to foreset and topset with little or no aggradation and is thought to represent high energy environment. These can also be complex as seen in figure 16.
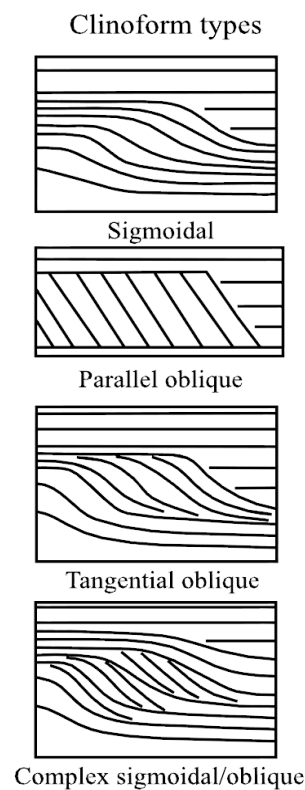
Figure 16 cartoons illustrating the different clinoform types, after Sangree and Windmier (1977).

Moreover, these two shapes may occur in the same progradational system, which then reflect changes in relative sea level rate and the interplay with sediment supply rate (Brown, 1996). However, there are still uncertainties in the quantification of the factors influencing the different shapes (Pirmez et al., 1998).

The shape of the clinoforms basinward dipping profile is affected by relative sea level, subsidence, eustasy, sediment supply, depositional regime and sediment type.

In addition, the shape is thought to indicate different depositional environments (Pirmez et al., 1998). Also, in a depositional, dip-oriented profile the successive positions of the shoreline along delta and shoreface-scale clinoforms, in a stratigraphic succession allow identification of the shoreline trajectory (Helland-Hansen & Gjelberg, 1994).

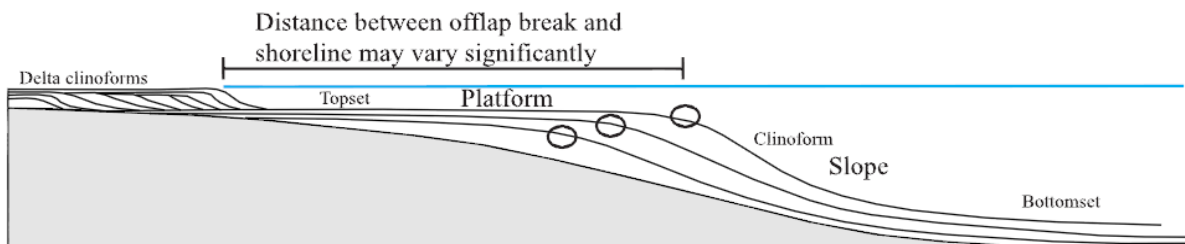Figure 17,showing geometric elements, modified from Emery and Myers (1996)

Trends between shelf-edge trajectories (figure 18) and depositional environments may be used to predict lithology in areas with few wells or limited seismic control (Bullimore, 2005). During normal regression a dominance of the rate of sediment supply over the rate of sea level rise results in rapid progradation, a low amount of accommodation space in the topset and the prediction of fluvially influenced/ dominated delta front sandstones and thin channel and floodplain deposits in the lower coastal plain area (indicated by low angle positive trajectories). A higher positive angle on the trajectories (A in figure 18) suggests a closer balance between rates of sediment supply and relative sea level rise. This results in more accommodation space in the coastal plain area. On the other hand, negative trajectories (C in figure 18) are associated with bypass and erosion in the topset and foreset areas. However, not all negative trajectories have basin floor fan deposits. In addition, low angle negative or flat (B in figure 18) trajectories represent a situation where a lack of incision at the shelf –slope break could result in storage of all sediment on the slope, and a lack of basin floor fan deposits can be predicted. Several studies like Plink-Bjørklund et al. (2001), Steel et al. (2000) and Bullimore (2005) seem to confirm this observation. Moreover, shoreface sandstones associated with low angle negative trajectories often will be thin and with poor reservoir quality due to slumping. The best reservoir sand associated in this type of environment will be at the maximum basinward extent of the shelf edge.

Here a flattening of the shelf-edge trajectory prior to the sea level rise will allow thicker sand deposits to accumulate. Nevertheless, slumping could still impede reservoir thickness and preservation (Bullimore, 2005) resulting in poor reservoir quality.
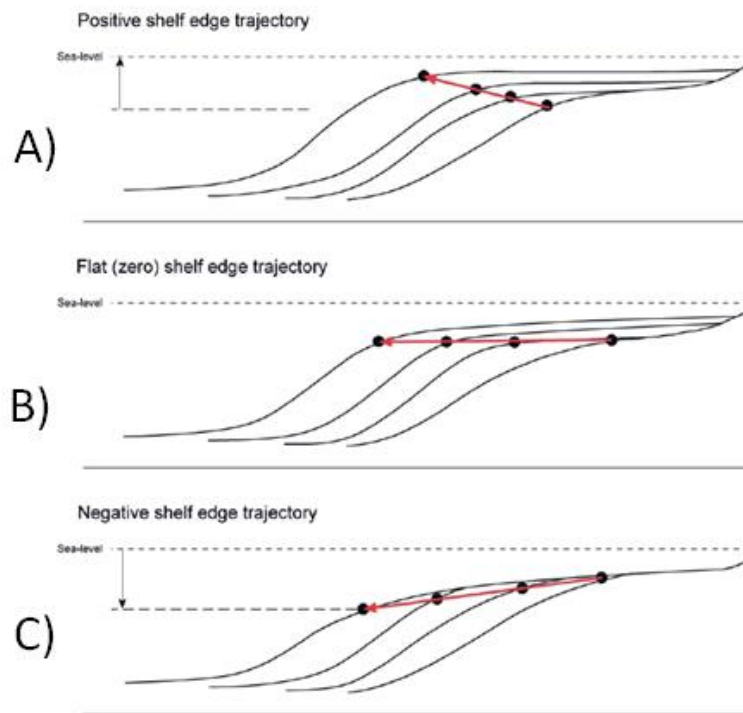
Figure 18 illustrating the different clinoform trajectories, modified after Steel & Olsen 2002.

Pirmez et al. (1998) modelling of clinoforms showed that increasing grain size results in steeper clinoforms with more abrupt rollover. In addition, larger grain size resulted in narrower sedimentation rate profiles with deposition mainly on the upper foreset.

Below follows a table (table 1) summarizing different authors opinions about clinoforms and relation to depositional environment and sediment grain size.

Author	Year	Angles	Sediment accumulation	Clinoform shape	Other
Brown	1996			Concave slope morphology -not disturbed by the interference -strongly prograding system	
Morton & Suter	1996			Strongly prograding - associated with coarse grained sediment	
Pirmez et al.	1998	Higher angle- coarser grains	Shallow water: sediment bypass topset region	Shape indicate different depositional environment	
			Incresing water depth: deposition at foreset, sediment. Pattern prograding		
Adams & Schlager	2000			Sigmoidal shape -interference between wave dominated shelf transport and gravity driven slope transport	
Plink-Bjørklund & Steel	2002			Flat/negative trajectories are associated with more fluvially dominated dep. systems	
				Positive trajectories are associated with wave dominated processes.	
Steel & Olsen	2002			Shelf edge trajectories are influenced by rates of sediment supply and changes of relative sea level	
Steel & Proebski	2003		2 types of shelf margin deltas with different sediment accumulation		
Deibert et al.	2003		Delivery of sand to shelf edge -no guarantee of delivery to deep water		
			Evidence of sand on the basin floor -channels on shelf edge or submarine fans		
Galloway	2004				Muddy rivers typically create fluvial or tide dominated delta, while sand rich rivers are fluvial or wave dominated
Bullimore et al.	2005			Low angle descending trajectories -no effective bypass of sediments to deep marine	
				Sigmoidal/ Oblique clinoform shapes associated with different energy levels -	The youngest clinothems deposited in a progradational succession are typically eroded and onlapped by deep water facies
				nowadays more complicated and related to accomodation rates	
				Obligue progradation - commonly associated with deltaic progradation. Consequence: commonly composed of silisiclastic with high sand content	
				Slope controlled by the rate of progradation, water depth and composition of sediments	
Henriksen et al.	2010			Flat/ descending trajectories -fluvial dominated	
				Aggradational/ positive trajectories -wave dominated	
Evy G-Clark	2011	Higher angle - coarser grain			Protruding shape- fluvially dominated

Table 1: Summary table regarding clinoform interpretation

Klappmyss Fm. stratigraphy

As previous mentioned Glørstad-Clark et al. (2011) interpreted the prograding clinoforms observed in early Triassic to be platform-margin deltas. The Klappmyss Formation is penetrated at the toe of one of these clinoforms in the Hegg well (figure 19) located on the Samson Dome, and this well will therefore have main focus. As mentioned previously the Klappmyss Fm. has had little attention regarding exploration potentials and is only penetrated by 25 wells in total (Appendix B) where one as the primary target (well 7228/9-1S). This well showed no gas shows in Klappmyss Fm.

Nevertheless, as highlighted in figure 19, both the Bamse and the Hegg well had good shows. However, since there is no core from Bamse, this well will not be further discussed. Both well 7122/7-4S (Goliat S) and Pandora (7228/7-1A) has core from the Klappmyss Fm, and will be further mentioned in this paper. Moreover, the Goliat S well had a 32m thick oilzone in Klappmyss Fm., while Pandora had gas (estimated volume of $4*10^9Sm^3$ recoverable gas). Figure 19 shows the location of these wells.
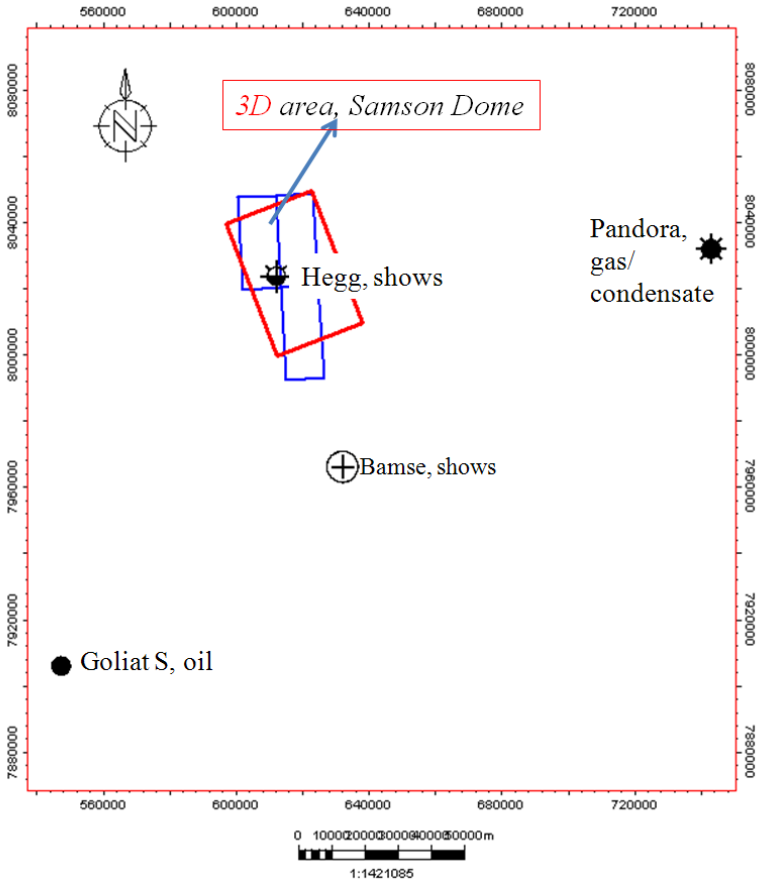

Figure 19 illustrating the location of four wells of interest and the 3d seismic cover.

I believe it is also worth mentioning that Russian wells have successively drilled the Klappmyss formation with oil and gas discoveries in well Krestovaya and Admiraltskaya located east of Bjarmeland platform (see figure 20). However, logs or more specific information about these fields are limited. In addition, as seen on map in figure 20, several other Triassic discoveries have been found on the Russian side of Barents. Kildinskaya Severnaya 82 and Murmanskaya 22 both had the discovery in Upper Triassic sandstones, a common reservoir in the Norwegian Barents (personal communication with A.Stoupakova), nevertheless the other Triassic discoveries closer to Bjarmeland platform remains unknown whether the discovery is in the Kobbe, Klappmyss or Havert Formation.
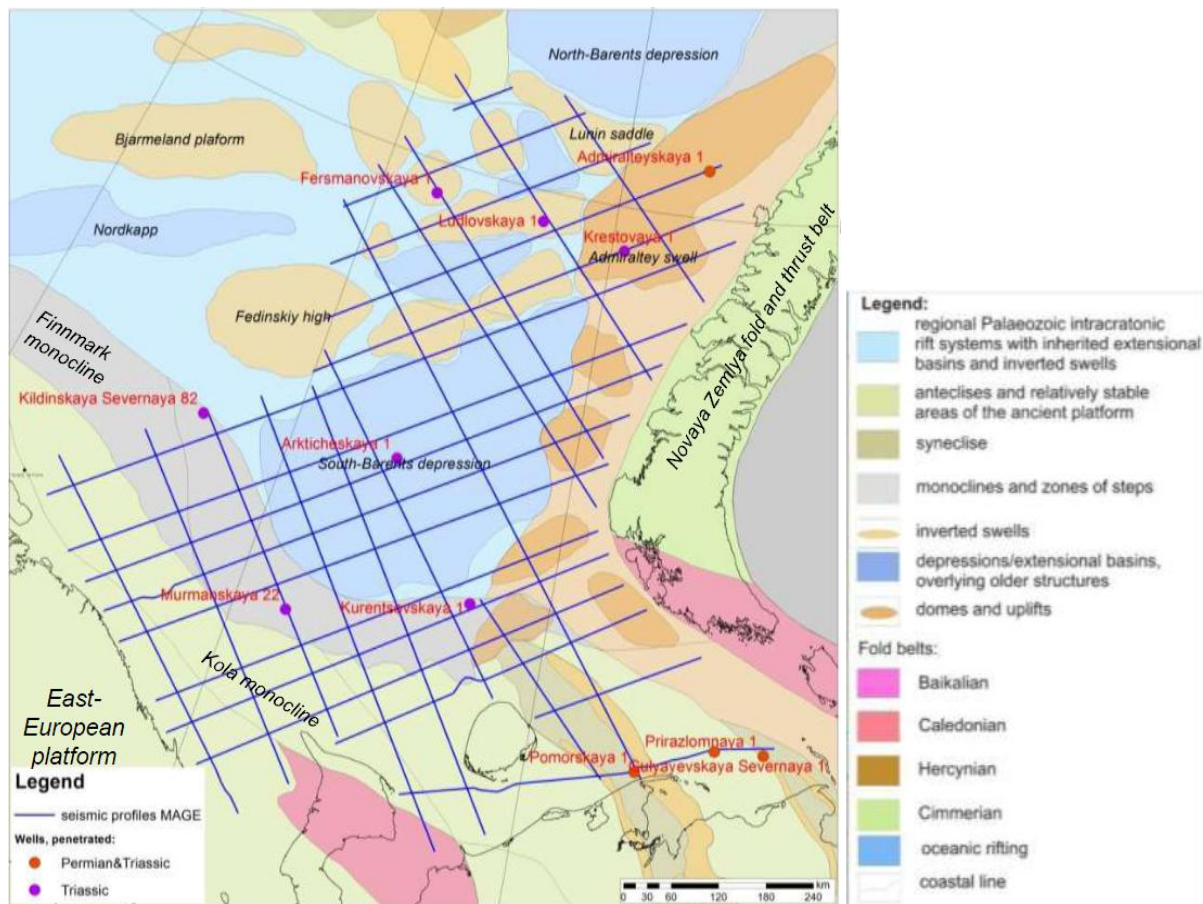

Figure 20 showing location of the Russian wells compared to the Bjarmeland Platform and the focus area in this study, after Stoupakova, 2011.

Observations

Logs from the Hegg, Goliat S and Pandora wells will be evaluated where main attention will be given to the Hegg well. Moreover, seismic character and clinoform observations will be highlighted mainly within the focus area (lower Klappmyss). In addition, some regional lines will be shown to illustrate the main pattern of the Klappmyss Fm. unit.

Figure 21 shows the location of the wells, while figure 22 shows the seismic to log relationship between these three wells. Note that the wells are widely spaced and affected by salt in the image.

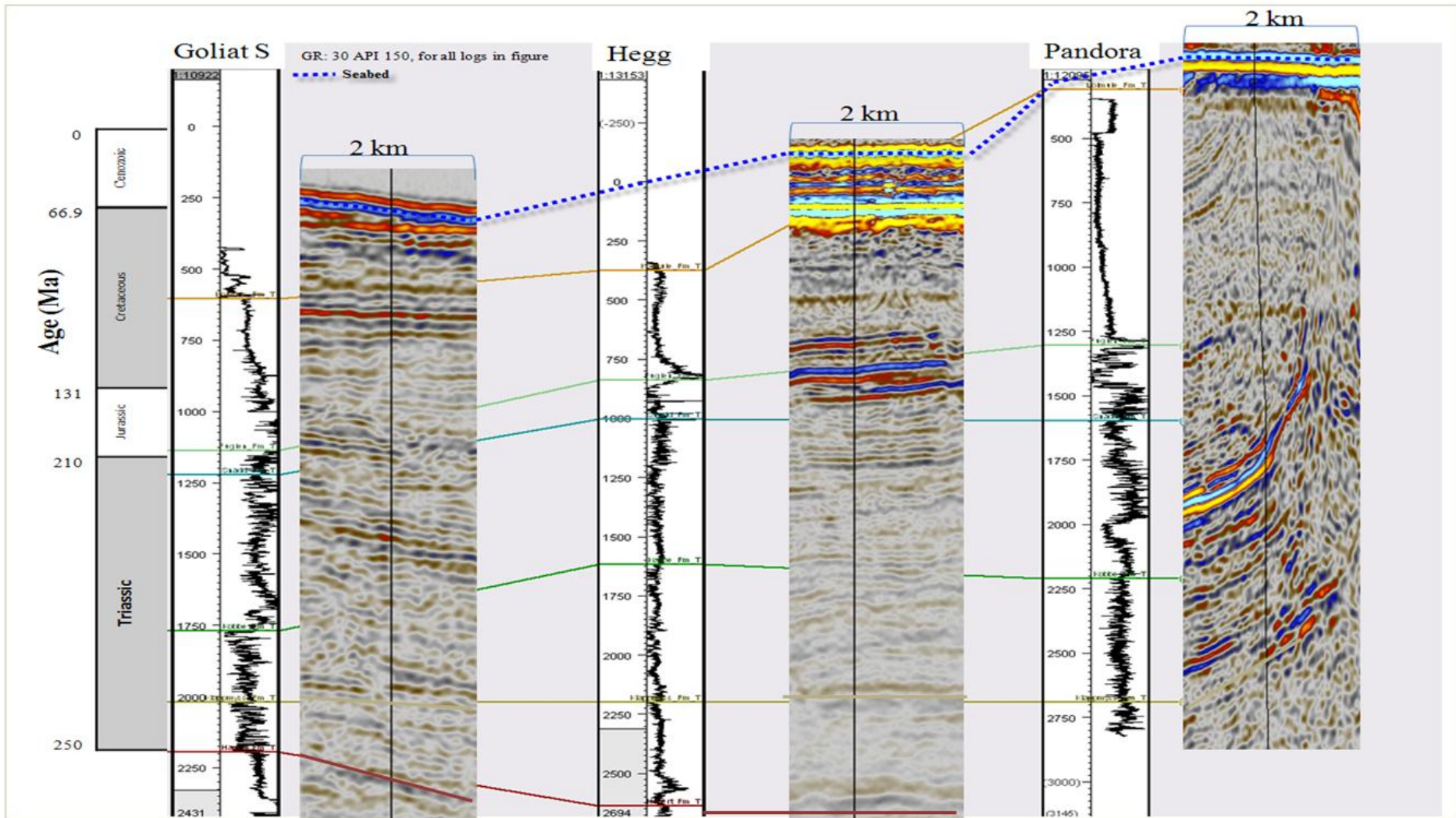Figure 21 illustrating the different Basins/Platforms in the Barents Sea and the 3 well locations.

Figure 22 showing seismic to well relation between the 3 wells in focus. Same GR range in all wells.

Pandora (7228/7-1A)

The main objective of this well, drilled in 2001 was to test the hydrocarbon potential of Upper and Middle Triassic sandstones. The Klappmyss interval was encountered at 2741m (MD) and drilled for 140m without entering the below lying Havert Formation. The core was taken at 2836 m depth and is 28m thick (http://factpages.npd.no/factpages/Default.aspx?culture=en).

Figure 23 shows core photos and logs from the Pandora well. Dominant lithology is mudstone and siltstone but with some beds consisting of very fine sandstone. In addition a single bed of 0.1cm mudclast with coarse grain size occurs. Horizontal lamination and ripples in lenticular bedding is observed as well as a wide diversity of trace fossils. Based on the amount of trace fossils this is interpreted as a fully marine environment (Distal bay), where the lenticular ripples indicate a quiet depositional environment. Overall reservoir quality in Pandora is low (less than 15% porosity and 0.1mD permeability), and the well was permanently abandoned in 2001 as a discovery (http://factpages.npd.no/factpages/Default.aspx?culture=en). Location of the well can be seen in figure 21.

GR in the Pandora well is in the interval 65-116 API (figure 24). This well shows higher average GR compared to the Hegg well (figure 26), which could indicate that the Hegg well is more sand prone in general. In addition, the gamma ray seems funnel shaped especially at the lower part of the log indicating coarsening upward cycles (regression). Moreover, Pandora has some short intervals with drastically change in density/neutron (figure 24). The caliper log is in gauge (figure 24), indicating stability in the borehole and no washout or mud-cake development, which means that instability, has not affected the logs.
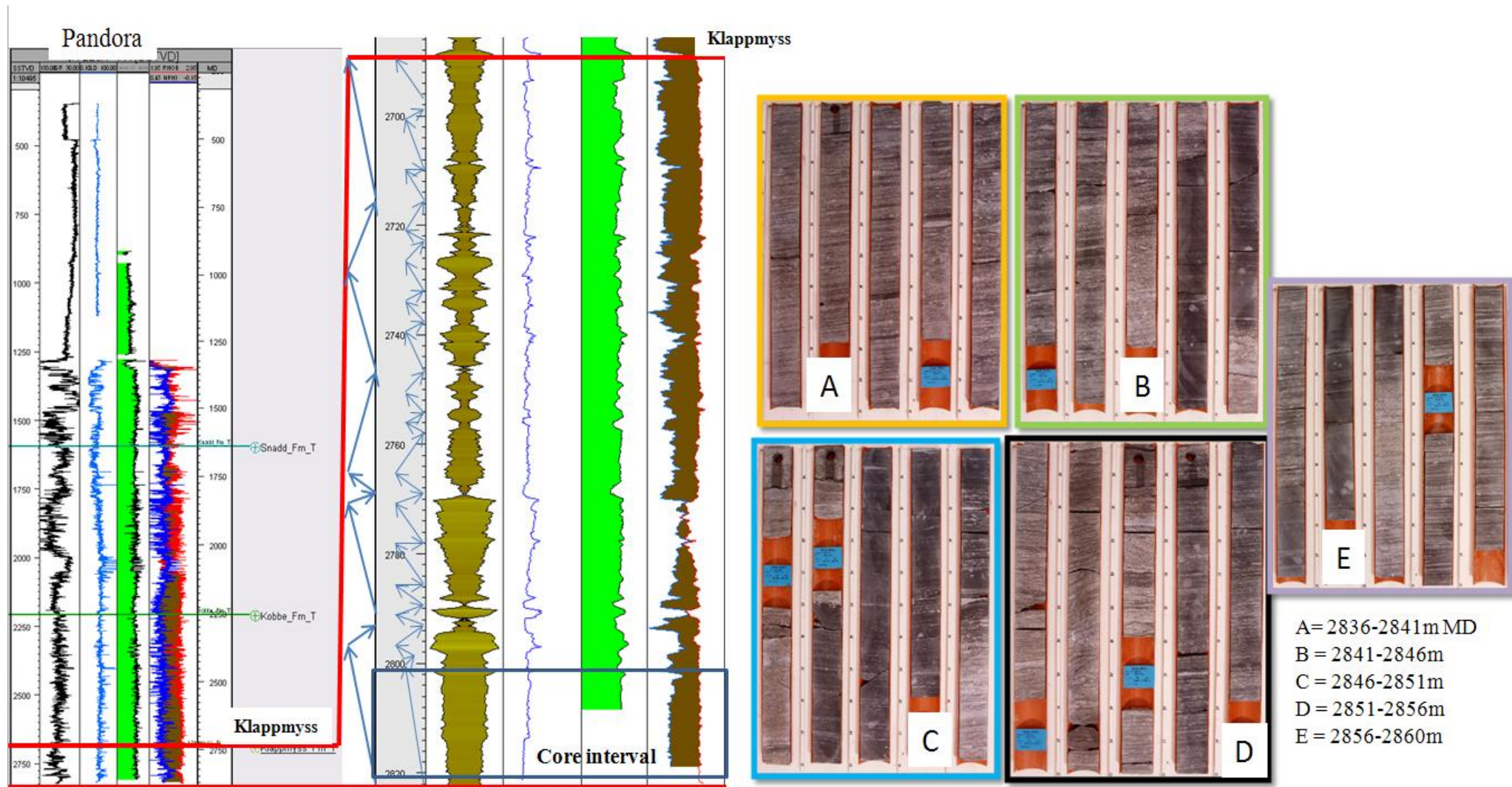
.

Figure 23 showing logs for the Pandora well as well as core photos.

Goliat S (7122/7-4S)

The Goliat S well was drilled in 2006 and were the fourth appraisal well on the Goliat discovery. Main objective were to prove OWC and confirm oil and gas in Triassic. The Klappmyss Fm. was penetrated at 2042 m depth and the interval is 175 m thick. Oil was discovered at several intervals in Klappmyss Fm (http://factpages.npd.no/factpages/Default.aspx?culture=en).

The 11.42m thick core from the Goliat S well is seen in figure 25. This core consist of coarse to fine sandstone at the top (2052-2055.3m) interbedded with massive, well sorted shale clasts interpreted to represent a tidal channel. The next interval from 2055.3 to 2059.6 m consists of a fining upward pattern, where 2.6m thick sandstone is observed interpreted to represent a tidal bar. In addition, medium scale cross-bedding and mud couplets is described indicating tidal reworking. This interval also shows high amount of plant fragments. The lowermost part going from 2059.6 – 2063.4m consist of fine grained thin bedded greenish siltstone alternating with thin beds of very fine sandstone. Also here ripple marks occur and this interval is interpreted as a tidal mud flat. Opposite to the Pandora well, Goliat S has several intervals with good permeability, where average permeability for samples with more than 20% porosity are 230mD (Appendix). Goliat S is planned to start producing at the end of 2013. Location of the well can be found in figure 21.

Gamma ray values in the Goliat S well lies between 60-110 API (figure 24). Moreover, the GR pattern has a blockier signature in Klappmyss indicating aggradation. Compared to the Pandora well, Goliat S seems more sand prone (lower GR and more blocky). But as in the Pandora well, Goliat S shows a drastically change in the density/neutron log. Several minor crossovers and a thick interval with low neutron/ high density are observed (figure 24). Also this well has caliper log on gauge.
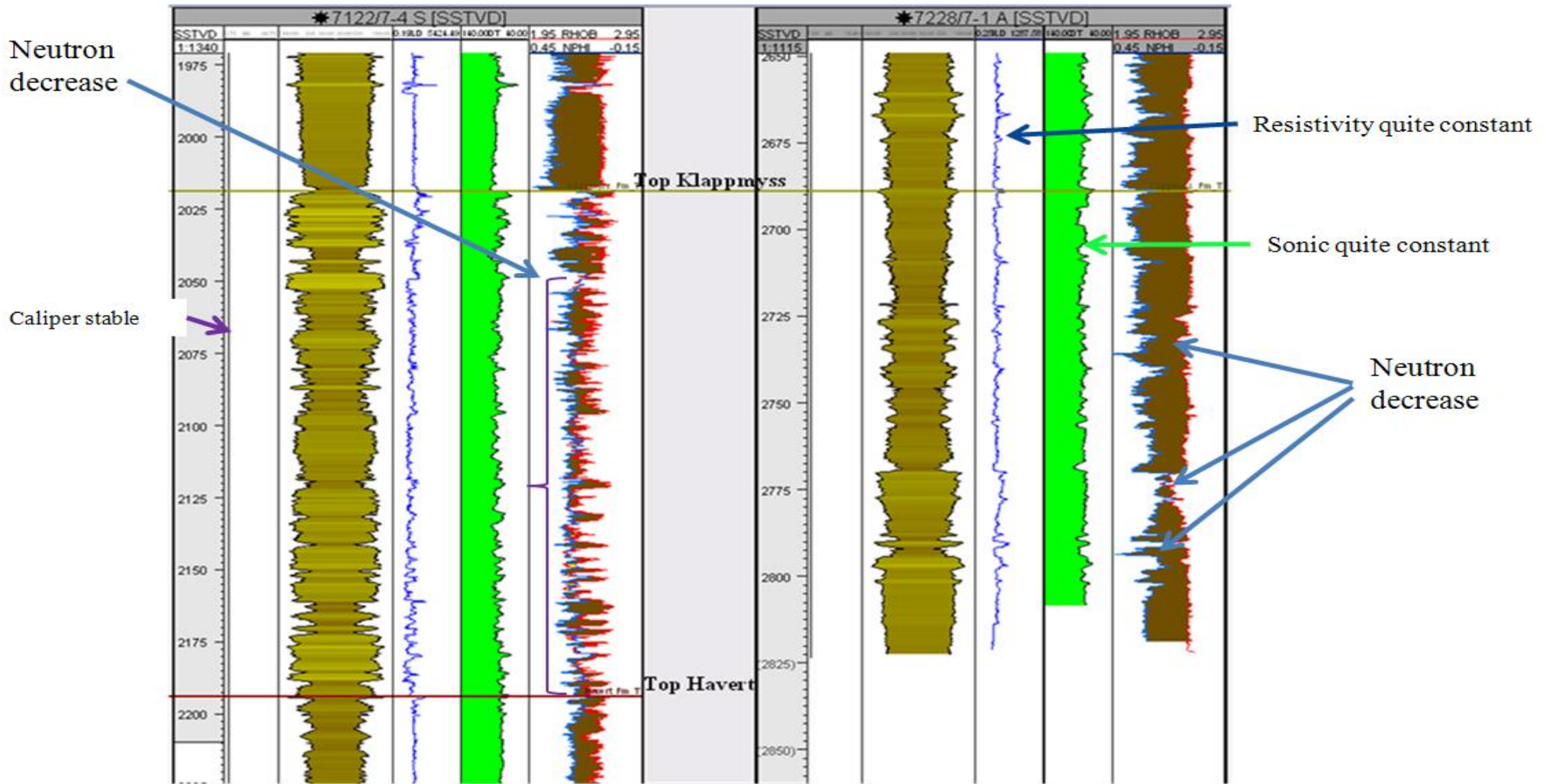
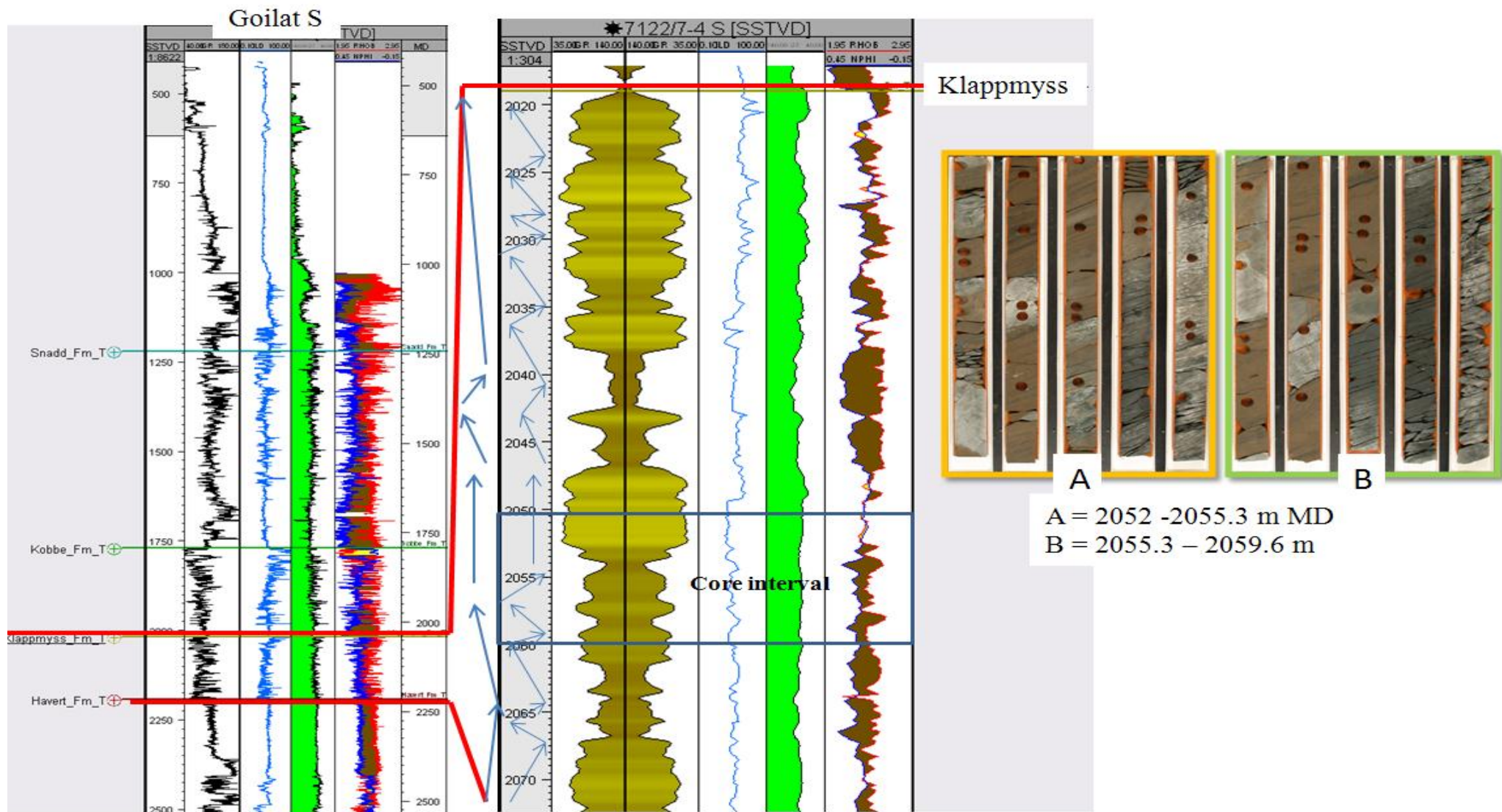Figure 24 where pointed out different log observations in the Goliat S well and the Pandora well.

Figure 25 showing logs for the Goliat S well together with core photos.

Table 2 below illustrate gamma ray log pattern, facies interpretation and sequence stratigraphic framework for both Goliat S and Pandora at the interval where core is obtained. Location of these wells can be seen in figure 21.

Well	Gamma-ray log pattern	Well-log signature	Facies interpretation based on core description	Sequence stratigraphic framework
Goliat S 7122/7-4S (11.42m thick core)		Spiky and fining upwards	Tidal mud flat	Transgression
		Spiky and coarsening upward	Tidal bar	Progradation or transgression
		Fining upward	Tidal channel	Transgression or retrogradation
Pandora 7228/7-1 A (28m thick core)		Blocky and aggradational	Distal Bay fill	Aggradation

Table 2 illustrating GR pattern, interpretation and sequence stratigraphic framework for the Goliat S and Pandora well. The Hegg well does not have core and is therefore not mentioned.

Hegg (7224/7-1)

The Hegg well (7224/7-1) is drilled on the Samson Dome and is the well closest to the project area. The objective of this well was to test sandstone reservoirs in Jurassic and Triassic ages and carbonaceous rocks of Permian age. Klappmyss Fm. was penetrated at 2222m MD, and this interval is 440m thick. Good gas shows were indicated at the lower Klappmyss interval which is the main interest interval in this study (prograding clinoforms). This interval at about 2500m depth consists of Marl at the top with underlying claystone, where drilled. Permeability measurements for Klappmyss were not performed. Neither was core taken for this interval. The well was permanently abandoned in 1988 with shows.

As will be noticed during the following chapters the interval of interest (lower Klappmyss Fm.) begins with the upper interpreted horizon "Top lowstand". However, this horizon name

is not descriptive because as I went along with this study I realized that the seismic does not provide enough detail to observe system tracts. Nevertheless, I chose to keep the name.

Gamma ray values for this well are in the range 55-60 API (figure 26) while a bit lower for the deepest part (around 40 -45). Resistivity and sonic logs remains quite constant through the Klappmyss interval from 2200m to 2663m. However, a minor shift on the neutron log is observed in the lower Klappmyss interval starting with the interpreted horizon "Top lowstand" (figure 26). Stacking pattern in the Hegg well shows an overall coarsening upwards trend in the Klappmyss Fm. which represent a 3rd order sequence (Glørstad-Clark et al., 2011).
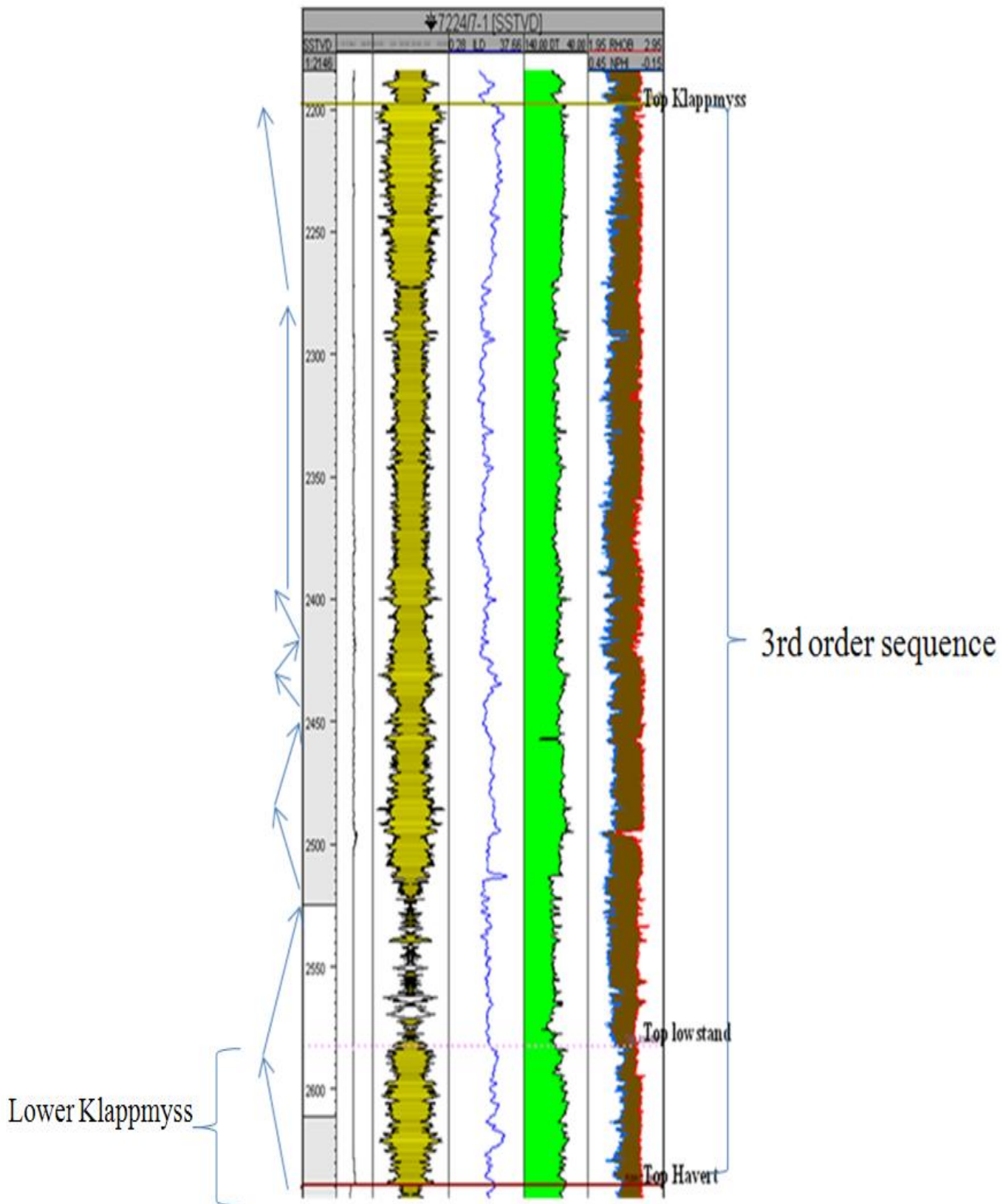
Figure 26 showing stacking pattern and logs for the Hegg well. The whole Klappmyss Fm. is displayed and lower Klappmyss interval is indicated.

The interpreted Top Klappmyss Fm. is seen in figure 26 and represents the horizon picked in seismic believed to represent top of the formation. Also interpreted horizon named Top lowstand and Top Havert is shown in the figure. Top Havert represent base of the interpreted Klappmyss Fm. interval. The stacking pattern of the lower Klapmyss (prograding clinoforms/ interval between Top lowstand and Top Havert) comprise of coarsening-upwards parasequences indicating transgressive/ regressive cycles (figure 27). A total of four prograding clinoforms is observed within the lower Klappmyss interval.

Horizon *"Top lowstand"* is interpreted at 2585 m depth and has a sharp character on the log profile showing high GR above. In addition, several possible flooding events are indicated in figure 27, representing the interpreted FS surface and MFS.
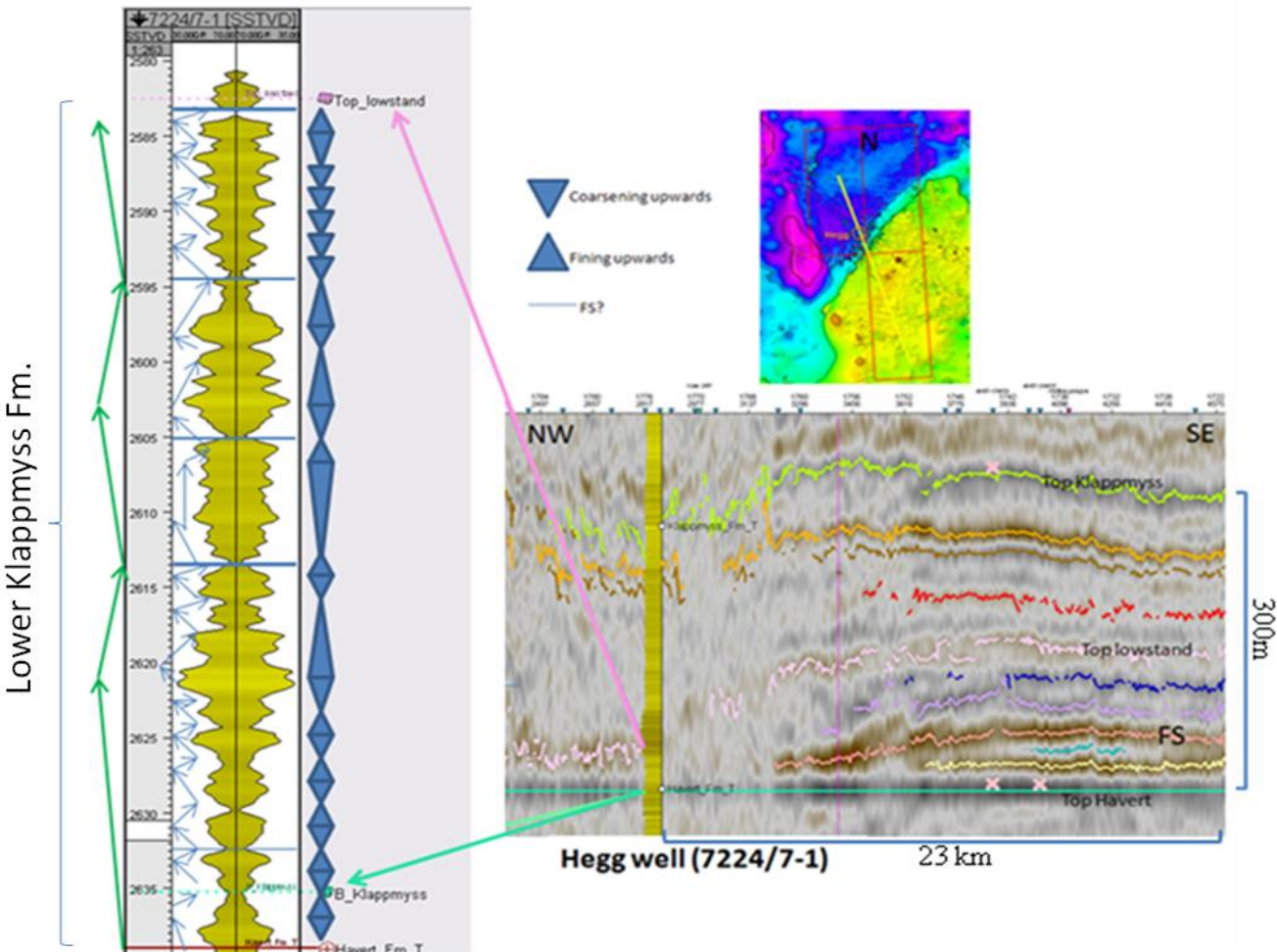
Figure 27 zoomed in on the lower Klappmyss interval showing the well to seismic relationship. Map indicate position of the seismic line.

Seismic character

Five interpreted horizons representing the lower Klappmyss Fm. and top of the Klappmyss Fm. will be discussed. These were chosen based on the area of interest (prograding clinoforms/ platform-margin delta) and by the ability to contribute to a detailed understanding of the clinoforms in Klappmyss Formation close to the Hegg well (figure 27). This chapter starts by introducing some regional 2D seismic lines showing the main pattern of Klappmyss Fm. Then the description will focus on the lower Klappmyss Fm.

As observed on the 2D seismic line going through Hegg and Pandora well seen in figure 29 the pink and red horizon downlapping on Top Havert horizon in east direction. Furthermore, close to the salt dome next to Pandora well the Klappmyss Fm. seems to thin out, which indicate that the Klappmyss Fm. is much thinner here compared to at the Hegg well. It can though be assumed that much of the Klappmyss Fm. was drilled in the Pandora well, even if it did not penetrate the underlying Havert Fm..
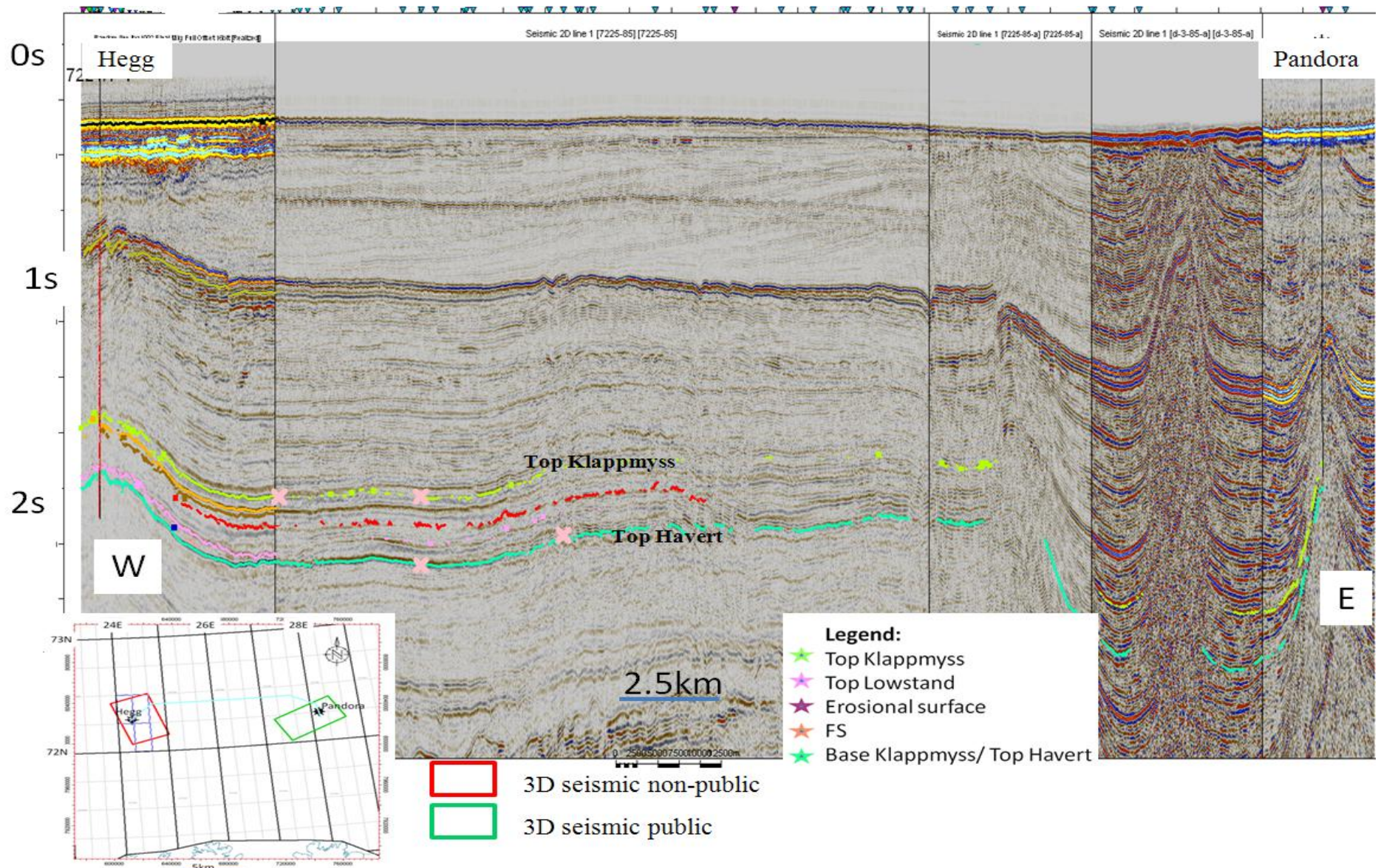
Figure 29 showing seismic line from the Hegg well to the Pandora well.

Further when looking at the seismic 2D line going through Hegg and Goliat S well, also here a thinning of the Klappmyss Fm. can be observed.

Even if the top of the Klappmyss Fm. is above the main object interval (lower Klappmyss) it was interpreted to contribute to a detailed overview of the thickness variations in the whole formation. The seismic interpretation of Top Klappmyss follows a very distinct negative amplitude reflector throughout most of the data set. However, close to both Goliat S and Pandora this reflector is difficult to trace due to major faulting and salt structure.

As mentioned earlier and seen on the seismic lines between Goliat S, Hegg and Pandora there are some visible thickness variations in the Klappmyss Formation. The formation seems to pinch out both towards Pandora and Goliat S compared to the Hegg well. Further the formation seems to thin out towards northwest and South as seen in figure 31. This thickness trend is confirmed by the seismic lines shown in figures 31 and 32.
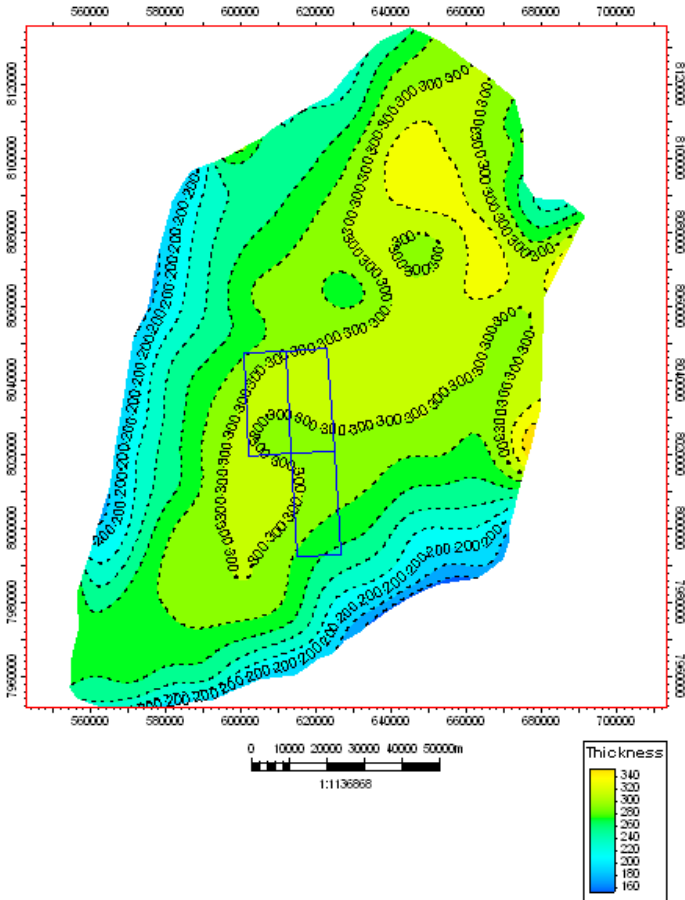
Figure 30 time-thickness map of the Klappmyss Fm. Notice thickest interval within the licence area represented by the three squares.
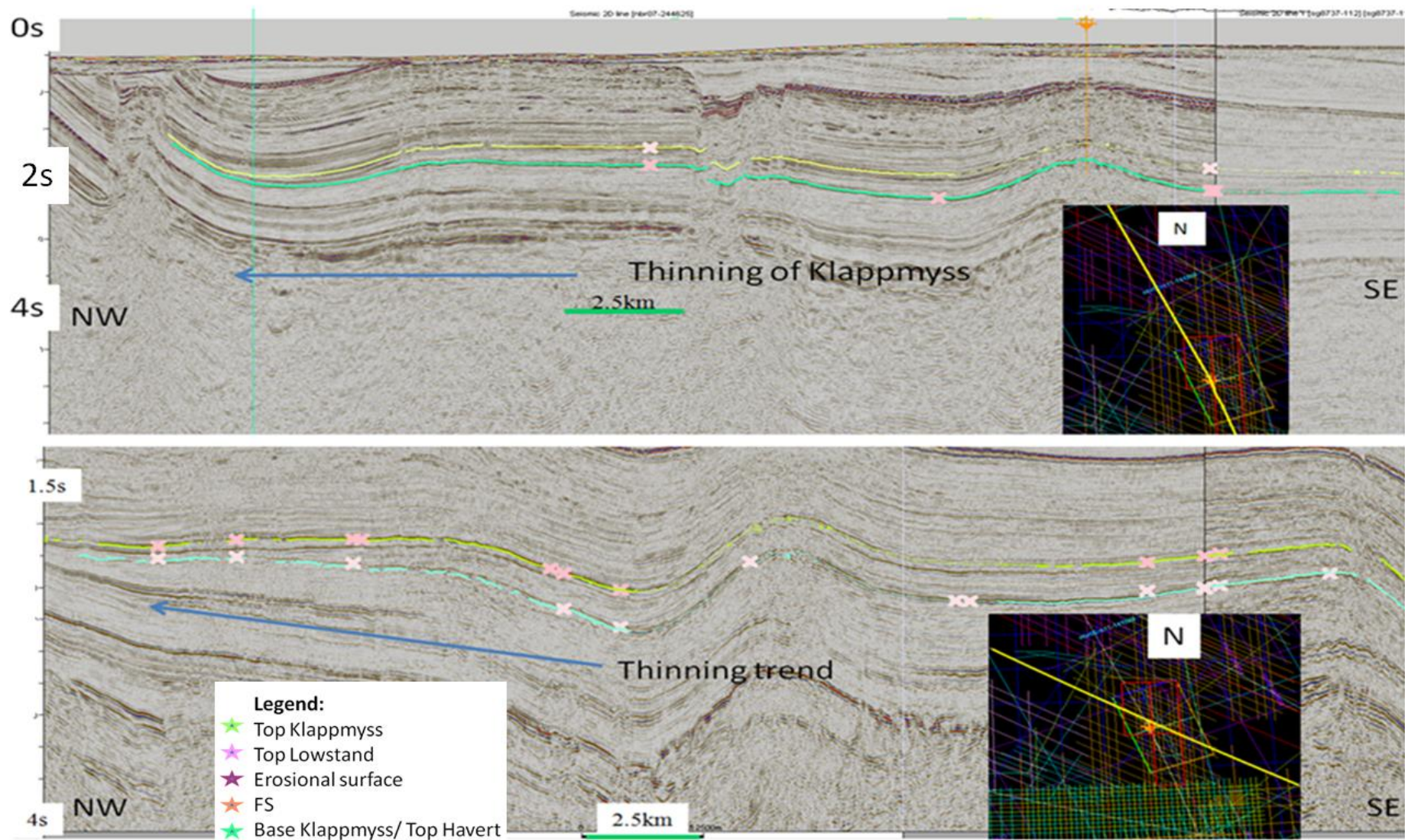
Figure 31 showing two different seismic lines . The Hegg well is in the image.
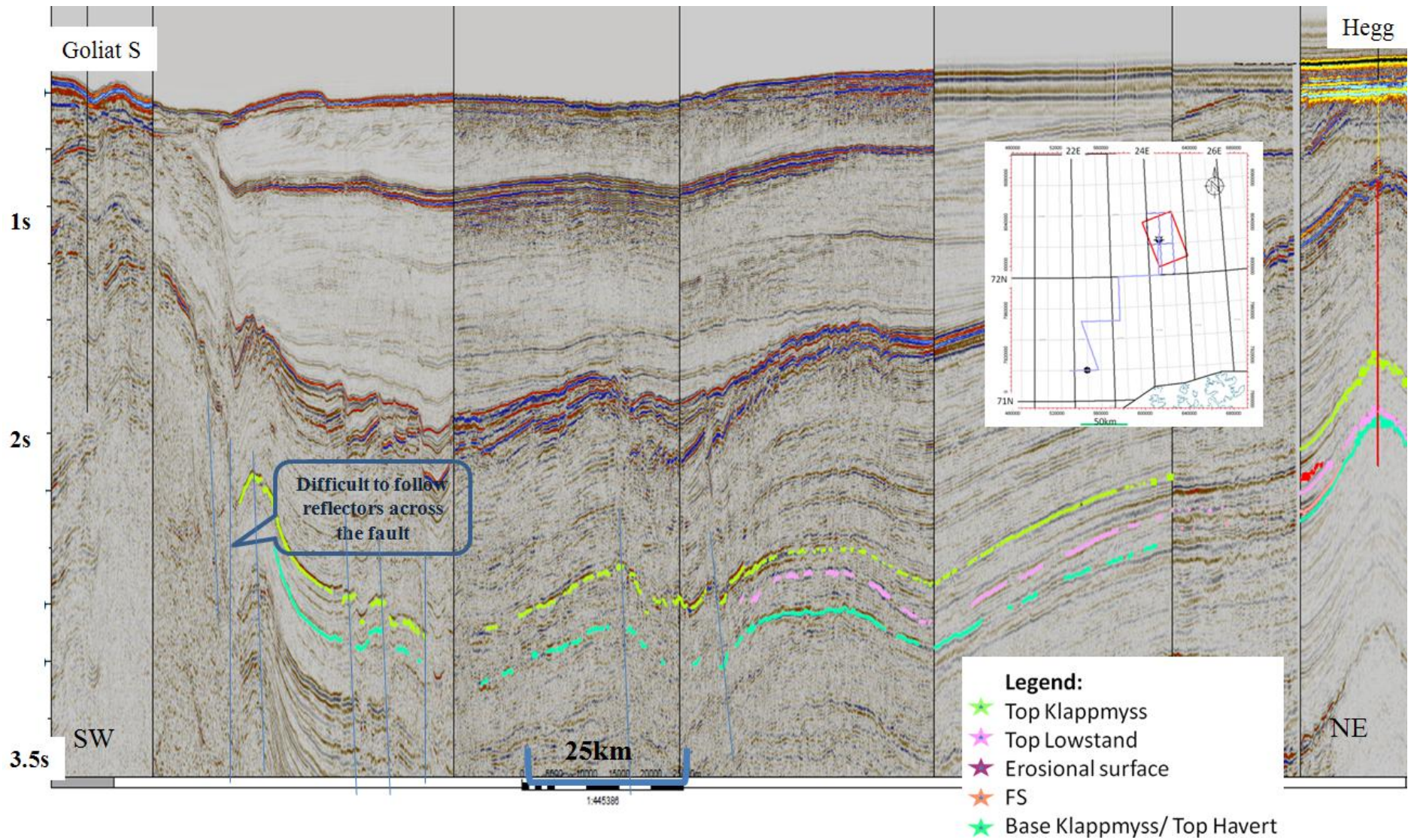
Figure 32 Iterpreted SW-NE striking seismic line with well 7122/7-4S (Goliat S) and 7224/7-1 (Hegg).

Lower Klappmyss interval

Lower Klappmyss interval was further divided into two units. 1) Lower unit consisting of a sequence boundary which is the top of Havert Formation and the top is MFS (FS horizon in seismic). 2) Upper unit bounded by MFS (FS horizon) and a flooding surface (Top lowstand horizon). Both these units will be further discussed regarding well log and seismic character.

Lower unit

Well log character

In figure 33 below, the lower unit consist of coarsening upward stacking pattern followed by fining upward indicating a transgressive event, which is interpreted to represent maximum flooding surface. This represents a 4th order sequence and could be related to subsidence and/or sea level rise. This unit might also be narrower than indicated on the figure (uncertainty in which FS representing MFS).
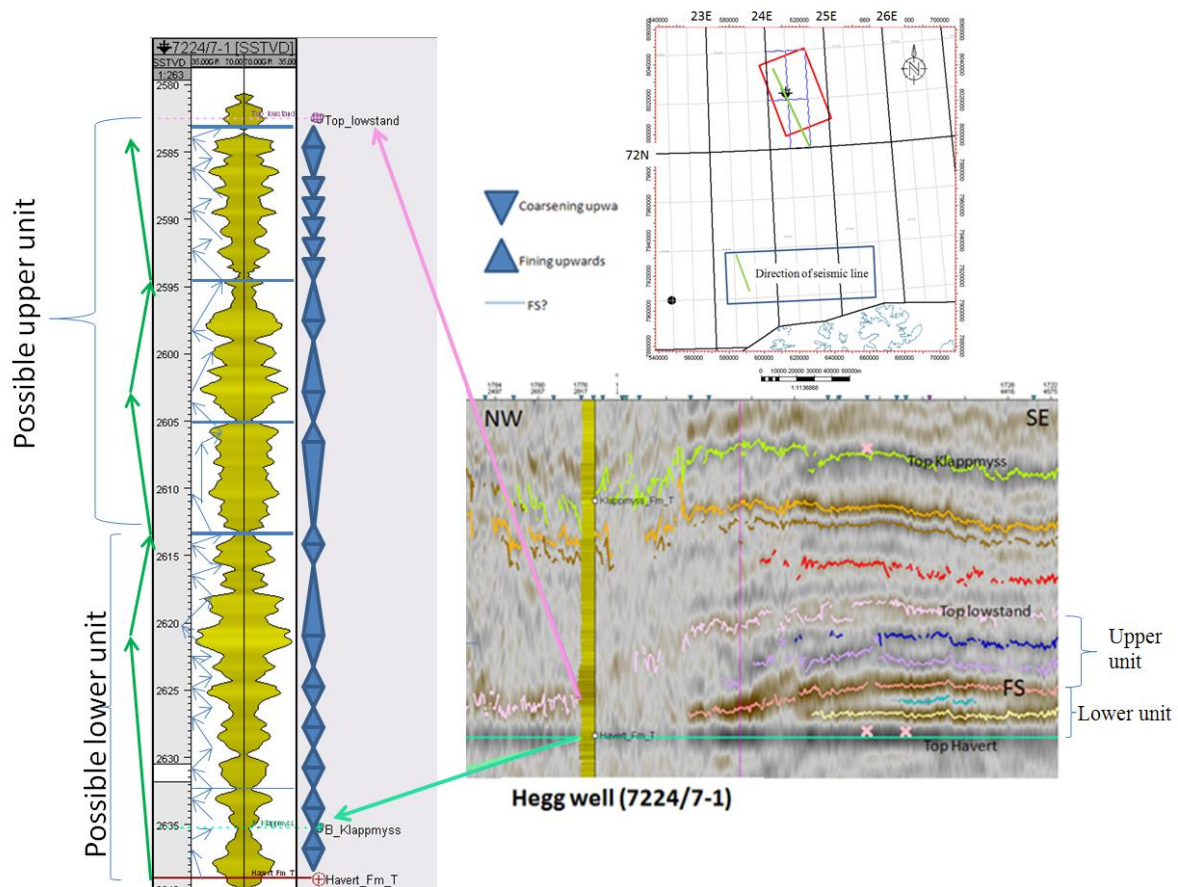
Figure 33 repeated zoomed in log on the lower Klappmyss, where upper and lower unint within this interval is highlighted. Map shows position of the seismic line.

Seismic character

Base Klappmyss/Top Havert

The seismic interpretation of Top Havert (figure 34 A) follows a very distinct negative amplitude reflector throughout most of the data set. However, close to both Goliat S and Pandora this reflector is difficult to trace due to major faulting and salt structures. The relatively flat nature of this reflector made it a favourable horizon to flatten when interpreting in more complex areas with faulting and salt structure affecting the image. Further, this reflector represent base of the Klappmyss Fm. and was useful in isopach map illustrating thickness variations in the formation within my dataset.

FS

FS horizon (figure 34 B) has a strong positive amplitude value and is easily traceable. This is interpreted to be maximum flooding surface due to the observations of downlapping clinoform reflectors, and the recognition of back stepping (retrogradational) reflector below.
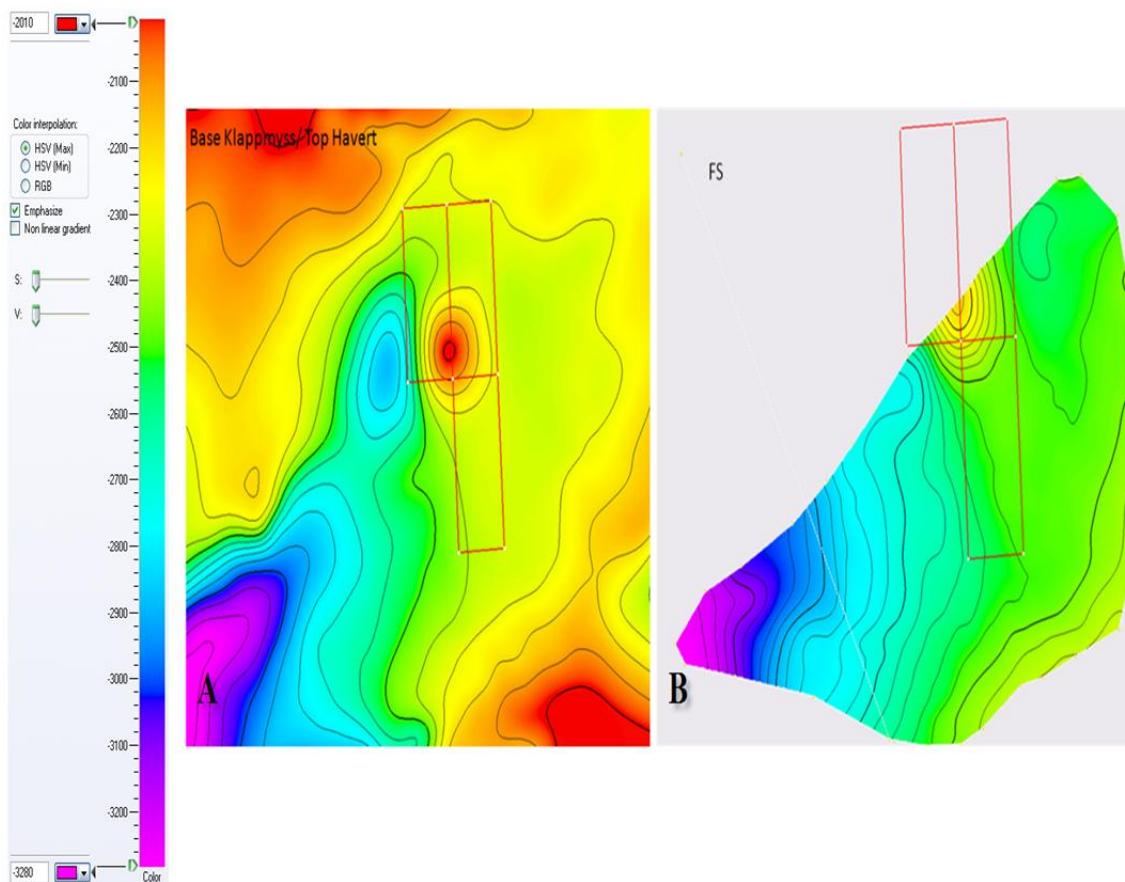
Figure34 Structural maps of A) Base Klappmyss and B) FS horizon.

Isopach map between Top Havert and FS indicate thicker interval towards the Hegg well (figure 35). As highlighted on this figure east-west oriented geometries are observed, which might reflect tidal sand banks.
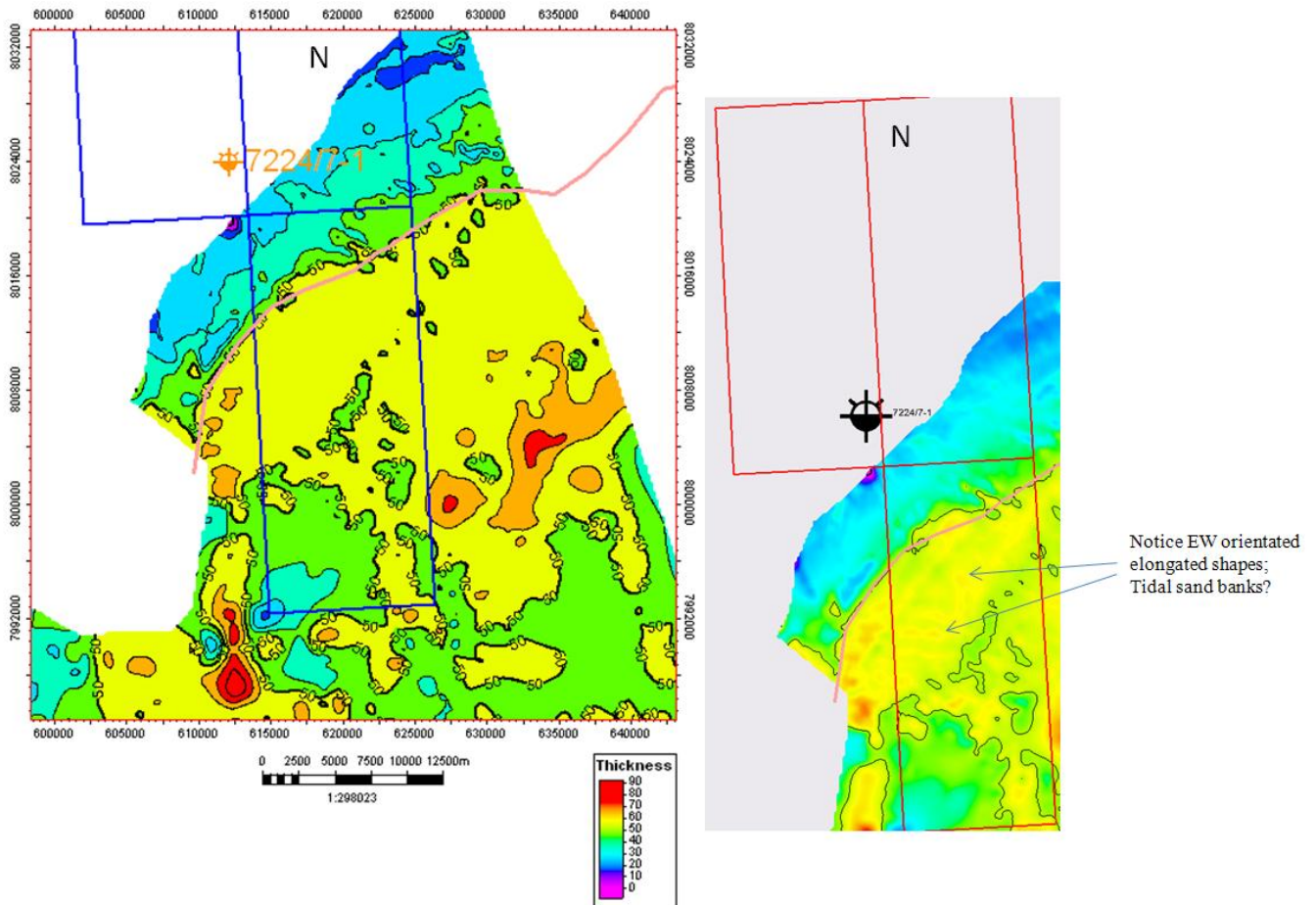
Figure 35Time thickness maps between interpreted Base Klappmyss and FS. Snapshot on the right side is abit zoomed out compared to the leftmost as noticed by the three squares representing the licence area.

Upper Unit

Well log character

As seen in figure 33 the upper unit consist of several coarsening upward cycles separated by possible flooding surfaces. It also seems to represent a parasequence of prograding cycles. These are 4th order sequences. As with the lower unit this could be related to subsidence, sea level changes (or changes in sediment supply).

Seismic character

Erosional surface

This reflector follows a positive amplitude value, but is not traceable in most of the dataset (figure 36 A) and is only interpreted in a limited area. The reflector is not observed close to the Hegg well or further northwards, and has the strongest reflectors to the east direction of the Hegg well. Moreover, this horizon represents the prograding clinoforms with the steepest angles seen in figure 39 and will be further discussed regarding clinoform angles.

Top Lowstand

Top lowstand (figure 36 B) is identified based on a clear positive amplitude value throughout the dataset. This horizon represent top of the lower Klappmyss Fm. interval which define the top of my main interval of interest. This reflector is right above the prograding clinoforms and seems to represent a flooding surface based on downlap architecture on to Top Havert and low gamma ray.
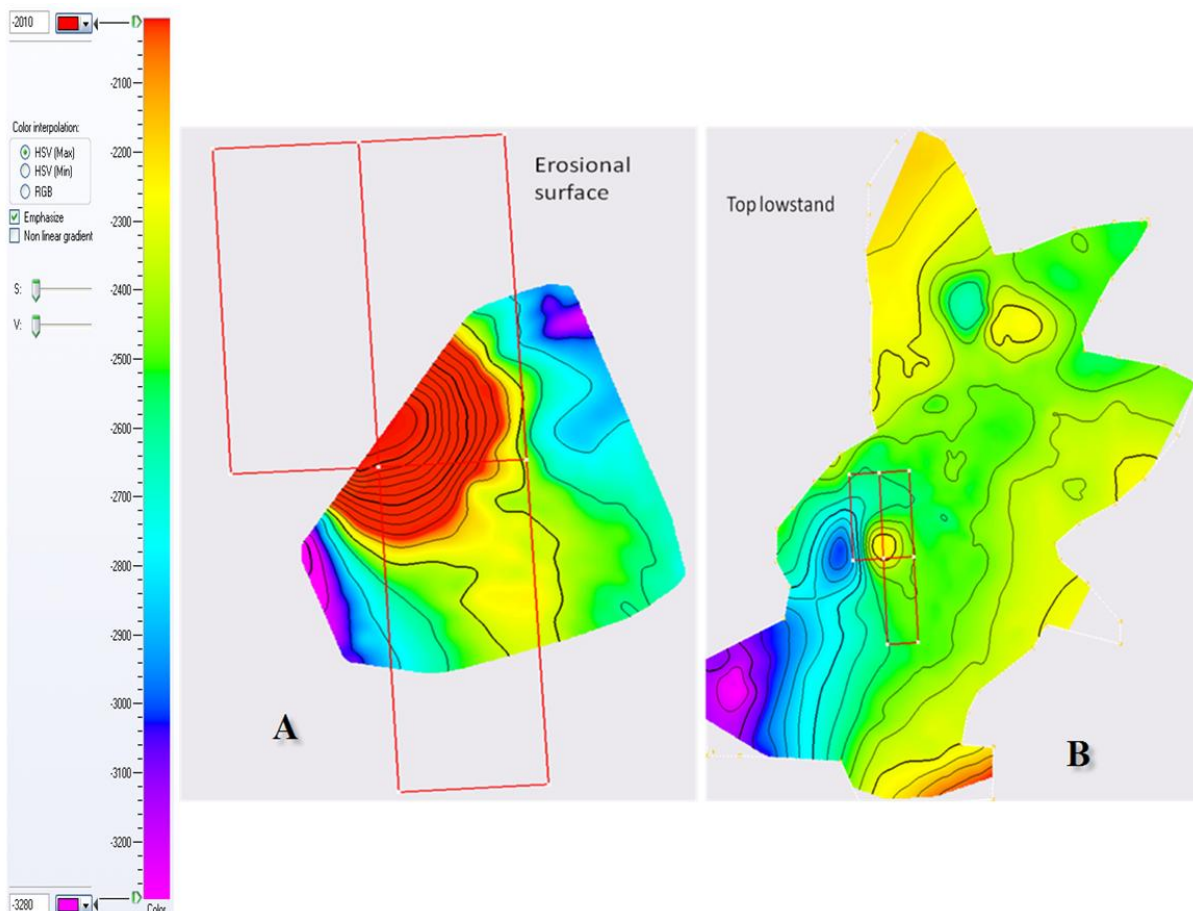
Figure 36 Structural maps of the two horizons representing the upper unit. Note the licence area for scaling purpose.

Thickness map between Top lowstand and FS (upper unit) reveal a thicker wedge shaped area outlined in black (figure 37).
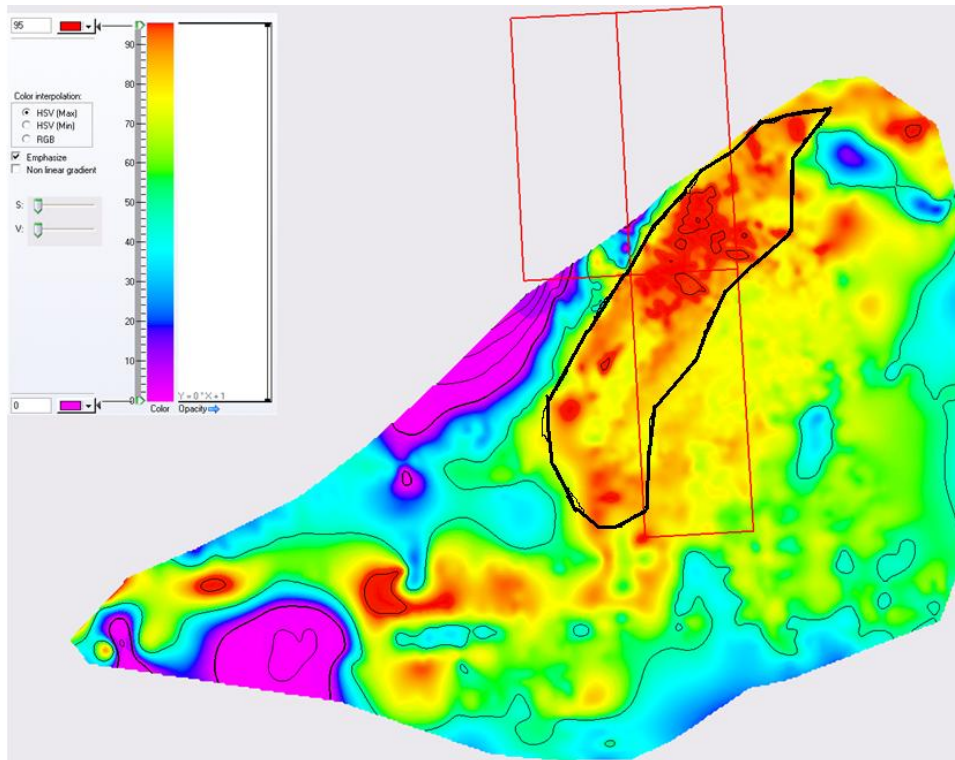
Figure 37 Time thickness map between the FS surface and the Top lowstand horizon.

Summarized the Klappmyss Fm. seems to be thickest around the Samson Dome within area of interest (licence). Moreover, the lower Klappmyss Fm. can be further divided into two separate units which have different characters observed on seismic and well logs.

Amplitude

Both average amplitude and variance amplitude maps were generated. However, neither of these helped in minimising the uncertainty of finding hydrocarbons in the area of interest. Seen in figure 38 A; Average amplitude between top and base Klappmyss Fm. illustrate the masked area (area disturbed by several faults). B) Constructive interference can be seen in the bright area where Top lowstand downlap onto Base Klapmmyss and cause a tuning effect. C) Variance cube for Top Havert indicate the faults in the masked area. These amplitude attributes were performed for all interpreted horizons, but since these did not contribute towards any conclusion, the amplitude will not be further considered in this paper.
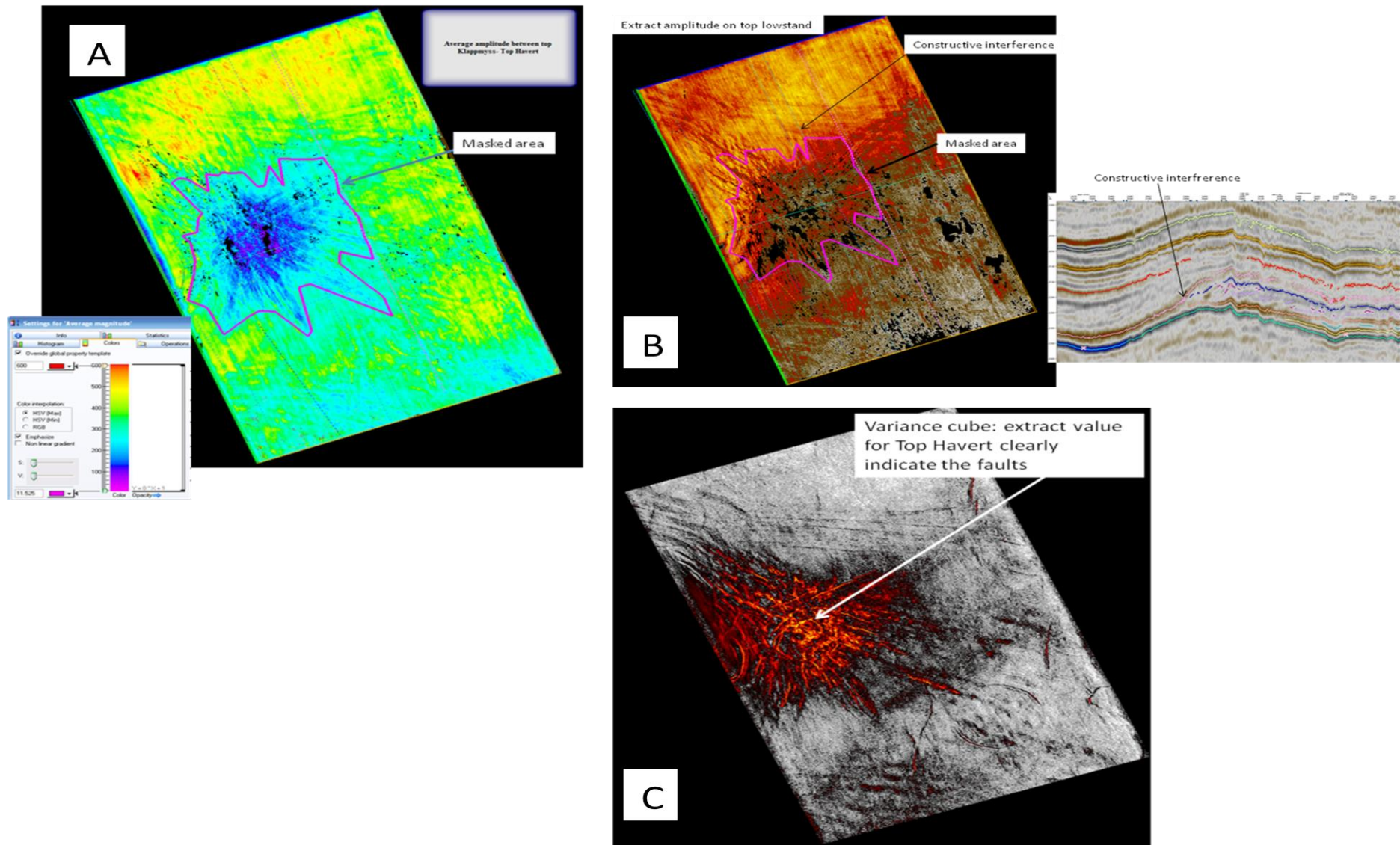
Figure 38 showing selected snapshots from the amplitude maps.

Clinoform trajectory trends

As mentioned under stratigraphic considerations in previous chapter, clinoform trajectory trends can help predict lithology and depositional environment. In the studied seismic data set it is possible to identify two different classes of clinoform trajectory trends. Note that although the terms high-angle and low angel are used, these are relative terms.

As seen on the seismic line below in figure 39 a northwest-southeast oriented line east of the Hegg well shows a flat to slightly negative trajectory trend. FS horizon is flattened, acting as a time line to improve the interpretation (ease the recognition of the clinoform trend). The seismic line shows oblique clinoform facies with steep geometries and with no or thin topsets. Moreover, reflectors are observed to step out a distance of 5-6 km prograding significantly with little aggradation (i.e. Not building upwards). Below FS the seismic reflectors terminate abruptly stepping back towards the southeast and being apparently drowned by the horizon named FS. This flat to negative trajectory is represented by a package of four clinoforms that are strongly progradational. Moreover, some of the tops of the clinoform s seem planned off.

In contrast to figure 39 the clinoform trajectory trend in figure 40 is positive. The clinoform shape is sigmoidal with lower angles and clear topsets. Prograding reflectors are observed to step out a distance of about 5 km and show some aggradation (i.e. building upward). As in figure 39 the seismic reflectors below FS terminate abruptly stepping back towards the southeast and being apparently drowned by the horizon named FS. This positive trajectory is typified by a package of three clinoforms that are strongly progradational and where each successive break of clinoform slope is positioned slightly above and more basinward than the previous one.
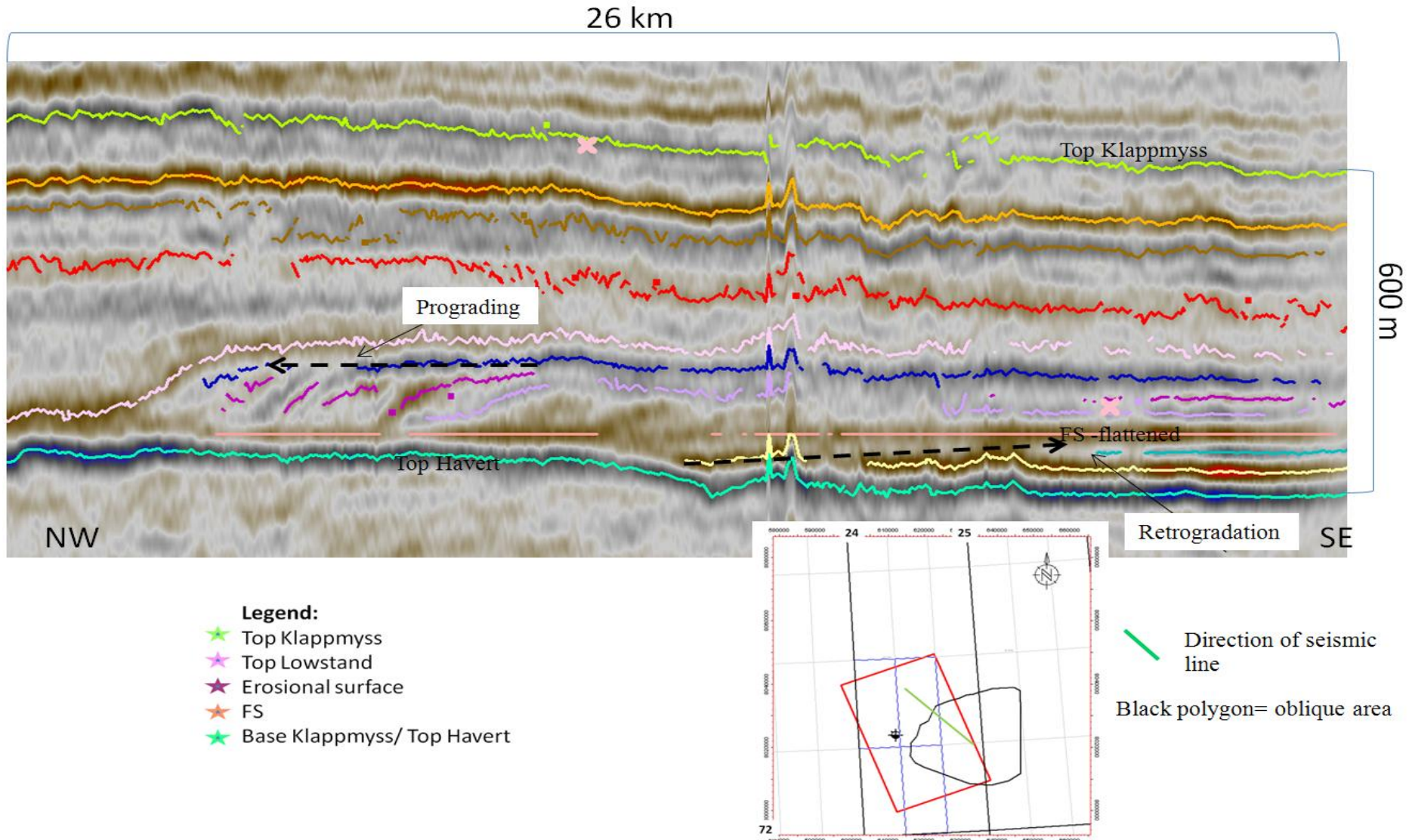
Figure 39 illustrating the prograding clinoforms and the direction of the trajectory (flat to slightly negative). Map illustrate direction of the seismic line. 3D seismic is represented by red square.

24 km

Hegg well

Top Klappmyss

570 m

Base Klappmyss

FS

NW

SE

Legend:
★ Top Klappmyss
★ Top Lowstand
★ Erosional surface
★ FS
★ Base Klappmyss/ Top Havert

Direction of seismic line

Black polygon= oblique area
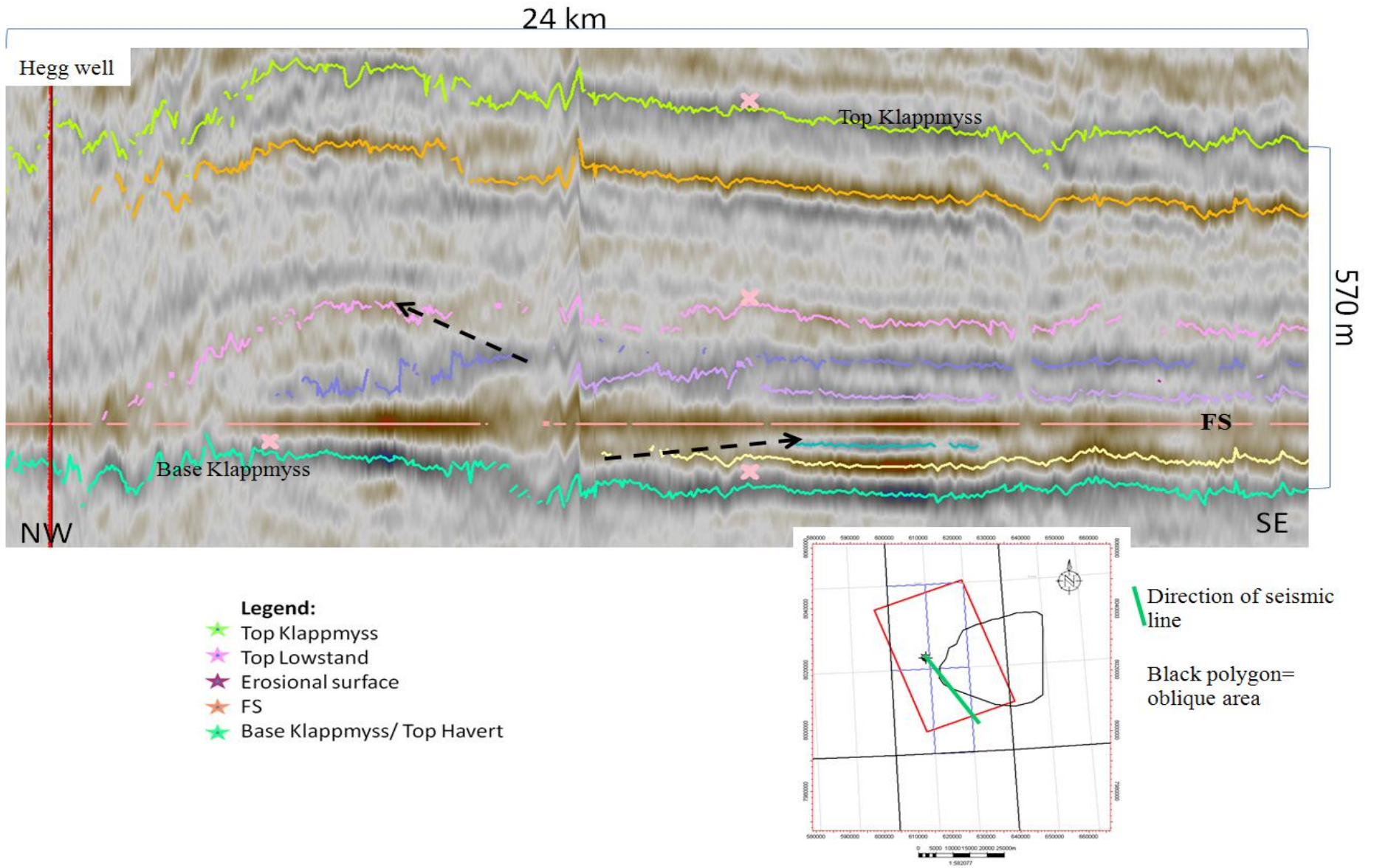
Figure 40 illustrating the prograding clinoforms, notice the clinoform trajectory positive trend. Map illustrate position of the seismic line.

By mapping out the area with oblique seismic facies (figure 41) it is recognisable that this polygon fits the area with the thick wedge shaped geometry on the isopach map between Top lowstand and FS horizons.
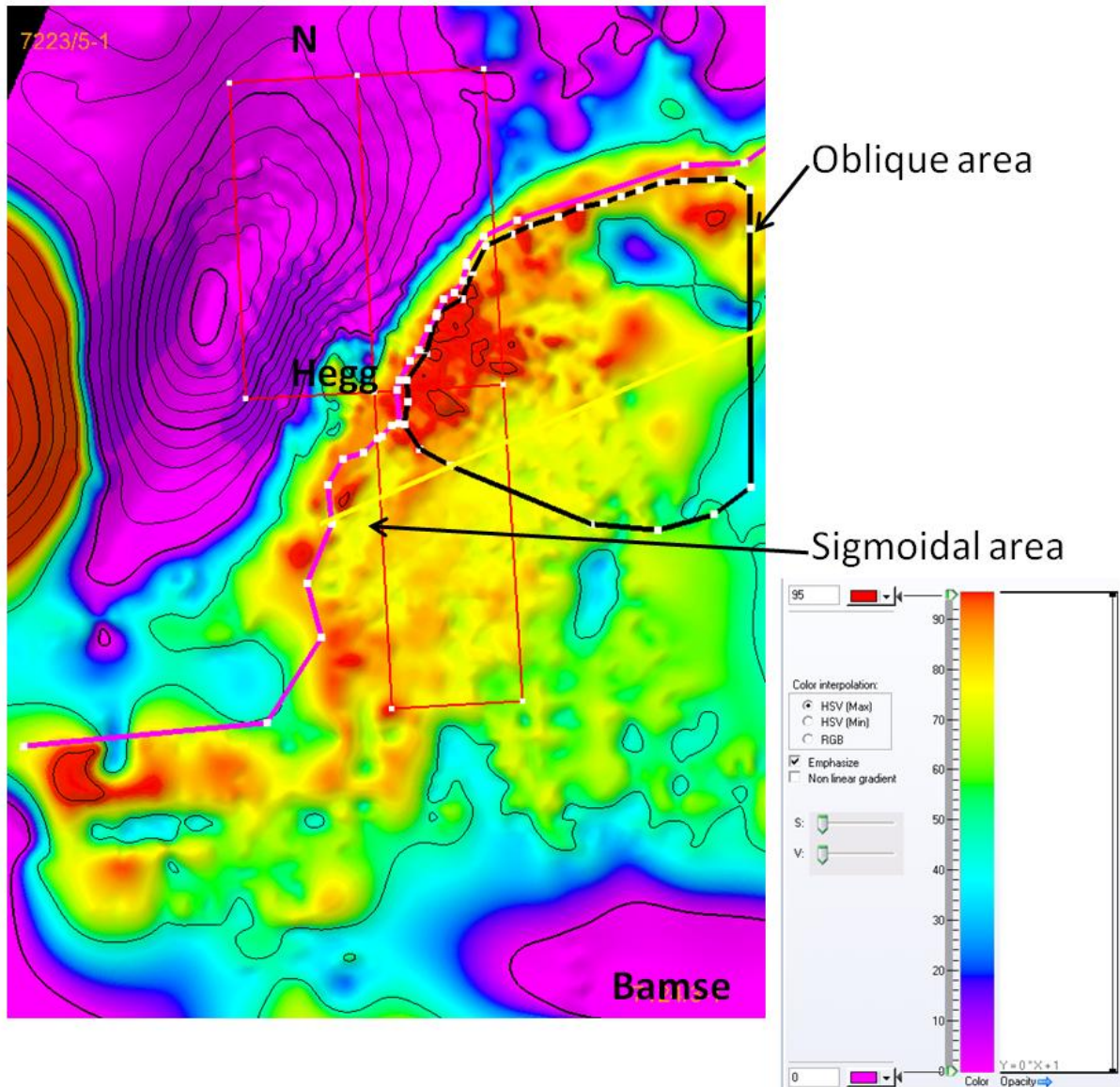
Figure 41 Time thickness map shown together with polygon outlining the oblique clinoform area.

Maximum progradation starting after the flooding suface is illustrated by polygons in figure 42. Thickness of the clinoforms indicating water depth gives 136m at the last prograding clinoform at horizon "Top lowstand". It is also noteworthy to mention the protruding geometry on maximum progradation following this horizon, where a change in shape from the flat FS polygon is seen.

53
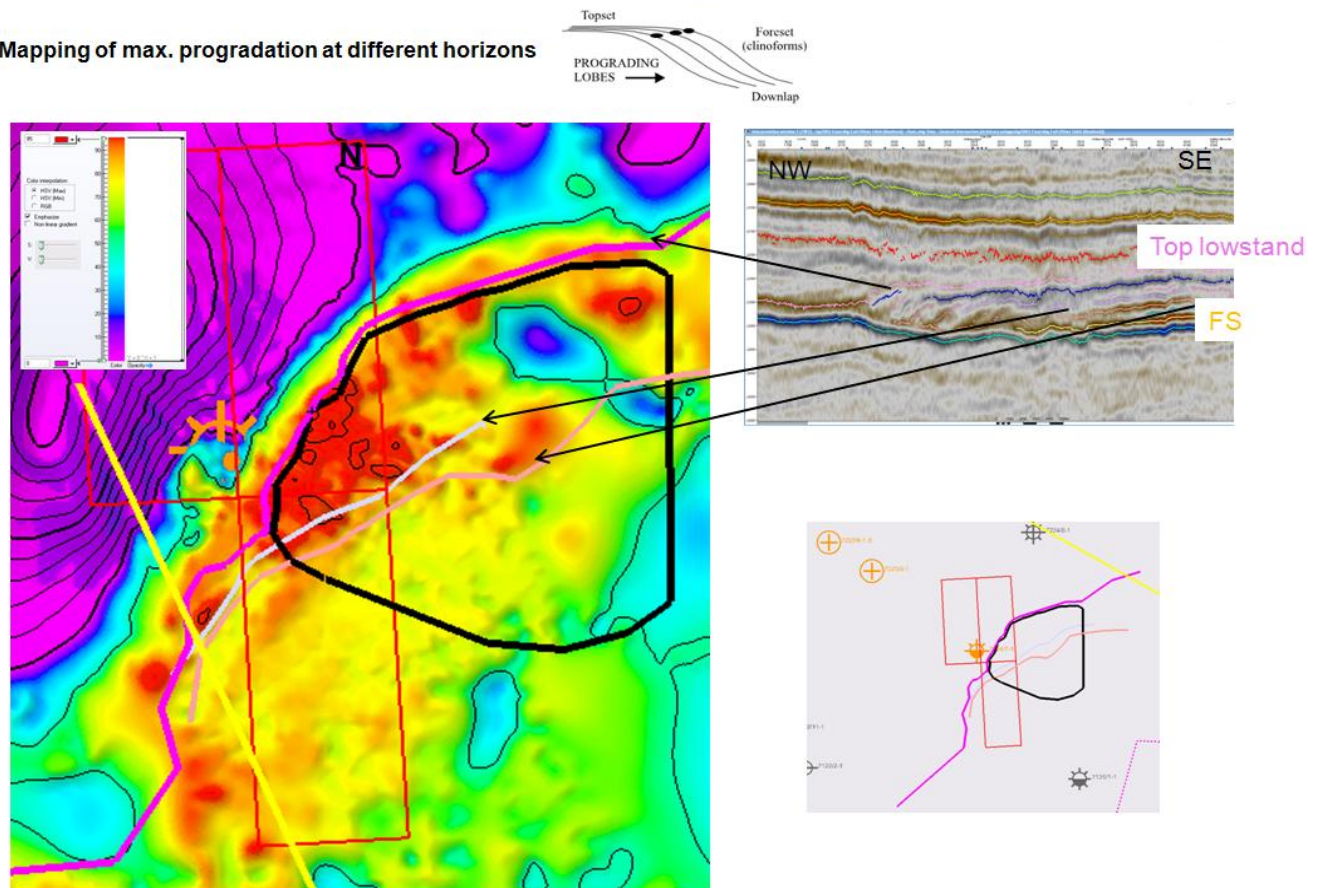
Figure 42 illustrating the shape of the prograding clinoforms.

Clinoform angles

Clear differences in clinoform angles were observed in the upper unit. As seen in figure 43 the clinoform angles in the oblique seismic area seems higher compared to those observed in the sigmoidal shaped area. A more detailed description of the clinoform angles will follow under discussion.
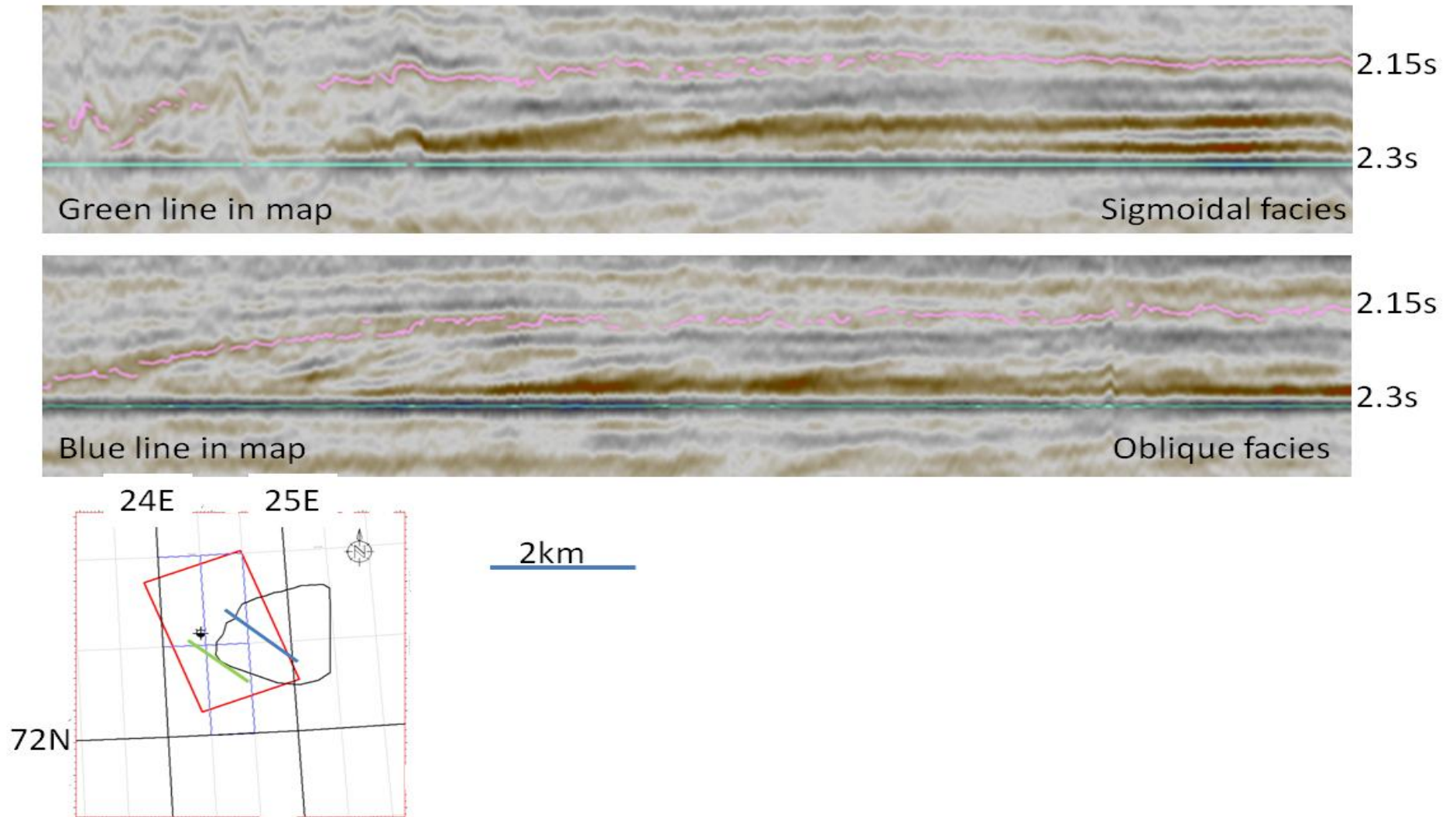
Figure 43 showing one seismic line going through the sigmoidal shaped seismic facies (top) and oblique facies (bottom), Map showing location of the seismic lines, and red square represent the 3D seismic cover over the Samson Dome. Vertical scale represent scale on the seismic. Both seismic images are flattened on Top Havert horizon. Pink horizon represent Top lowstand horizon while green line Top Havert.

Discussion

The discussion is divided into four separate sections. These consist of well log interpretation, seismic and thereby clinoform analysis, petroleum implications where preliminary volumes will be given and at the end previous studies.

Well interpretation

The higher gamma ray values in the Goliat S well compared to the Pandora could be interpreted to explain smaller sediment grain size in the Pandora well (more muddy). This might contribute to the lower permeability in the Pandora well, since smaller grains (more sorted) have lower porosity and thereby often lower permeability. Core photos (figure 22 and 23) seem to confirm that Pandora is more mud and silt prone than Goliat S. In addition, the funnel shaped gamma ray profile seen in the Pandora well is interpreted to represent coarsening upward pattern indicating regression. The Goliat S well has a more blocky gamma ray indicating intervals with more aggradational stacking pattern.

The horizon *"Top lowstand"* representing top of the lower Klappmyss interval, is showing increasing GR which probably is caused by lithology transition from marl to shale indicating a transgressive event. Moreover, the decrease in the neutron log could possibly be related to hydrogen presence in all three wells, and represent gas in Pandora, oil in Goliat S and gas shows in the lower Klappmyss interval.

A correlation between the Goliat S and the Hegg well are seen in figure 44. Here lower Klappmyss Fm. is correlated with the upper interval of Klappmyss in the Goliat S well using stacking pattern. Both show coarsening upward cycles. As seen from this correlation the lower Klappmyss interval seems thicker in Goliat S than Hegg. Moreover, Goliat S seems to miss the package above this interval. This scenario could have several reasons like different subsidence rates, uplift at the Golias S area etc. To test the correlation I would suggest biostratigraphy and a detailed study in fault and terrace structural movement around the Goliat S well.

Figure 44 showing a possible correlation between the Goliat S and the Hegg wells.

Seismic interpretation
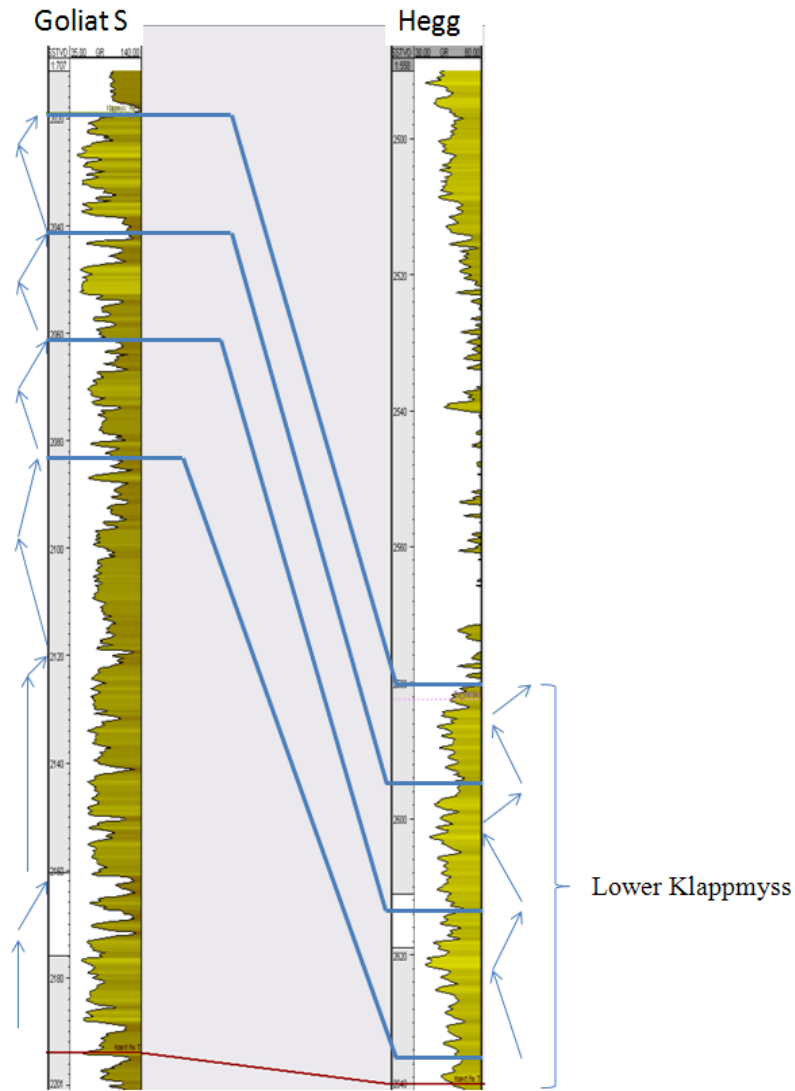
Mentioned earlier in this paper, seismic facies can contribute in the prediction of environment at time of deposition/progradation. Higher energy environment is seen as oblique shaped, while lower energy as sigmoidal. Since this study shows both observed in the same system, this is interpreted to reflect changes in relative sea level rate and the interplay with sediment supply rate at the same time. The oblique area is interpreted to represent area with higher sediment supply by probably a high energy river; while the sigmoidal shaped area could represent the shoreline area.

The upper unit of the Lower Klappmyss Fm. consists of prograding clinoforms representing a platform-margin delta, interpreted by Glørstad-Clark et al. (2011). Moreover, angles of the clinoforms are interpreted elsewhere to represent grain size variation. Therefore (see stratigraphic consideration chapter) the variation in clinoform slopes has been interpreted over the Hegg prospect as seen in table 3. These clinoform angles were separated between the oblique and sigmoidal shaped facies and revealed differences in angles as seen in table 3.

	Horizon:	Sigmoidal area a (m)	b (m)	Angle (Degree)		Obligue area a (m)	b (m)	Angle (Degree)
	Top lowstand	221.1	5000	2.5		190.3	2400	4.5
Before decompaction	FS	96.9	7800	0.7		101.2	7900	0.73
	Light purple	153.9	7700	1.15		148.7	7500	1.14
	Dark purple	not present				117.8	800	8.4
	Horizon:	Sigmoidal area a (m)	b (m)	Angle (Degree)		Obligue area a (m)	b (m)	Angle (Degree)
	Top lowstand	311.7	5000	3.6		269.6	2400	6.4
After decompaction	FS	281	7800	2		286.7	7900	2
	Light purple	153.9	7700	3.3		421	7500	3.2
	Dark purple	not present				117.8	800	11.8

Table 3 summarizing the angle calculations

The angles measured from the seismic will have been shallower from that at deposition by sediment compaction. In order to estimate the angle at time of deposition, porosity-depth trends were used to predict/prognose sediment thickness when deposited.1.5-2 km uplift is used in the calculation after Henriksen et al. (2011) study on uplift history in the Barents Sea. In table 3 also angles after decompaction can be seen. Porosity- depth relationship and the formula used in the estimation is seen in figure 45.

$$S = \frac{Si(1-\text{ø})}{1-\text{ø}*}$$

S = Sediment thickness decompacted
Si = Sediment thickness at present
Ø = Porosity at burial depth
Ø* = Porosity at surface
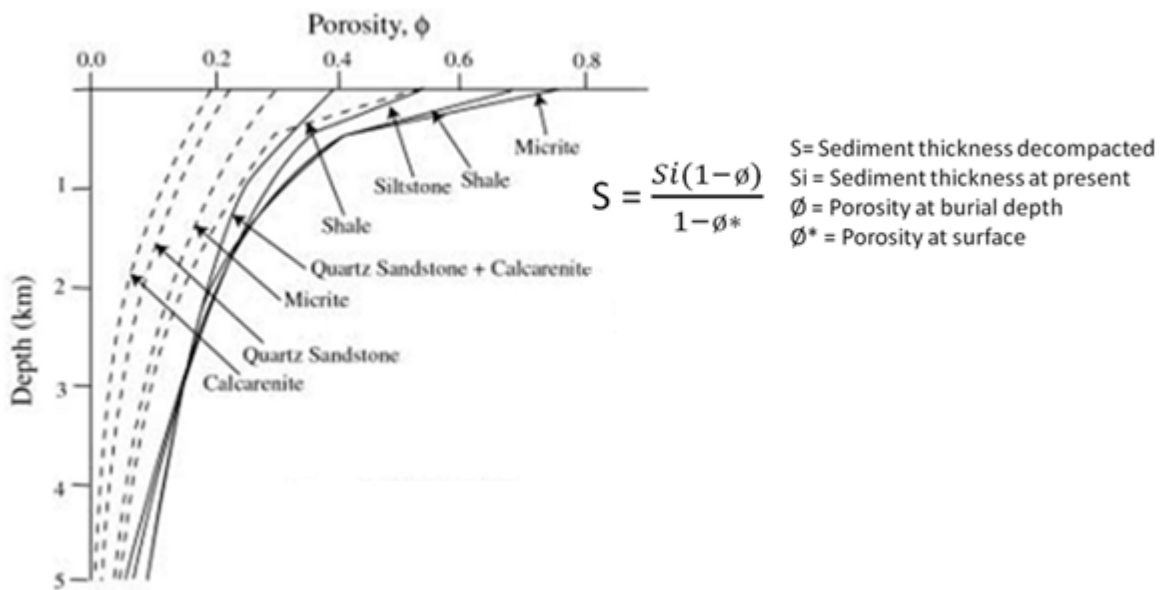
Figure 45 showing the porosity-depth curve used in the decompaction.

For illustrative purpose a seismic line is shown in figure 46. Here a change in angle during decompaction (from 8.4 degrees to 11.8) in the oblique area can be observed.
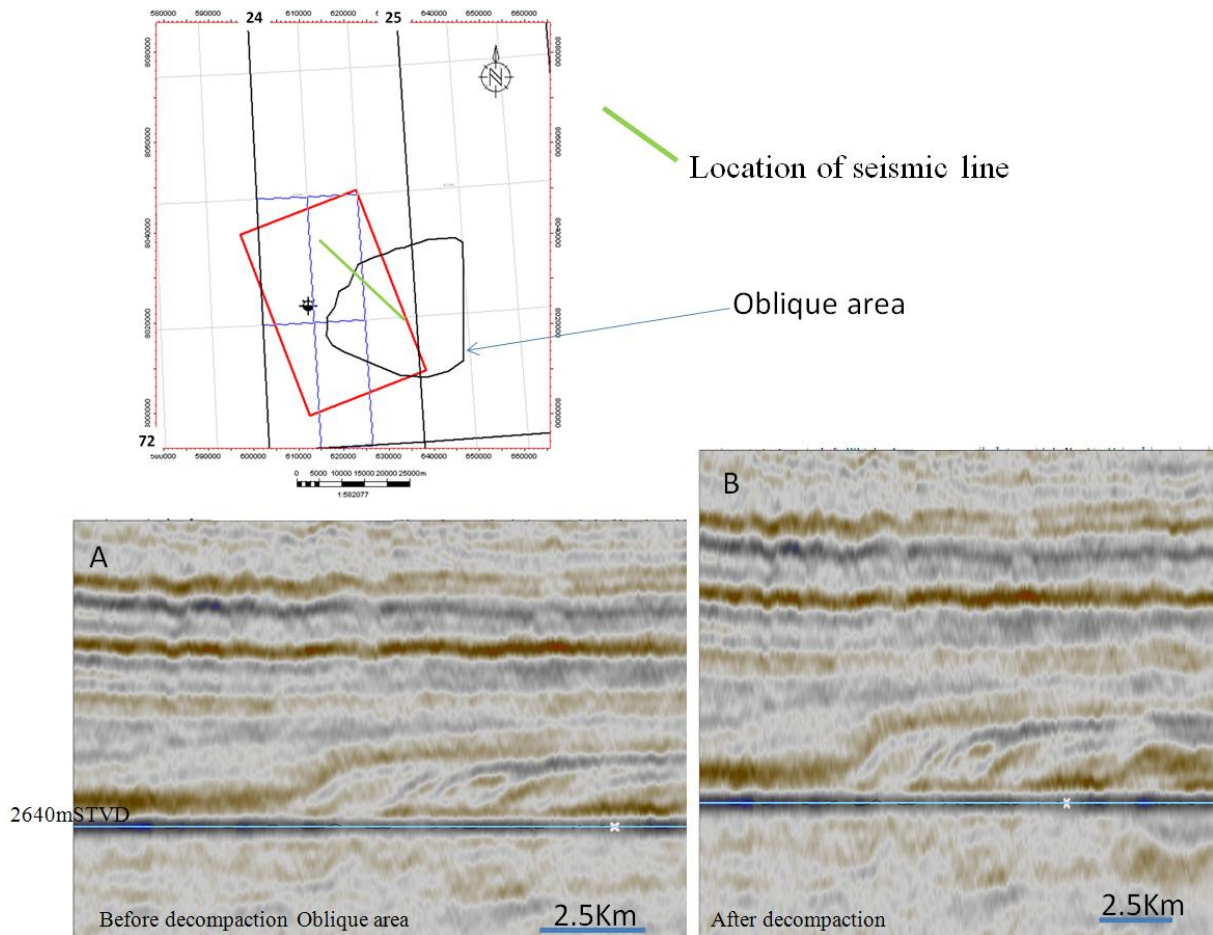
Figure 46 illustrating the differences in angles on the steepest oblique clinoform before and after decompaction.

As seen in the table the oblique area has steeper angles compared to the sigmoidal, where the steepest angle is 8.4 degrees. Compared, the steepest angle in the sigmoidal area is only 2.5 degrees. Considering Pirmez et al (1998) study which concluded that higher clinoform angles correspond to coarser grain size and the wide acknowledgement (E. Glørstd-Clark et al., 2011, Steel et al., 2002) it seems reasonable to believe this is true. Therefore, the oblique area is interpreted to have coarser grain size compared to the sigmoidal. This also fits well with the idea of a river system feeding the delta with coarser grains compared to the well sorted and finer grained sediments found at the coastline. However, considering the well data and core descriptions Klappmyss Formation seems to consist mainly of fine grained material (mostly silt) and there seems to be little sand in the system. But, Bullimore et al. (2005) states that oblique progradation commonly is composed of sediments with high sand contents which add confidence to the interpretation of sand content in the oblique part. In addition, Russian wells producing from the Klappmyss Fm. confirms sand and reservoir potentials.

Regarding clinoform trajectory trends, both flat to negative and positive trends is seen in the system. The flat/negative trend in the oblique area might represent a situation where a lack of incision at the shelf –slope break result in storage of all sediment on the slope, and a lack of basin floor fan. This could help explain why no sand was drilled in the Hegg well. In addition, no evidence of significant volumes of sand bypassing the shelf or upper slope environment is found, because no channels and no submarine fans on the time equivalent basin floor are observed in the seismic data. The low angle negative trajectory is suggested to represent progradation during falling and subsequent early rise of relative sea-level. Moreover, the positive trend in the sigmoidal area suggests a closer balance between rates of sediment supply and relative sea level rise and is interpreted to represent progradation during rising relative sea-level where deltaic units are deposited and preserved in the topset area.

Isopach maps indicate tidal sand banks in the lower unit of the Klappmyss Fm. (figure 35) as well as a thick wedge shaped area located within the observed oblique seismic facies is seen in the upper unit (figure 41). This is interpreted as a change in environment; from being tide dominated towards more wave dominated. Moreover, the protruding geometry of the uppermost clinoform (Top lowstand horizon) indicates a fluvial dominated system. Henriksen et al. (2010) seems to agree, saying that flat trajectories represent fluvially dominated system while positive wave dominated.

This means that the lower Klappmyss Fm. interval consists of a lower unit (figure 33) which was tide dominated allowing retrogradation. The upper unit, on the other hand seems to become wave dominated, where the oblique area correspond to fluvial dominance with transportation of sediments in a higher energy system.

A reconstruction of this possible scenario is seen in figure 47 illustrating the paleogeography. First in A) a tide dominated system allowing eustary and back stepping of the seismic reflectors where some sand bars (elongated yellow parallel to direction of tidal flow) are obtained followed by B) a prograding delta system where a high energy river transport coarse grains to the delta (dotted yellow in figure B) and builds out the platform-margin delta.
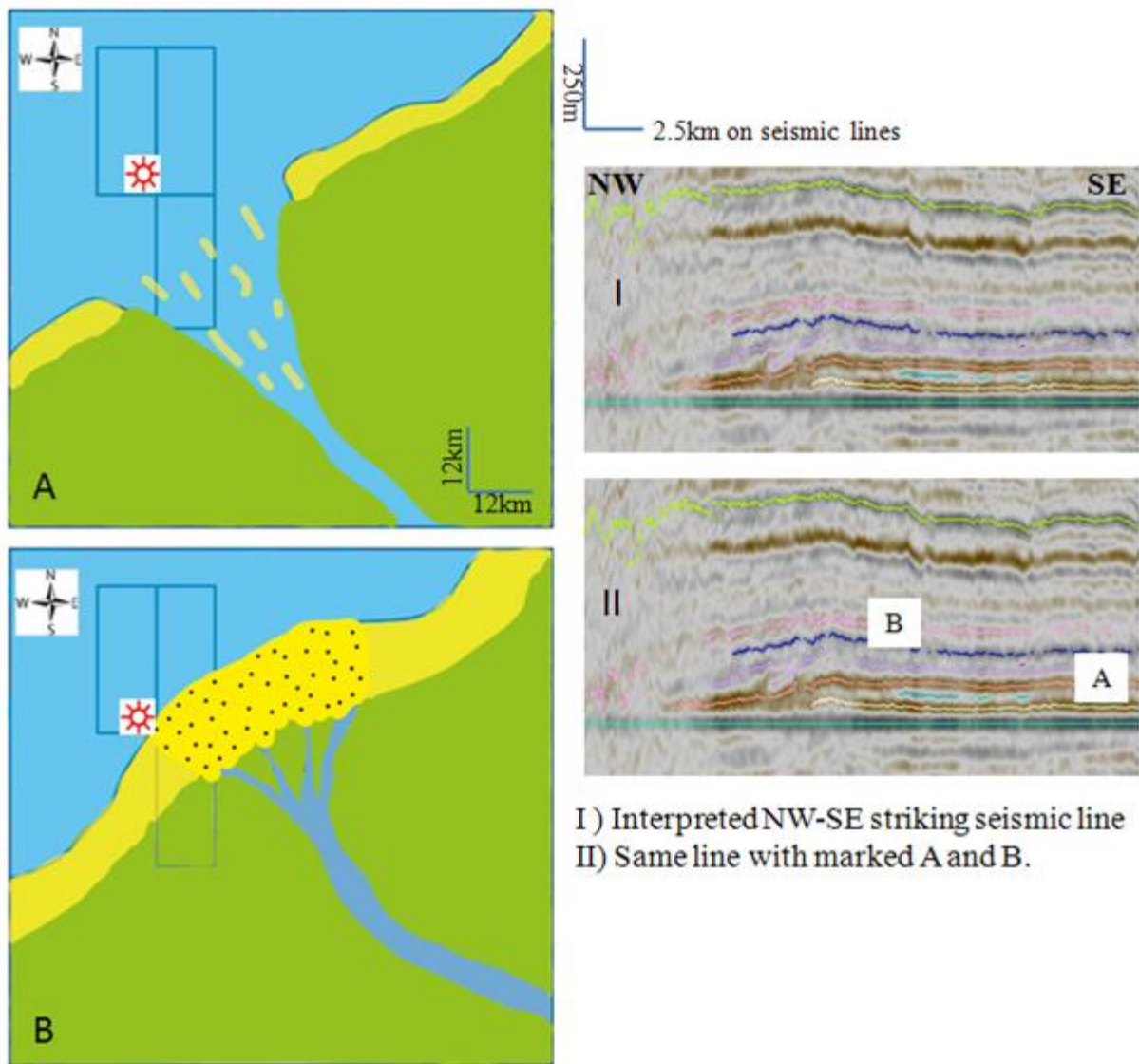
Figure 47 reconstructed paleogeography for the lower Klappmyss interval consisting of two units. A) The flooding event (retrogradation) followed by B) the prograding platform-margin delta development.

Petroleum significance

Volume calculations were carried out using Monte Carlo simulation in GeoX software to get some ideas about the economic value and to get some insight in how this is done. Since reservoir volumes and risk were not a major objective in this study, some of the input values in the calculation are more general and not adjusted to this special case. However, keeping in mind the reconstructed paleogeography, the two different units will have different reservoir quality and this should ideally be incorporated in the calculation.

Type III Kerogen is most likely based on the deep burial history and the finding of mostly gas/ gas shows in this formation. So, even if the Goliat S well contain oil in the Klappmyss Fm. this is rather unlikely in the deeper Samson Dome area. Therefore the input in the calculation and simulation used a gas case as a basis. Several values (see appendix D) were chosen to represent this reservoir. Recovery factor were chosen between 0.5-0.8 since this is a common recovery in gas reservoirs. Moreover, porosity was chosen in the range between 0.15-0.26. These values were picked based on porosities measured in the Pandora and the Goliat S wells in the Klappmyss Formation. Since the sand accumulation in a platform-margin delta with flat/negative clinoform trajectory often consist on thin layers, net/gross ratio were chosen in the 0.15 to 0.4 interval, but this is highly subjective. Moreover, the Bg (gas formation factor) were calculated using values (pressure,temperature etc.) measured in the Hegg well. However, this value should be discussed with a reservoir engineer to get an even more realistic value.

Figure 48 and 49 illustrate the volume distribution using 10000 realizations. P90 represent the volume of gas given success with a 90% chance of getting 553.9 (10^9) scf of gas, or more. Similar P50 represent the 50% chance of getting a given volume or more (given success) and similar the P10. Figure 48 represent volumes in place while figure 49 recoverable volumes. In addition mode= 491.4 (10^9) scf representing the volume that is appearing most often, and med (median) = P50 is shown.

Type: MC(10000)	
Mean	583.5
Std	199.1
P99.5	218.9
P95	310.3
P90	353.9
P75	437.6
P50	555.9
P25	699.0
P10	850.3
P05	954.4
P0.5	1261.7
Min	N/A
Max	N/A
Med	555.9
Mod	491.4
P10:90	2.4

X and Y-axis types Lin-lin

Inplace.Accumulation size Non Assoc. Gas [1e9 scf]
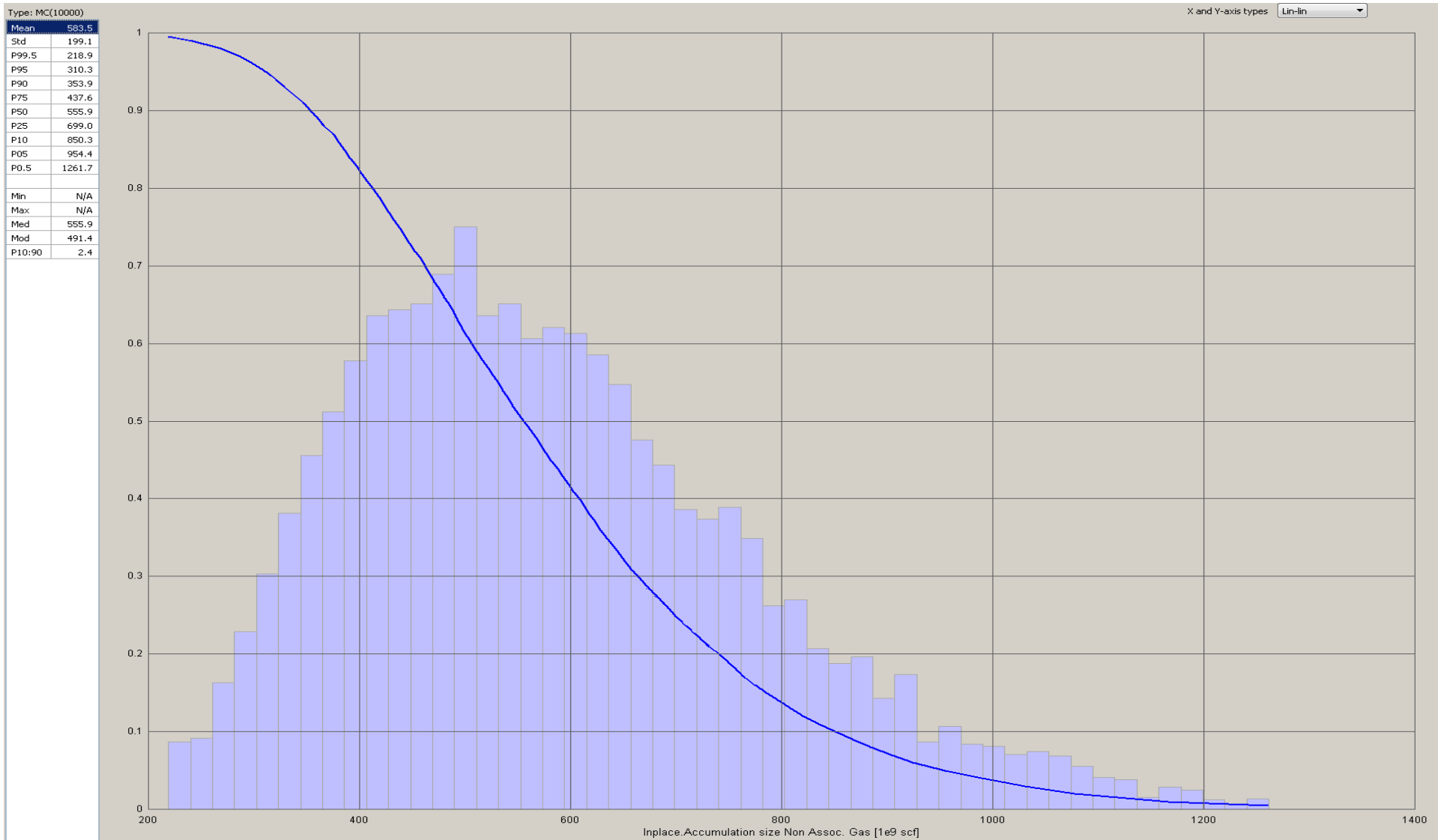
Figure 48 Inplace accumulation gas. P90= 353.9, P50= 555.9 and P10= 650.3 (all in 10^9scf).
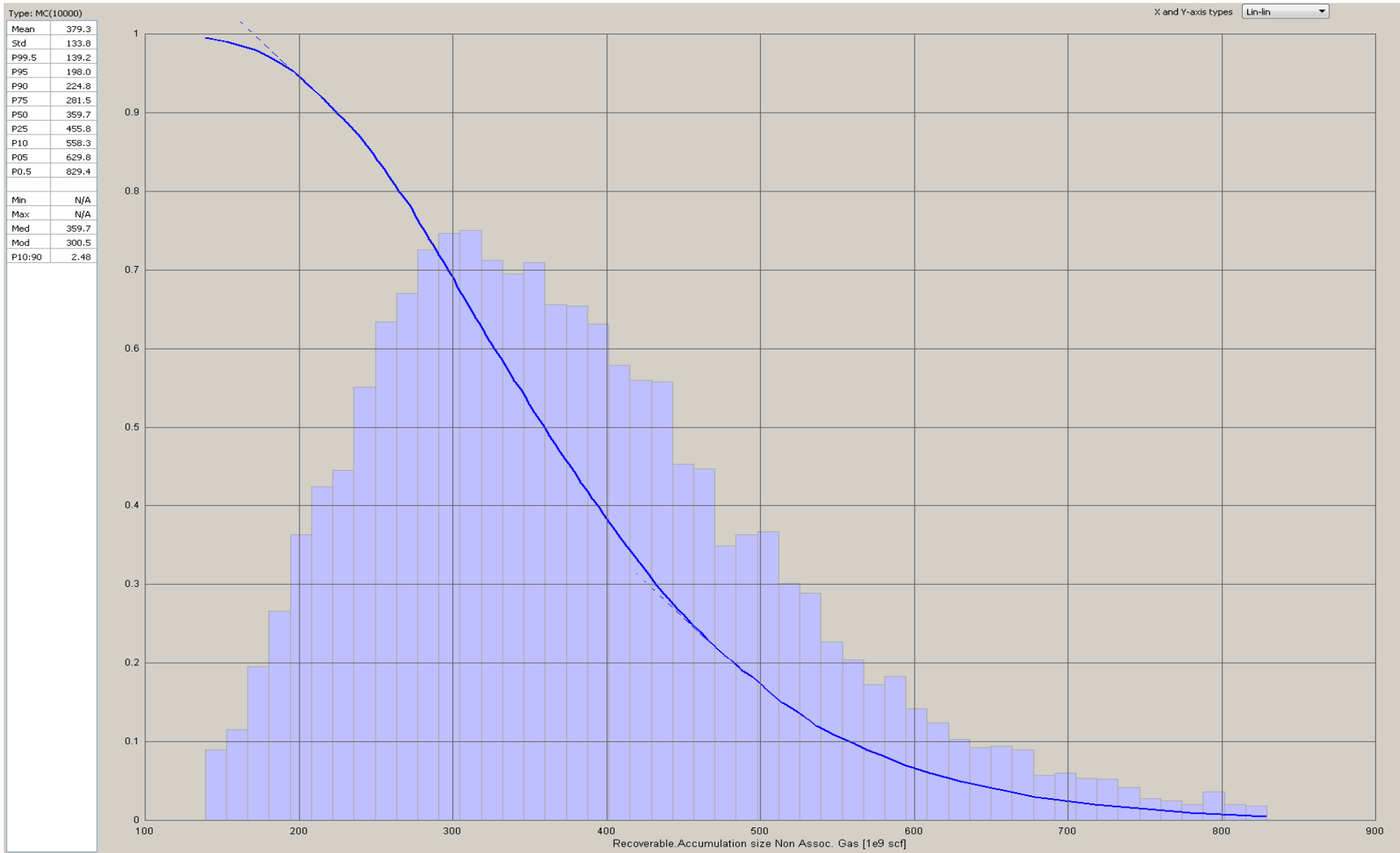
Figure 49 Recoverable accumulation gas. P90= 224.8, P50= 359.7 and P10= 558.3 (all in 10^9scf).

Figure 50 illustrate the Area vs. depth curve and shows the Gas/water contact at 2850m.
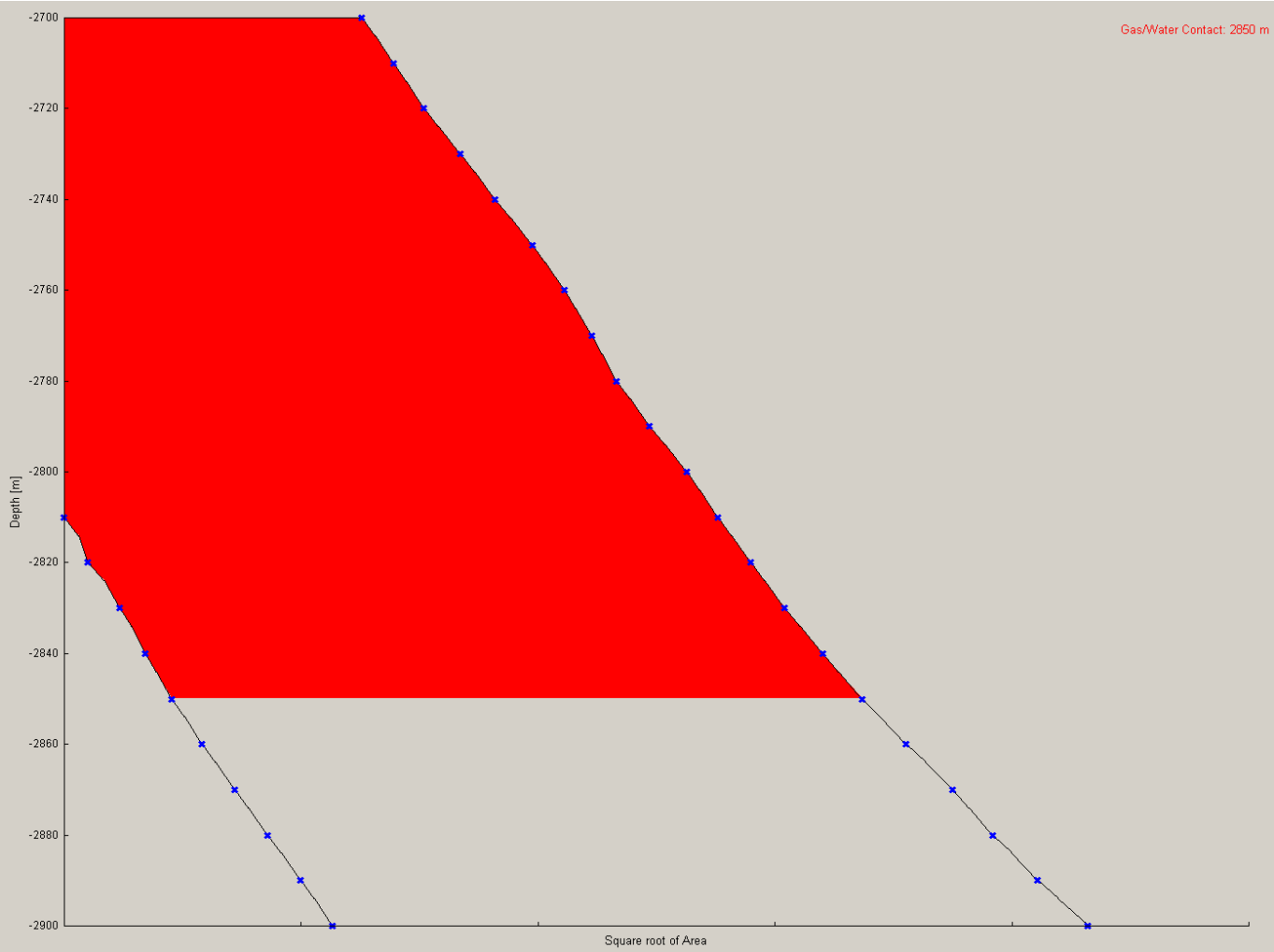
Figure 50 Area vs. Depth curve

The figure below (figure 51) represent the tornado chart in this case. This chart illustrate which values having the highest impact on the calculation (sensivity analysis). Here it is seen that the HC water contact plays the most important role, which means that the calculation is most sensitive to this value. Similar the recovery factor play the least important value, meaning a change in this value will have less impact on the calculation compared to the net/gross ratio or HC water contact.
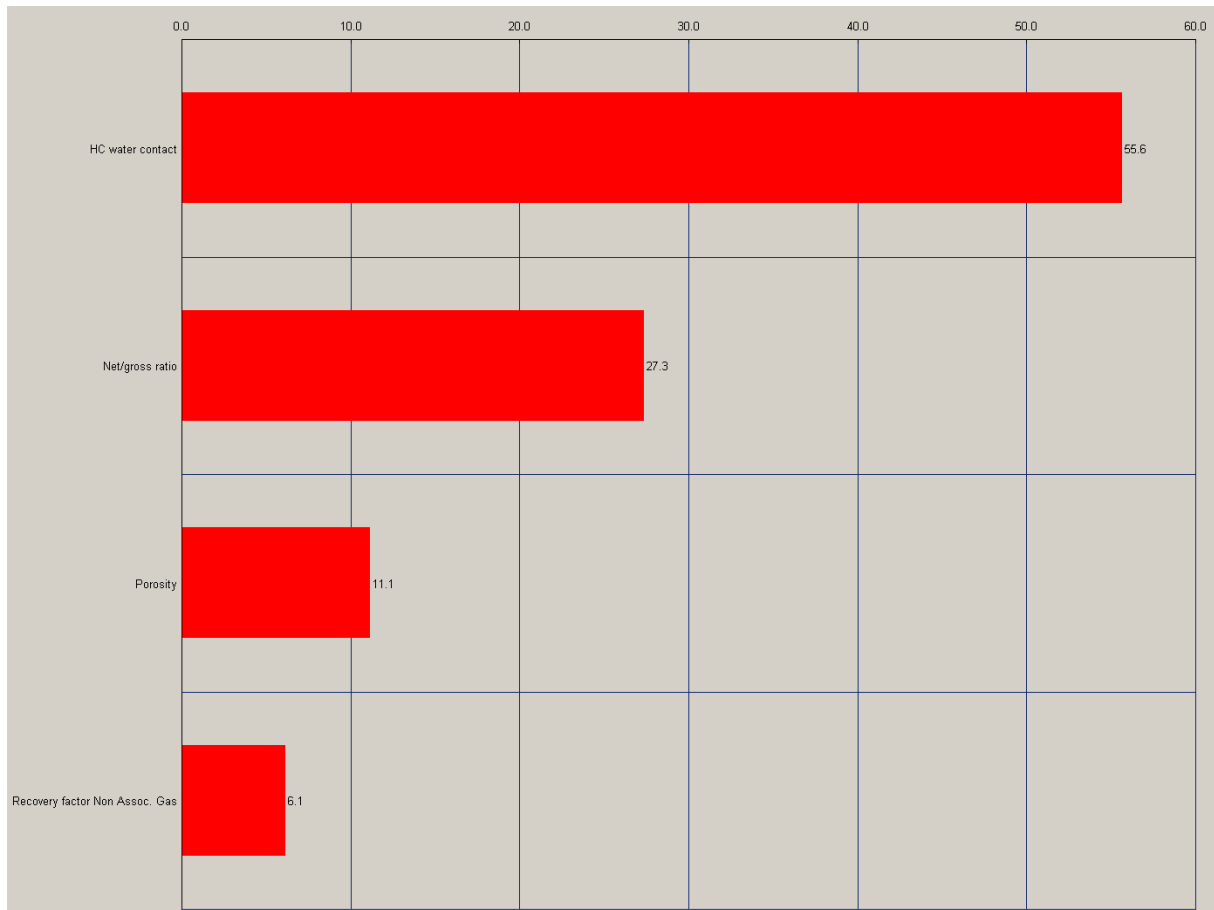
Figure 51 Tornado chart for this gas case

To get some insight into risk analysis, also a risk analysis were preformed. However, this was mainly to learn the step and the input values are guiding values only. As seen in appendix D, values for reservoir, source and trap (presence and effectiveness) were considered. These values represent probabilities. This means that a reservoir effectiveness of 0.5 means that the probability of having an effective reservoir is 50%. This low value were chosen based on permeability measurements in the Klappmyss Fm., were values often have been low (tight reservoir). Sandstones associated with low negative clinoform trajectories are often thin and with low quality due to slumping. Moreover, reservoir presence was given a 25% probability but is rather uncertain. Considering observations of high angle (coarse grain) clinoforms and sand presence in the Goliat S well this probability could be higher. Both source presence and effectiveness were given high probabilities (1 and 0.8) due to an already proven source potential in several wells. This was also the case for the trap mechanism, which also is considered to be proven.

Previous studies

Compared to previous studies, refereeing to Glørstad-Clark`s studies (2010/2011) on the more regional aspect of Triassic, the observations in this study fits well. The position and geometry of the delta seems very similar (figure 7). We both get a protruding shape on the delta, and also the trajectory trends are very similar in both studies. However, this study adds a significant level of detail around the processes dominating the depositional environment and includes important clues from offset well data as to the reservoir quality potential.

Considering provenance studies indicating the Uralian Mountains to be the source for the sediment, the transportation distance is questioning the ability to preserve coarse grains. However, considering the Baltic shield to be the sediment source preservation of coarse grains seems more likely. Few papers have been found to confirm provenance for the Early Triassic sediments.

Conclusion

Several analyses on the clinoforms representing a platform-margin delta have been done. These analyses conclude with a high probability for sand being present. However, low reservoir quality represents a major uncertainty. A question to be answered is possibilities to preserve, or gain a higher permeability like chlorite coating or overpressure in the reservoir. Also net/gross is likely to be low due to thin sand accumulations. Best reservoir properties will be maximum basinward of the shelf margin, because here a flattening of the clinoform trajectory will allow thicker sand accumulations.

Reconstruction of the paleogeography indicates a change in environment from tide to wave domination; this is confirmed by the seismic facies and clinoform trajectories, indicating different energy, as well as time- thickness maps. The two units will therefore have differences regarding sand volume and quality (porosity/permeability).

In place volumes is estimated to be about; P90= 353.9, P50= 555.9 and P10= 650.3 (all in 10^9scf). Commercial value based on the volume estimation seems low, especially being a primary objective. Being a secondary target in a combined prospect is another issue. Also change in the future gas prices might change the value on long term.

This study confirms the regional findings of Glørstad-Clark, but adds a significant level of detail around the processes dominating the depositional environment and includes important clues from offset well data as to the reservoir quality potential.

Further studies on provenance in Bjarmeland Platform/Samson Dome area needs to be done to answer the question regarding source of the sediments. This could add valuable information regarding probabilities for coarse grains and sand presence. In addition, more quantitative studies on grain size vs. clinoform angles needs to be done to add more certainty into higher clinoform angles representing coarser sediments.

References

http://www.npd.no/publications/resource-reports/2011/chapter-2/

http://factpages.npd.no/factpages/Default.aspx?culture=en).

www.worldatlas.com/aatlas/infopage/barents.gif)

ADAMS, E.W., SCHLAGER, W., ANSELMETTI, F.S. 2001: *Morphology and curvature of delta slopes in Swiss lakes: lessons for the interpretation of clinoforms in seismic data.* International Association of sedimentologists. Sedimentology 48, 661-679.

BROWN, L.F., 1996.*Seismic Sequence Stratigraphy: Its role in Petroleum Exploration and Development.* JAPEC. Geological Society Burlington House, Piccadilly, London. Course notes, 161.

BULLIMORE, S.A., HENRIKSEN, S., LIESTØL, F.M., HELLAND-HANSEN, W., 2005. *Clinoform stacking patterns, shelf edge trajectories and facies association in Tertiary coastal deltas, offshore Norway: implications for the prediction of lithology in prograding systems.* Norwegian Journal of Geology 85, 169-187.

CATUNEANU, O. 2002. *Sequence stratigraphy of clastic systems: concepts, merits and pitfalls.* Elsevier. Journal of African Earth Sciences 35 p. 1-43.

DEIBERT, J.E., BENDA, T., LØSETH, T., SCHELLPEPER, M., STEEL, R.J. 2003: *Eocene clinoform growth in front of a storm-wave dominated shelf, central basin, Spitsbergen: no significant sand delivery to deepwater areas.* Journal of sedimentary research, Vol. 73, No. 4 pp 546-558.

DENGO, C.A., RØSSLAND, K.G., 1992: *Extensional tectonic history of the western Barents Sea. Structural and tectonic Modeling and its Application to Petroleum Geology* edited by R.M. Larsen. H. Brekke, B.T., Larsen and E. Talleraas. NPF Special Publication 1, pp.91-107. Elsevier. Amsterdam. Norwegian Petroleum Society (NPF), 1992.

EMERY, D., MYERS, K.J. 1996. *Sequence Stratigraphy*. Blackwell Science, Oxford. P. 297.

FALEIDE, J.I, GUDLAUGSSON, S.T. & JACQUART, G., 1984: *Evolution of the western Barents Sea.* Marine and Petroleum Geology 1, pp. 123-150.

FALEIDE, J.I., VÅGENES, E. & GUDLAUGSSON, S.T., 1993: *Late Mesozoic- Cenozoic evolution of the south-western Barents Sea. Petroleum Geology of Northwest Europe; Proceedings of the 4th Conference* (edited by J.R. Parker). Petroleum Geology 86 Ltd. Published by The Geological Society, London, 99- 933-950.

GABRIELSEN, R., FÆRSETH, R.B., JENSEN, L.N., KALHEIM, J.E., RIIS, F., 1990. *Structural elements of the Norwegian continental shelf, part I: the Barents Sea region,* Norwegian Petroleum Directorate Bulletin 6, 47.
GALLOWAY, W.E. 2004. *Terrigenous Clastic Depositional Systems and sequences – Application to Reservoir Prediction, Delineation, and Characterization*. AAPG. Course notes.

GLØRSTAD-CLARK E., BIRKELAND. E.P., NYSTUEN, J.P., FALEIDE, J.I., MIDTKANDAL, I. 2011*: Triassic platform-margin deltas in the western Barents Sea.* Elsevier Ltd. Marine and Petroleum Geology 28 pp. 1294-1314.

GLØRSTAD-CLARK, E., FALEIDE, J.I., LUNDSCHIEN, B.A., NYSTUEN, J.P. 2010: *Triassic seismic sequence stratigraphy and paleogeography of the western Barents Sea area.* Elsevier. Marine and Petroleum Geology 27 pp. 1448-1475.

GUDLAUGSSON, S.T., FALEIDE, J.I., JOHANSEN & S.E., BREIVIK, A.J., 1998: *Late Paleozoic structural development of the South-western Barents Sea.* Marine and Petroleum Geology 15, pp. 73-102.

HELLAND-HANSEN, W. & GJELDBERG, J.G. 1994. *Conceptual basis and variability in sequence stratigraphy; a different perspective.* Sedimentary Geology 92, 31-52

HENRIKSEN, S., HELLAND-HANSEN, W., BULLIMORE, S. 2010. *Relationship between shelf-edge trajectories and sediment dispersal along depositional dip and strike: a different approach to sequence stratigraphy.* EAGE. Basin researchvol. 23, Issue 1 p.3-21.

HENRIKSEN, E., BJØRNSETH, H.M., HALS, T.K., HEIDE, T., KIRYUKHINA, T., KLØVJAN, O.S., LARSSEN, G.B., RYSETH, A.E., RØNNING, K., SOLLID K., STAUPAKOVA, A. 2011: *Uplift and erosion of the greater Barents Sea: impact on prospectivity and petroleum systems.* Artic Petroleum Geology. Geological Society, London, Memoris 35, 271-281.

JOHANSEN, S.E., GUDLAUGSSON, S.T., SVANÅ, T.A., FALEIDE, J.I., 1994. *Late Paleozoic evolution of the Loppa High, Barents Sea.* Part of unpublished PHD thesis, University of Oslo, Oslo, p.25.

MØRK, M.B. 1999: *Compositional variations and procenance of Triassic sandstones from the Barents shelf.* Journal of sedimentary research, Vol. 69, No. 3, pp 690-710.

NØTTVEDT, A., CECCHI, M., GJELDBERG, J.G., KRISTENSEN, S.E. LONOY, A, RASMUSSEN, A., RASSMUSEN, E., SKOTT, P.H. 1993. *Svalbard- Barents Sea correlation: a short review.* In: Vorren, T., Bergsager, E., Dahl-Stamnes, Ø., Holter, E., Johansen, B., Lie, E., Lund, T. (Eds), Arctic Geology and Petroleum Potential. Norwegian Petroleum Society (NPF). Special Publication, vol. 2. Elsevier, Amsterdam, pp. 363-375.

NØTTVEDT, A., JOHANNESEN, E.P., SURLYK, F., 2008. *The Mesozoic of western Scandinavia and east Greenland.* Episodes 31, 59-65.

PLINK-BJØRKLUND, P. And STEEL, R., 2006. *Type II Shelf Margin, Høgsnyta, Norway: An Attached Slope Turbidite System,* in T.H. Nilsen, R.D. Shew, G.S. Steffens, and J.R.J. Studlick, eds., Atlas of Deep-water Outcrops: AAPG Studies in Gelogy 56.

PROEBSKI, S.J., STEEL, R.J. 2003: *Shelf-margin deltas: their stratigraphic significance and relation to deepwater sands.* Elsevier science. Earth-Science Reviews 62 pp 283-326.

PIRMEZ, C., PRATSON, L.F., STECKLER, M.S. 1998: *Clinoform development by advection-diffusion of suspended sediment: Modeling and comparison to natural systems.* Journal of geophysical research, Vol. 103. No. B10. pp 24, 141-24, 157.
RØNNEVIK, H.C., 1981: *Geology of the Barents Sea.* Petroleum Geology of the continental Shelf of North-West Europe, pp. 395-406. Institute of Petroleum, London, 1981.

SANGREE, J.B., WINDMIER, J.M., 1977. *Seismic stratigraphy and global changes in sea-level, 9.: seismic facies and depositional facies,* In: Payton, C. (Ed), Seismic Stratigraphy-Applications to Hydrocarbon Exploration. The American Association of Petroleum Geologists, Memoir, vol. 26. AAPG, Tulsa, pp. 165-184.

STEEL, R., CRANBAUGH, J., SCHELLPEPER, M., MELLERE, D., PLINK-BJØRKLUND, P., DEIBERT, T. & LØSETH, T. 2000. *Deltas versus rivers on the shelf edge: their relative contributions to the groeth of shelf margins and basin floor fans (Barremian and Eocene, Spitsbergen).* In: GCSSEPM Foundation 20th Annual Research Conference, Deepwater Reservoirs of the World. 981-1001. Houston.

STEEL, R. & OLSEN, T. 2002. *Clinoforms, Clinoform Trajectories and Deepwater Sands.* In Armentrout, J.M. & Rosen, N.C. (eds), Sequence Stratigraphic models for exploration and production: Evolving Methodology, Emerging Models and Application Histories. 367-381. Special Publication GCS- Society of Economic Paleontologists and Minerals.

STEMMERIK L., WORSLEY, D. 2005. *30 years on . Arctic Upper Palaeozoic stratigraphy, depositional evolution and hydrocarbon prospectivity.* Norwegian Journal of Geology, Vol. 85. Pp. 151-168. Trondheim.

STOUPAKOVA A.V., HENRIKSEN, E., BURLIN, Yu.K., 2011. *The geological evolution and hydrocarbon potential of the Barents and Kara shelves.* Geological Society, London, Memoirs v.35. p. 325-344.

TORSVIK, T.H., CARLOS, D., MOSAR, M., COCKS, L.R.M. & MALME, T., 2002: *Global reconstructions and North Atlantic palaeography 440Ma to Recent.* In: Eide, E.A. (coord), BATLAS – Mid Norway plate reconstruction atlas with global and Atlantic perspectives. Geological Survey of Norway, pp. 18-39.

VAIL, P.R., MITCHUM, R.M.J., THOMSON, S.I., 1977. *Seismic stratigraphy and global changes of sea-level, part 3: relative changes of sea-level from coastal onlap.* In: Payton, C. (Ed), seismic Stratigraphy- Application to Hydrocarbon Exploration. The American Association of Petroleum Geologists, Memoirs, vol .26. AAPG, Tulsa, pp. 63-81.

WORSLEY, D., 2006: *The post-Caledonian geological development of Svalbard and the Barents Sea.* Norsk Geologisk Forening. Abstracts and Proceedings, no. 3, 2006, pp. 5-21.

ZIEGLER, P.A. 1989. *Evolution of the north Atlantic – an overview.* In: Tankard, A.J. Balkwill, H.R., (Eds), Extensional Tectonics and stratigraphy of the North Atlantic margins. American Association of Petroleum Geologists, Memoir, vol. 46. Canadian Geological Foundation and AAPG, Tulsa, pp. 11-129.

ZIEGLER, P.A. 1988. *Evolution of the Artic-North Atlantic and the western Tethys.* In: American Association of Petroleum Geologists, Memoir, No, 43. AAPG, Tulsa. P. 198.
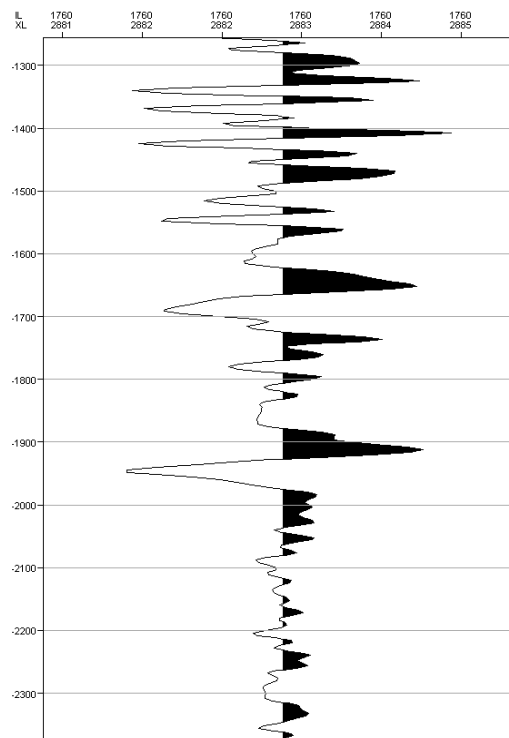
Appendix

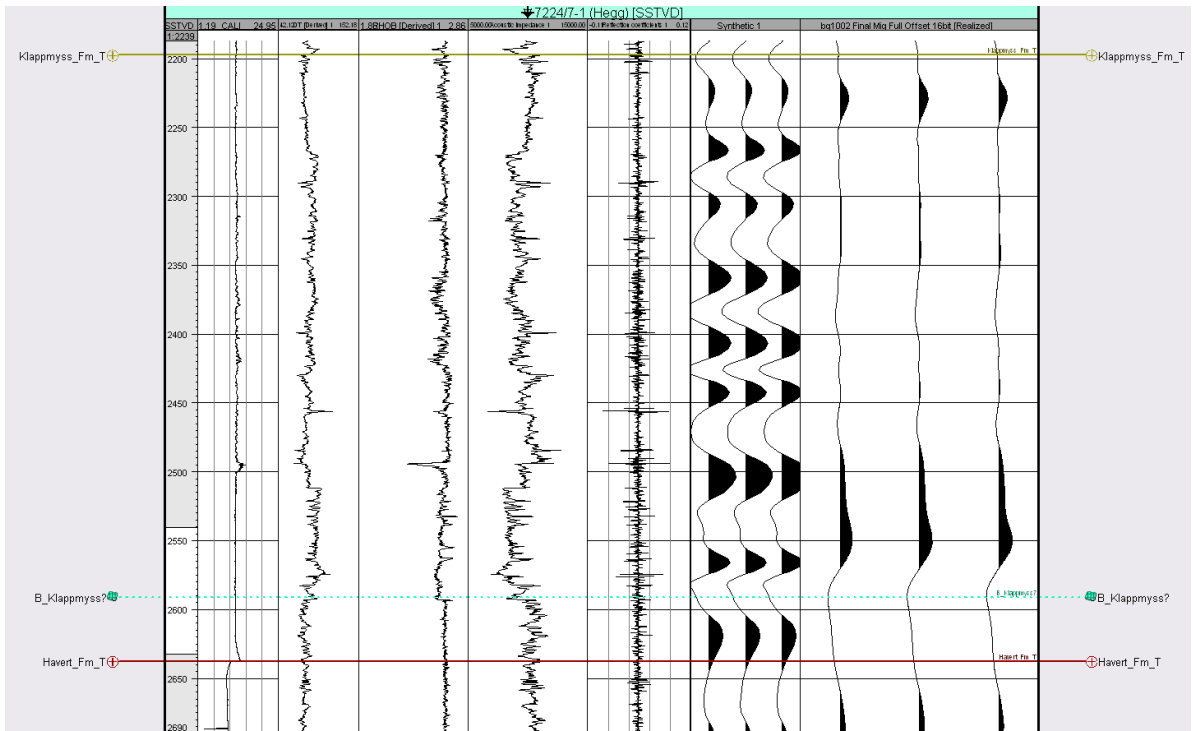## A) Synthetic seismic & frequency

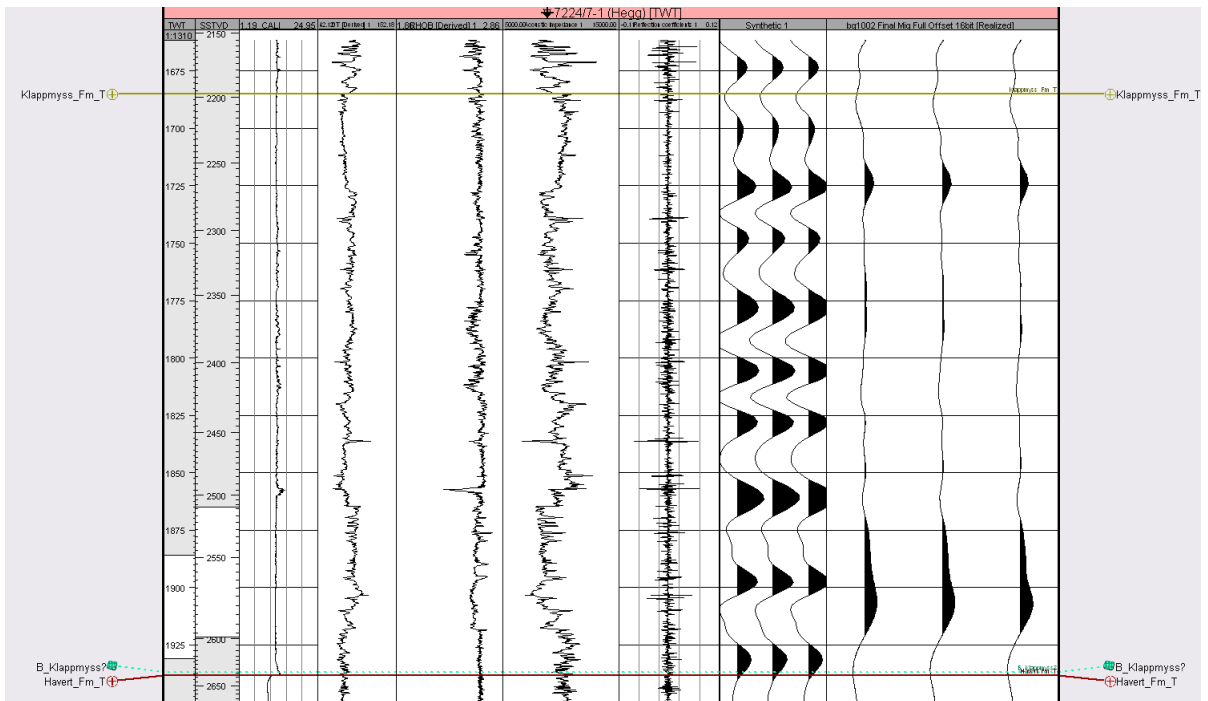Frequency obtained by summing all peaks. Frequency contribute in resolution calculation on the seismic.
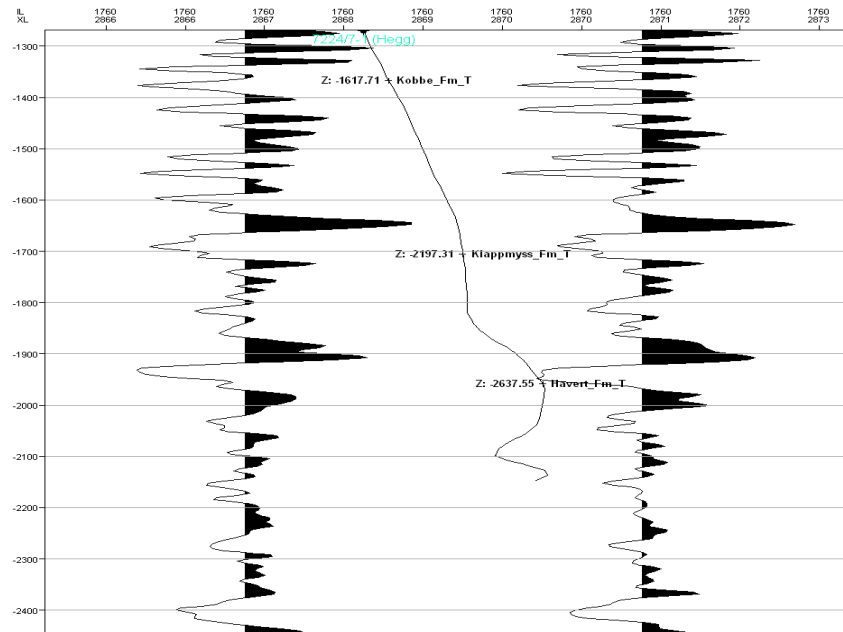
28 Hz

27 Hz

Snapshot of the created synthetic at Klappmyss level before bulkshift.

After bulkshift 20ms

B) Well information

Penetrating wells	End of drilling	Top depth (m)	Bottom depth (m)
7120/1-1	15.11.1985	2315	2373
7120/1-1 R	26.12.1985	2315	2373
7120/1-1 R2	21.07.1986	2315	2373
7120/9-2	20.10.1984	4245	4806
7120/12-2	11.09.1981	3095	3552
7120/12-4	16.04.1984	685	992
7121/1-1 R	23.08.1986	2605	2786
7122/7-3	08.01.2006	2044	2212
7122/7-4 S	25.11.2006	2042	2217
7122/7-5	23.12.2006	2126	2228
7124/3-1	20.10.1987	2334	2671
7125/4-1	07.03.2007	1561	1615
7125/4-2	01.12.2008	1683	1750
7128/4-1	26.02.1994	748	1008
7128/6-1	08.11.1991	734	1002
7222/6-1 S	10.03.2008	2464	2674
7223/5-1	14.01.2009	2451	2549
7224/7-1	19.06.1988	2222	2663
7226/2-1	19.07.2008	2325	2930
7226/11-1	11.04.1988	2303	2913
7228/2-1 S	20.12.1989	3574	3984
7228/7-1 A	02.02.2001	2741	2881
7228/9-1 S	07.05.1990	2097	2638
7229/11-1	15.12.1993	2353	2804
7324/10-1	19.08.1989	2272	2512

Callout annotations:
- Goliat S: Oilbearing at 2040,5. OWC at 2072,5m
- Bamse: Oil & gas shows, deepest at 2346m
- Obesum: Gas prone source rock at 2579-2675m
- Hegg: Gas shows
- Pandora: Gas
- Organic rich shale

Table summarizing all wells that have penetrated the Klappmyss Fm.

C) Seismic

2D SURVEYS	Bulkshift (ms)	Quality	Date	Comments	Survey Company
npd-fi-83	20	Chaotic in Klappmyss. Multiple of seabed	1983	Low frequency	NPD
npd-bjre-84	40	Good	1984	Low frequency	NPD
fwgs-84	0	Good	1984	Low frquency	
npd_nolo-85_aker_geo	0	Affected by salt and several faults	1985	Low frquency	NPD
st8611	0	Good	1986	Low frquency	
npd_fjoe2_86-aker-geo	20	Good	1986	Low frquency	NPD
st8813	0	Good	1988	Low frquency	
sg9715	0	Weak reflectors	1997	Low frquency	
bss01	0	Good	2001	Good	
nbr07re09 (2D)	-7	Good	2007	Good	Fugro
nbr06re11	-3	Good strong reflectors	2011	Good	Fugro

Table showing 2D seismic information

3D SURVEYS	Bulkshift (ms)	Quality	Date	Comments	Survey Company
st9403	-7	Good	94		
bg1002	20	Good	2011		CGGVERITAS

Table showing 3D seismic information

Time-Depth converting

Hegg (7224/7-1)

	TWT (ms)	OWT (ms)	OWT (s)	Depth (m)	Isochron secs owt	Isochore m	Vint m/s
MSL	0	0	0	0			
					0.17959	269	1498
Seabed	359.18	179.59	0.17959	269			
					0.25841	579	2241
Fuglen	876	438	0.438	848			
					0.5307	1790	3373
Havert	1937.4	968.7	0.9687	2638			

Time/ depth convertion table, showing the calculations

D) Volume & risk

Parameter [Units]	Dist. type	Mean	Std. dev.	Min (Lo)	Central	Max (Hi)
Wet gas shrinkage factor [decimal]	Const	0.95	0.0		0.95	
Gas expansion factor (1/Bg) [scf/cf]	Const	200.0	0.0		200.0	
Condensate yield [STB/1e6 scf]	Const	2.0	0.0		2.0	
Recovery factor Non Assoc. Gas [decimal]	StrBeta	0.65	0.0583	0.5	0.65	0.8
Recovery factor Condensate [decimal]	StrBeta	0.65	0.0583	0.5	0.65	0.8

Parameter [Units]	Dist. type	Mean	Std. dev.	Min (Lo)	Central	Max (Hi)
Net/gross ratio [decimal]	StrBeta	0.275	0.0486	0.15	0.275	0.4
Porosity [decimal]	StrBeta	0.196	0.0216	0.15	0.19	0.26
Gas saturation [decimal]	Const	0.47	0.0		0.47	

Calculation input

Risk factor	P(play)	P(segment | play)	Overall
Reservoir Presence	1.000	0.250	0.250
Reservoir Effectiveness	1.000	0.500	0.500
Source Presence	1.000	1.000	1.000
Source Effectiveness	1.000	0.800	0.800
Trap Presence	1.000	1.000	1.000
Trap Effectiveness	1.000	1.000	1.000
> Marginal play probability	1.000		
> Conditional segment probability		0.100	
> Unconditional probability		0.100	
> Dry hole risk		0.900	

Risk input

Scenarios	Dist. type	Mode	Mean	Std. dev.	P90	P50	P10	Overall probabi...
Failure								0.900
Success volume	MC(10000)	300.5	379.3	133.8	224.8	359.7	558.3	0.100
Unconditional segment	MC(10000)-r		37.9	121.4	0.0	0.0	139.2	1.000

Recoverable volumes